Existence and stability of standing pulses in neural networks

by

Yixin Guo

B.S. Heilongjiang University

M.A. University of Pittsburgh

Submitted to the Graduate Faculty of

Arts and Sciences in partial fulfillment

of the requirements for the degree of

Doctor of Philosophy

University of Pittsburgh

2003

UNIVERSITY OF PITTSBURGH

FACULTY OF ARTS AND SCIENCES

This dissertation was presented

by

Yixin Guo

It was defended on

June 5, 2003

and approved by

G. Bard Ermentrout, Professor, Mathematics Dept.

Jonathan Rubin, Assistant Professor, Mathematics Dept.

William C. Troy, Professor, Mathematics Dept.

Xiao-Lun Wu, Associate Professor, Physics Dept.

Committee Chairperson: Carson C. Chow, Associate Professor, Mathematics Dept.

EXISTENCE AND STABILITY OF STANDING PULSES IN NEURAL NETWORKS

Yixin Guo, Ph.D.

University of Pittsburgh, 2003

This dissertation studies a one dimensional neural network rate model that supports localized self-sustained solutions. These solutions could be an analog for working memory in the brain. Working memory refers to the temporary storage of information necessary for performing different mental tasks. Cortical neurons that show persistent activity are observed in animals during working memory tasks. The physical process underlying this persistent activity could be due to self-sustained network activity of the neurons in the brain.

The term 'bump' has been coined to imply a spatially localized persistent activity state that is sustained internally by a network of neurons. Many researchers have analyzed the bump state using firing rate models with either the Heaviside gain function or a saturating sigmoidal one. These gain functions imply that neurons begin to fire once their synaptic input reaches threshold, and the firing rate saturates to a maximal value almost immediately. However, cortical neurons that exhibit persistent activity usually fire well below their maximal attainable rate. To resolve this paradox, I study a single population rate model using a biophysically relevant firing rate function.

I consider the existence and the stability of standing single-pulse solutions of an integro-differential neural network equation. In this network, the synaptic coupling has local excitatory coupling with distal lateral inhibition and the non-saturating gain function is piece-wise linear. A standing pulse solution of this network is a synaptic input pattern that supports a bump state. I show that the existence condition for single-pulses of the integro-differential equation can be reduced to the solution of an algebraic system. With this condition, I map out the shape of the pulses for different coupling weights and gains. By a similar approach, I also find the conditions for the

existences of dimple-pulses and double-pulses. For a fixed gain and connectivity, there are at least two single-pulse solutions – a "large" one and a "small" one. However, more than two single-pulses can coexist depending on the parameter range. To have standing single-pulses, the gain function and synaptic coupling are both important.

I also derive a stability criteria for the standing pulse solutions. I show that the large pulse is stable and the small pulse is unstable. If there are more than two pulse solutions coexisting, the first pulse is the small one and it is unstable. The second one is a large stable pulse. The third pulse is wider than the second one and it is unstable. More importantly, the second single-pulse (which could be a dimple pulse) is bistable with the "all-off" state. The stable pulse represents the memory. When the network is switched to the "all-off" state, the memory is erased.

To my parents, my husband and my son

Acknowledgments

I would like to express my sincerest appreciation and gratitude to my adviser, Professor Carson Chow, for his guidance, patience, encouragement and understanding. Through the course of this thesis, I have had not only enormous help but had his generous advice as well. I feel lucky to be his student.

I extend my appreciation and thanks to my committee members, Professors G. Bard Ermentrout, Jonathan Rubin, William Troy and Xiao-Lun Wu for their willingness to be members of my thesis committee. This work benefited from their invaluable suggestions and comments.

I express my appreciation to Professors Bryce McLeod, Xinfu Chen and Bjorn Sandstede for their valuable time and insightful disscusions. I would also like to thank all my friends and my fellow officemates for their tolerance and understanding.

Finally, I would like to express my appreciation and thanks to my parents for their absolute love and support not only during this work but all of my life. Without them, I would not be able to complete this work. Especially, I would like to express sincere thanks to my husband for being there when I needed him and to my lovely son who is growing up in my absence.

Table of Contents

List of Tables

List of Figures

Chapter 1
Introduction

1.1 Working memory and standing pulses

Working memory refers to the temporary storage of material necessary for performing different tasks [6]. For example, to understand a sentence, you need to remember the beginning until you get to the end. The physical process underlying working memory is persistent neural activity that is sustained internally in the brain, rather than driven by external input [63].

Cortical neurons that show persistent activity during memory tasks are observed in animal experiments [11, 25, 26]. For example, the animal's delayed saccadic eye movement is guided by the memory of the visual cue. Neurons in the dorsolateral prefrontal (PFC) cortex of monkeys are found to display elevated firing activity during a memory task and then are switched off abruptly when the memory is no longer required.

In the past three decades, different neural mechanisms that support persistent activity have been proposed, such as 'line attractors' [61] or 'bump attractors' [3, 9, 41, 65]. A 'bump attractor' is a spatially localized stable persistent activity state.

A number of neural network models have been shown to support bump states. G.B. Ermentrout [18] gives a thorough review of these models and their solutions obtained by different methods. Amari studied a neural network [3, 34] with lateral-inhibition type coupling on a one-dimensional domain. The network supports a pattern of excitation (above threshold activation) on an open and finite interval on the domain. Amari calls this synaptic pattern a localized excitation, and later G. B. Ermentrout calls it a standing pulse [18]. A standing pulse is a 1-D version of a bump attractor. A localized excitation and a standing pulse refers to a synaptic input pattern that has only one excited region on a finite and open interval. More recently, different excitation patterns have been discovered [31, 43, 42]. These new patterns have excited regions composed of a union of two (or more) disjoint, finite and open intervals. They can be regarded as standing pulses because they are localized and stationary. To avoid confusion, in this thesis, I call a standing pulse with only one

finite and open excited region a (standing) single-pulse or 1-pulse. I call a standing pulse with two disjoint, finite and open interval excited regions a (standing) double-pulse or 2-pulse.

1.2 Previous work

1.2.1 Amari's model

In [3], Amari shows the existence of localized excitations for a neural network modeled by the following equation:

$$\frac{\partial u(x,t)}{\partial t} = -u(x,t) + \int_{-\infty}^{\infty} w(x-y) f[u(y,t)] dy + h + s(x,t) \tag{1.1}$$

This equation describes neuronal behavior in a lateral-inhibition network of a single-layer of neurons along a one-dimensional spatial domain. Function $u(x,t)$ is the synaptic input to neurons located at position $x \in (-\infty, \infty)$ at time $t \geq 0$, and it denotes the *level of excitation* of a neural element. The coupling function $w(x)$ determines the *connection* between neurons. The nonnegative and monotonically non-decreasing function $f[u]$, called the gain function, denotes the *firing rate* at x at time t. In Amari's model, $f[u]$ is the Heaviside function $\Theta(u)$,

$$f[u] = \Theta(u) \equiv \begin{cases} 0 & u \leq 0 \\ 1 & u > 0 \end{cases}$$

In the absence of $s(x,t)$, *i.e.*, $s(x,t) = 0$, Amari studies the existence and the stability properties of stationary solutions of (1.1), i.e. solutions of

$$u(x) = \int_{-\infty}^{\infty} w(x-y) f[u(y)] dy + h. \tag{1.2}$$

A neuron at x is excited when $u(x) > 0$. Let

$$R[u] = \{x | u(x) > 0\}$$

be the excited region of $u(x)$. A solution $u(x)$ of (1.2) for which $R[u] = (0, a)$ is a bounded,

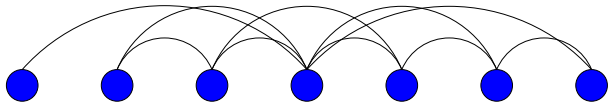

Figure 1.1. A network of N integrate-and-fire neurons.

---

connected, open interval is defined to be a single-pulse solution. Amari proves that equation (1.2) has zero, one or two single-pulse solutions for a general form of lateral-inhibition connections $w(x)$. He develops a stability criterion that shows when two single-pulse solutions coexist with the "large" of them being stable and the "smaller" being unstable.

1.2.2 Integrate-and-fire networks

Laing and Chow [41] study the properties of bumps in networks of spiking neurons using an integrate-and-fire model. They consider a network of N integrate-and-fire neurons (figure 1.1) whose membrane potential, v_i, obeys

$$\frac{dv_i}{dt} = I_i - v_i + \sum_j w_{ij}\alpha_j(t), \qquad \alpha_j(t) = \exp(-\beta t) \tag{1.3}$$

I_i is the input current applied to neuron i. The connection weight between neurons i and j is w_{ij}. In a one-population network, each neuron excites nearby neurons and inhibits distant ones (figure 1.2.) Each time the voltage reaches the threshold from below the neuron fires. The voltage then immediately resets to $v_i = 0$, and a synaptic pulse $\alpha_j(t)$ is sent to all connected neurons.

From the integration of differential equation (1.3), they obtain the spike response form

$$v_i(t,s) = I_i + \eta(t-s) + u_i(t) \tag{1.4}$$

with synaptic input

$$u_i(t) = \sum_{l \in \text{spikes}} \sum_{j \in \text{neurons}} w_{ij}\epsilon(t - t_j^l)$$

where $\epsilon(t)$ is a synaptic filter and $\epsilon(t) = \displaystyle\int_0^t e^{s-t}\alpha(s)ds$.

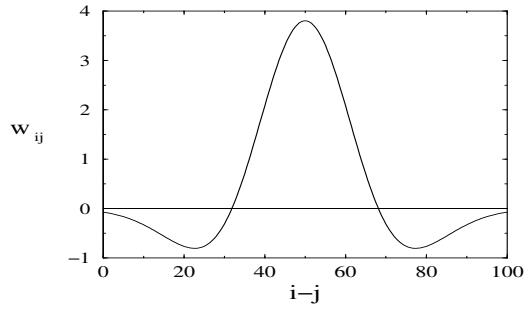

Figure 1.2. Weight function for $i = 50$, $N = 100$.

They also write

$$u_i(t) = \sum_j w_{ij} \int_0^\infty \epsilon(s) A_j(t-s) ds \tag{1.5}$$

where $A_j(t)$ is the "activity" of neuron j and

$$A_j(t) = \sum_l \delta(t - t_j^l)$$

where the sum over l is over all past firing times.

For a large network, input to a neuron is almost constant if the firing times of the neurons are uncorrelated. Then the neural activity is simply the firing rate of a neuron given synaptic input $u(t)$, *i.e.* $A_j(t) = A(t) = f[u(t)]$. For integrate-and-fire neurons, when the threshold is scaled to 1, (see figure 1.3)

$$f[u] = \begin{cases} \dfrac{1}{\ln\left(\frac{u}{u-1}\right)} & u > 1 \\ 0 & u \le 1 \end{cases} \tag{1.6}$$

For a continuous network with infinitely many neurons, the sum in (1.5) becomes an integral.

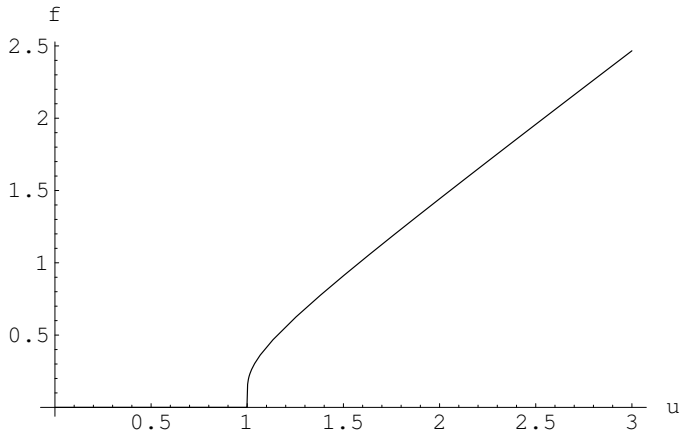

Figure 1.3. Neural activity $f[u]$ for integrate-and-fire networks.

Therefore

$$u(x,t) = \int_\Omega w(x-y) \int_0^\infty \epsilon(s) f[u(y,t-s)] ds dy \tag{1.7}$$

If $\alpha(t) = \delta(t)$, then $\epsilon(s) = e^{-s}$. Differentiating (1.7), yields a population rate model

$$\frac{\partial u(x,t)}{\partial t} = -u(x,t) + \int_\Omega w(x-y) f[u(y,t)] dy \tag{1.8}$$

Laing and Chow [41] compare stationary pulse profiles of the population rate model (1.8) and the network of integrate-and-fire neurons (1.3). Figure (1.4) is a space-time raster plot of the firing times of a stationary pulse from a numerical simulation of a network of 100 integrate-and-fire neurons. Figure (1.5) shows the profiles ($\circ$, $+$, $\times$) of the average firing rate (neural activity) for the integrate-and-fire with three different values of β. The solid line is the profile from the population rate model. It corresponds to the stationary solution of the equilibrium equation (1.9). The agreement is very good especially for small values of β.

$$u(x) = \int_\Omega w(x-y) f[u(y)] dy \tag{1.9}$$

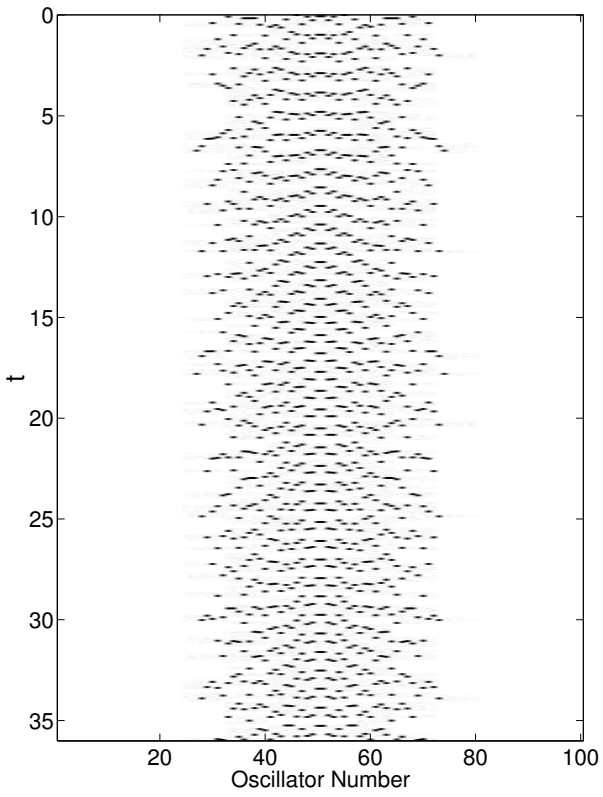

Figure 1.4. Localized persistent state.

Laing and Chow, 2001

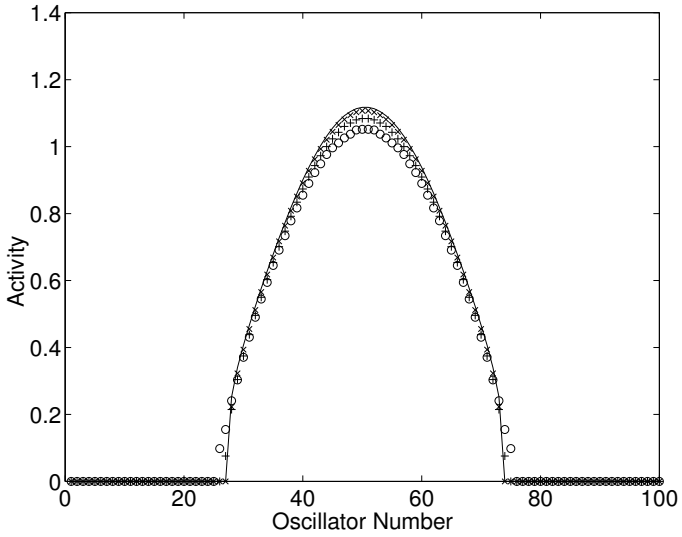

Figure 1.5. Average firing rate.

Laing and Chow, 2001

1.3 Motivation

In [3], Amari approximates the firing rate by the Heaviside gain function. This means that neurons fire above threshold and saturate to their maximum rate immediately. The Heaviside gain function makes the equilibrium equation (1.2) mathematically tractable. However it neglects a very important biophysical fact that though persistent activity is observed at firing rates of around 25 to 60 Hz, neurons can fire much faster and the saturating rate could be as high as 500 Hz. In other words, persistently active neurons fire at rates far below their saturated maximum. To examine this situation, I consider the Amari-like one-population rate model (1.8) using biophysically relevant firing rate functions (1.11).

Model (1.8) is of the same form as Amari's model except it has a different gain function $f[u]$. This can be seen by a change of variables $v = u - u_T$, where u_T is the threshold. This gives

$$\frac{\partial v(x,t)}{\partial t} = -v(x,t) + \int_\Omega w(x-y) f[v(y,t)] dy - u_T \tag{1.10}$$

In this case, $-u_T < 0$ is equivalent to $h < 0$ in Amari's model.

The neural activity (1.6) for integrate-and-fire neurons is the reciprocal of a logarithmic function when the synaptic input u is above threshold. It is difficult to analyze the population rate model (1.8) with this firing rate function. However we can approximate this firing rate function by a piecewise-linear function with the following form (see figure 1.6)

$$g[u] = \begin{cases} \alpha(u - u_T) + \beta & u > u_T \\ 0 & u \leq u_T \end{cases} \tag{1.11}$$

where $\alpha > 0$, $\beta > 0$ and $u_T > 0$ is the threshold.

Pinto and Ermentrout [53] consider a two-population Amari-like model (1.12)-(1.13) and look at the stability of the standing pulses:

$$u_t = -u + \int_{-\infty}^{\infty} w_{ee}(x-y)\Theta[u(y,t) - u_T] dy - \int_{-\infty}^{\infty} w_{ie}(x-y) v(y,t) dy \tag{1.12}$$

$$\tau v_t = -v + \int_{-\infty}^{\infty} w_{ei}(x-y)\Theta[u(y,t) - u_T] \tag{1.13}$$

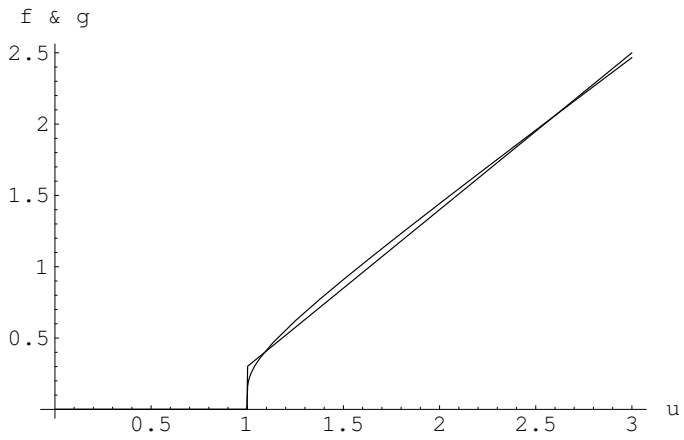

Figure 1.6. Comparing the gain function $f[u]$ for integrate-and-fire networks with a piecewise linear firing rate function $g[u]$ (1.11.) $\alpha = 1.1$, $u_T = 1$, $\beta = 0.3$.

---

where Θ is the Heaviside function. Here u and v represent the average neural activity in a population of excitatory (e) and inhibitory (i) neurons, respectively, at spatial point x and time t. w_{jk} is the coupling weight function representing the strength of connectivity from population j to k ($j, k \in \{e, i\}$). w_{jk} are bounded, nonnegative, even, and normalized. f_j is the firing rate of population j. For fast inhibition, *i.e.* $\tau = 0$, $v = w_{ei} * \Theta$, where the notation $*$ means convolution. Substituting this into (1.12) yields

$$u_t = -u + (w_{ee} - w_{ie} * w_{ei}) * \Theta(u - u_T). \tag{1.14}$$

Hence model (1.12)-(1.13) becomes the Amari model for fast inhibition with linear gain.

In [53], Pinto and Ermentrout use a singular perturbation technique to construct stationary standing single-pulse solutions of the two-population network with a general nonlinear firing rate function. But this construction results in only one standing single-pulse solution.

Pinto and Ermentrout [53] uses the pulse width to study the stability of standing single-pulses of system (1.12)-(1.13). They also analyze the linear stability of standing single-pulses. For the fast inhibition network, their results are consistent with Amari's. For more realistic inhibitory dynamics, *i.e.* $\tau > 0$, they demonstrate the loss of stability to a Hopf bifurcation. In their stability analysis, they adopt the saturating Heaviside gain function.

Coombes *et.al* [12] study the stationary patterns of

$$u(x,t) = \int_{-\infty}^{\infty} w(x-y) \int_{-\infty}^{t} \eta(t-s) f[u(y,s)] ds dy \tag{1.15}$$

When $\eta(t) = e^{-t}$, one can derive the Amari model (1.10) by differentiating both sides of (1.15). Using a sigmoidal firing rate function $f[u] = \dfrac{1}{1+e^{-\beta(u-u_T)}}$ (as $\beta \to \infty$, $f[u] = \Theta(u)$,) they derive an associated fourth order Hamiltonian system. Through this Hamiltonian system, they are able to find standing single-pulses and multiple-pulses. To analyze the stability of standing pulses, they develop an eigenvalue problem for a general firing rate function. But they only solve the eigenvalue problem for the Heaviside gain function case.

Laing and Troy [43, 42] also study the Amari model with a lateral-inhibition type of connection function $w(x)$ that has exactly one zero on $(0,\infty)$. They determine a simple set of assumptions on $w(x)$ and gain function f for which (1.8) has stationary single-pulse solutions [43]. They also investigate the existence and the stability of double-pulse solutions of the same model [42]. They find that double-pulse solutions exist but none of them are stable. However, they find both stable and unstable double-pulse solutions when they replace the $w(x)$ with only one zero on $(0,\infty)$ by an oscillatory $w(x)$ with three positive zeros.

In [43], Laing *et al.* study (1.8) using an oscillatory connection function and a continuous and saturating gain function $f[u] = 2e^{-r(u-u_T)^2}\Theta(u-u_T)$ where $b > 0$, $r > 0$ and threshold $u_T > 0$. In the limiting problem in which $r = 0$, $f[u]$ becomes the Heaviside function. When $r > 0$, their $f[u]$ saturates at 2. In this case, they show the existence of 'multiple-pulse' solutions by using an ordinary differential equation derived from the equilibrium equation of (1.8).

More recently, Rubin and Troy [58] consider Amari's model with the Heaviside gain function and an off-center synaptic architecture as an alternative to recurrent excitation. They show the existence of an unique single-pulse solution. This is different from the lateral inhibition network when two or more single-pulses can coexist. They also give a rigorous linear stability calculation to show that the unique single-pulse is stable.

In the work I mention above [12, 43, 53, 58, 42], the authors either use the Heaviside gain function or a saturating sigmoidal one. Amari's model with a non-saturating gain function has not been investigated. Therefore, I study Amari's model with the nonstaturating piece-wise linear

gain function (1.11). Notice that when $\alpha = 0$, (1.11) becomes the Heaviside gain function provided $\beta = 1$. Hence, my model generalizes Amari's.

Another reason to adopt gain function (1.11) is that I need a function that can support bistability with an inactive state. This piece-wise linear gain function serves this purpose. Both Amari's model and the integrate-and-fire model [41] have bistability with the pulse and the "all-off" resting state both being stable. Bistability is important because the population network is an analogue of working memory. The stable pulse represents the memory. When the network is switched to "all-off" state, the memory is erased.

Laing and Chow [41] have shown numerically that the activity profile of the population rate model (1.8) matches the the activity profile of the integrate-and-fire model (1.3). I ask the following questions about the following population rate model with the non-saturating firing rate function (1.11):

$$\frac{\partial u(x,t)}{\partial t} = -u(x,t) + \int_{\Omega} w(x-y) f[u(y,t)] dy$$

- When does a single-pulse (or a localized excitation) exist?
- When is it stable?
- What is the maximal firing rate?

To answer the above questions, I show the existence of stationary single-pulse solutions of (1.8) first. Then I investigate when a single-pulse exists according to the changes of the slope α in the gain function, the connection parameters a and A and also the threshold u_T. I also map out the parameter range for the maximum firing rates when single-pulses exist. Finally, I derive a criteria to test the stability of single-pulses.

Remark 1.1. *This thesis mainly investigates the existence and the stability of single-pulse solutions. However it does not mean that single-pulse solutions are the only form of solutions of the population rate model (1.8). There could be different forms of solutions, such as double-pulse solutions or even multiple-pulse solutions [31, 42].*

1.4 Outline

The work in this dissertation will explore the population rate model (1.8) with a non-saturating firing rate function in the form of (1.11). In Chapter 2, I show the existence of time-independent single-pulse solutions $u(x)$ of (1.8). I demonstrate the coexistence of two single-pulse solutions. One is "larger" and "wider", and the other is "smaller" and "narrower". I also discover that more than two pulse solutions can coexist. Upon proving the existence of the single-pulse solution, I further investigate in what range of parameters a, A, α and u_T such a solution exists and what the firing rates are.

In chapter 3, I examine the stability of single-pulse solutions by adding a small perturbation to it. After linearizing the dynamical system (1.8) around the stationary single-pulse solution, I derive an eigenvalue problem with two boundary (threshold points) terms which come from the discontinuity in the piece-wise linear firing rate function. Using a combination of analytical and numerical methods, I show that the 'larger" and "wider" single-pulse is stable and the other one is unstable. My stability analysis generalizes Amari's.

During the study of stationary single-pulse solutions of (1.8), other solutions were also discovered. For example, there can also exist double-pulses, which are solutions that have two disjoint open and finite intervals for which the synaptic input $u(x)$ is above threshold. In chapter 4, I give my strategy for constructing a double-pulse solution and discuss future directions.

Chapter 2

Stationary single-pulses

A stationary solution is a time-independent solution of the rate equation

$$\frac{\partial u(x,t)}{\partial t} = -u(x,t) + \int_{-\infty}^{\infty} w(x-y) f[u(y,t)] dy \tag{2.1}$$

The stationary solution of (2.1) satisfies the equilibrium equation (2.2)

$$u(x) = \int_{-\infty}^{\infty} w(x-y) f[u(y)] dy \tag{2.2}$$

where $f[u]$ is a piece-wise linear firing rate function. It is zero below threshold and linear with a positive slope above threshold. When the slope is set to zero, the piece-wise linear function becomes the Heaviside function. Therefore Amari's case is a special case in my study. I choose an exponential form of synaptic coupling function $w(x)$ because its Fourier transform is a polynomial in the transform variable. Then, I am able to apply a Fourier transform to decompose the convolution that appears on the right side of (2.2).

The bulk of the work in this chapter is on single-pulse solutions. The strategy to construct the single-pulse solutions is to convert the integral equation (2.2) into a fourth order ordinary differential equation (ODE). The ODE includes singular terms from the discontinuity in the firing rate function. A stationary single-pulse solution $u(x)$ of the rate equation corresponds to a homoclinic orbit of the ODE. A proof for the existence of a single-pulse then becomes a proof for the existence of a homoclinic orbit. Since the ODE has discontinuities across the threshold points, the ODE on the real line is reduced to three different linear ODEs on three regions separated by threshold points. I then match the solutions of the ODEs at the threshold points by a system of five equations. From this system, I am able to construct different single-pulse solutions. I can also follow solutions as the slope of firing rate function or synaptic coupling is changed in the network using the continuation program AUTO (used within the program XPPAUT [16]). With the help of AUTO and symbolic program packages, I am able to map out the parameter regimes for the existence of the single-pulses

for the firing rate model, which has never been done before.

2.1 Connection and firing rate

The neural network (2.1) has lateral-inhibition type connection $w(x)$ for which excitatory connections dominate for proximate neurons and inhibitory connections dominate at a greater distance. In general, $w(x)$ satisfies the following six properties.

1. $w(x)$ is symmetric, i.e. $w(-x) = w(x)$,
2. $w(x) > 0$ on an interval $(-x_0, x_0)$, and $w(-x_0) = w(x_0) = 0$,
3. $w(x)$ is decreasing on $(0, x_0]$;
4. $w(x) < 0$ on $(-\infty, -x_0) \cup (x_0, \infty)$;
5. $w(x)$ is continuous on $\Re$, and $w(x)$ is integrable on $\Re$;
6. $w(x)$ has a unique minimum x_m on $\Re^+$ such that $x_m > x_0$, and $w(x)$ is strictly increasing on (x_m, ∞).

In order to apply Fourier Transform to the equilibrium equation (2.2), the connection function is specified as:

$$w(x) = Ae^{-a|x|} - e^{-|x|}. \tag{2.3}$$

where a, A are parameters who satisfy condition $A > 1$ and $a > 1$ to guarantee that $w(x)$ has the shape shown in figure 2.1.

For the exponential connection (2.1), $x_0 = \dfrac{\ln A}{a-1}$, $x_m = \dfrac{\ln aA}{a-1}$. The area of the connection function $w(x)$ above the x-axis represents the excitation in the network, and the area below the x-axis shows how much inhibition is in the same network. The total area is $2(\frac{A}{a} - 1)$. The amount of excitation and inhibition depend on the ratio of A and a. If $A > a$, i.e. $2(\frac{A}{a} - 1) > 0$, excitation dominates in the network. If $2(\frac{A}{a} - 1) < 0$, inhibition dominates. In the balanced case, $A = a$, i.e. $2(\frac{A}{a} - 1) = 0$. From the analysis and numerical simulations I have done, to stabilizing the bump state, there cannot be too much excitation in the network. This will be illustrated in section 2.7.4.

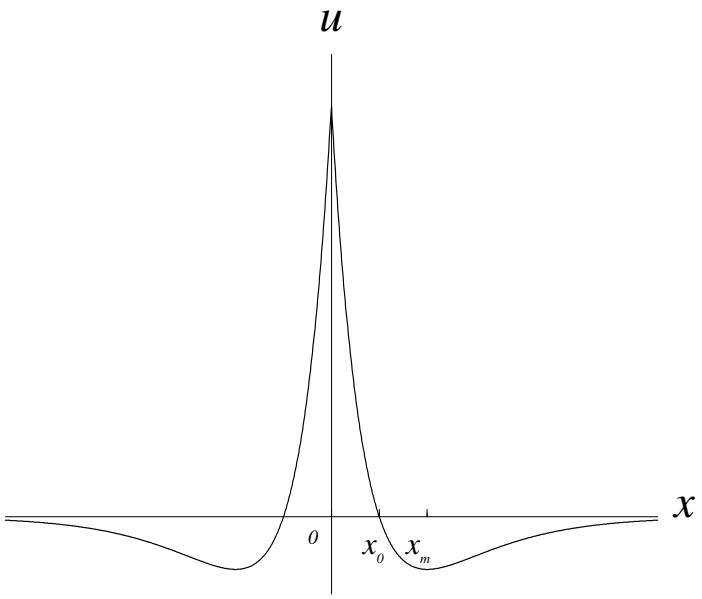

Figure 2.1. Coupling function with $A = 2.8, B = 1, a = 2.6, b = 1$.

The piece-wise linear gain function is of the form:

$$f[u] = \begin{cases} \alpha(u - u_T) + \beta & \text{if } u > u_T \\ 0 & \text{otherwise} \end{cases} \tag{2.4}$$

where u is the synaptic input, $\alpha > 0$ is the slope, $u_T > 0$ is the threshold, and $\beta > 0$ is the jump

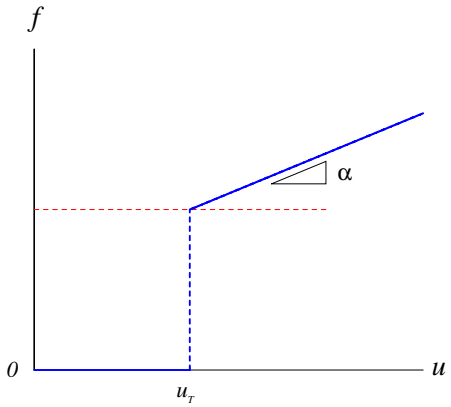

Figure 2.2. Piecewise-linear Gain function.

---

from rest to firing. The gain function can also be written as

$$f[u] = [\alpha(u - u_T) + \beta]\Theta(u - u_T) \tag{2.5}$$

where $\Theta(u - u_T)$ is the Heaviside function such that $\Theta(u - u_T) = \begin{cases} 1 & \text{if } u > u_T \\ 0 & \text{otherwise} \end{cases}$.

Gain function (2.5) does not saturate with a positive slope α. From this point on, I set $\beta = 1$. The gain function (2.5) turns into the Heaviside function when $\alpha = 0$. A different type of network with oscillatory connections and a continuous firing rate has been treated in [43]. Besides a different neuronal connectivity, the other major difference between their work [43] and this work is that their firing rate saturates to a maximum.

2.2 Constant solutions

One may first look into the constant solution of equation (2.2). It is obvious that zero is a solution of (2.2) for any positive threshold u_T, $\beta = 1$, and any values of parameters a, A, α.

Suppose equation (2.2) has a non-trivial constant solution u^0 and $u^0 > u_T$. The integral equation becomes

$$u^0 = \int_{-\infty}^{\infty} w(y) f[u^0] dy$$

i.e.

$$u^0 = f[u^0] \int_{-\infty}^{\infty} w(y) dy$$

With the exponential connection, $\int_{-\infty}^{\infty} w(y)dy = 2(\frac{A}{a} - 1)$, the constant solution satisfies

$$u^0 = 2f[u^0](\frac{A}{a} - 1) \tag{2.6}$$

From (2.6), for the piece-wise linear gain function, one can explicitly state when there are non-trivial

constant solutions as the ratio $\frac{A}{a}$ is either smaller than one or larger than one by the following two propositions

Proposition 2.1. *When $A < a$, for fixed a, A, u_T, $\alpha > 0$, there exists a non-trivial constant solution if both $u_T + 4\alpha u_T < 2$ and $t < 1 - \frac{u_T}{2(1-2\alpha u_T)}$ are true.*

Proof of proposition 2.1: Let $t = \frac{A}{a}$, then $t - 1 < 0$ because $A < a$, and $2\alpha(t-1) - 1 < 0$. The latter inequality gives $t < 1 + \frac{1}{2\alpha}$.

Substituting $f[u] = \alpha(u^0 - u_T) + 1$ into (2.6), the non-trivial constant solution u^0 is

$$u^0 = \frac{2(1-\alpha u_T)(t-1)}{2\alpha(t-1) - 1}$$

A non-trivial constant solution u^0 must satisfies two conditions:

(i) $u^0 > 0$ and (ii) $u^0 > u_T$.

Since $u^0 > 0$, $1 - \alpha u_T$ must be positive. Therefore, $\alpha u_T < 1$.

From condition (ii), the following inequalities must be satisfied,

$$\begin{aligned} \frac{2(1-\alpha u_T)(t-1)}{2\alpha(t-1)-1} &> u_T \\ 2(1-\alpha u_T)(1-t) &> u_T - 2\alpha u_T(t-1) \\ 2(1-t) &> 4\alpha u_T(1-t) + u_T \\ 2(1-2\alpha u_T)(1-t) &> u_T \end{aligned} \tag{2.7}$$

For (2.7) to be true, $1 - 2\alpha u_T > 0$ must be true. Therefore, $2\alpha u_T < 1$, *i.e.*, $4\alpha u_T < 2$.

From (2.7), $t < 1 - \frac{u_T}{2(1-2\alpha u_T)}$

$$1 + \frac{1}{2\alpha} - \left[1 - \frac{u_T}{2(1-2\alpha u_T)}\right] = \frac{1-\alpha u_T}{2\alpha(1-2\alpha u_T)} > 0$$

Since $1 - \frac{u_T}{2(1-2\alpha u_T)}$ must be larger than zero, $u_T + 4\alpha u_T < 2$ must be true. To satisfy both (i) and (ii), both $u_T + 4\alpha u_T < 2$ and $t < 1 - \frac{u_T}{2(1-2\alpha u_T)}$ must be true. $\Diamond$

For the case in which $\frac{A}{a} > 1$, the following proposition is proven.

Proposition 2.2. *For fixed a, A, such that $A > a$, positive α and threshold u_T, there is a non-trivial constant solution of equation (2.2) when either of the following conditions is satisfied:*

(a) $2\alpha u_T < 1$ *and* $\dfrac{1}{2\alpha} + 1 < t < 1 + \dfrac{u_T}{2(2\alpha u_T - 1)}$.

(b) $\alpha u_T > 1$ *and* $1 - \dfrac{u_T}{2(1 - 2\alpha u_T)} < t < \dfrac{1}{2\alpha} + 1$.

Proof of proposition 2.2: t is defined as the ratio of A and a. Then $t - 1 > 0$ since $A > a$.

Substituting $f[u] = \alpha(u^0 - u_T) + 1$ into (2.6) yields

$$u^0 = \frac{2(1 - \alpha u_T)(t - 1)}{2\alpha(t - 1) - 1} \tag{2.8}$$

u^0 must satisfy:

(i) $u^0 > 0$ and (ii) $u^0 > u_T$.

In order for $u^0 > 0$, $(1 - \alpha u_T)$ and $2\alpha(t - 1) - 1$ are either both positive or both negative.

Case 1: Both $(1 - \alpha u_T)$ and $2\alpha(t - 1) - 1$ are positive. Then $\alpha u_T < 1$ and $t > \dfrac{1}{2\alpha} + 1$.

From $u^0 > u_T$, the following inequality is derived

$$2(t - 1)(1 - 2\alpha u_T) > -u_T \tag{2.9}$$

Right hand side of inequality (2.9) is negative. If $(1 - 2\alpha u_T) > 0$, *i.e.*, $2\alpha u_T < 1$, the inequality is satisfied. Hence there exists a constant solution when $2\alpha u_T < 1$ and $t > \dfrac{1}{2\alpha} + 1$.

When $2\alpha u_T - 1 = 0$, inequality (2.9) is satisfied.

If $(1 - 2\alpha u_T) < 0$, (2.9) can be written as

$$t - 1 < \frac{u_T}{2(2\alpha u_T - 1)} \tag{2.10}$$

Hence $t < 1 + \dfrac{u_T}{2(2\alpha u_T - 1)} \left(> 1 + \dfrac{1}{2\alpha}. \right)$ Combining this condition with the conditions derived from $u^0 > 0$, there is a non-trivial constant solution if $2\alpha u_T < 1$ and $\dfrac{1}{2\alpha} + 1 < t < 1 + \dfrac{u_T}{2(2\alpha u_T - 1)}$.

Case 2: Both $(1 - \alpha u_T)$ and $2\alpha(t - 1) - 1$ are negative. Then $\alpha u_T > 1$ and $t < \dfrac{1}{2\alpha} + 1$.

From $u^0 > u_T$, the following inequality is derived

$$2(t - 1)(1 - 2\alpha u_T) < -u_T \tag{2.11}$$

$(1 - 2\alpha u_T)$ is always negative because $\alpha u_T > 1$.

(2.11) is satisfied if $t > 1 - \dfrac{u_T}{2(1-2\alpha u_T)}$. One can also show that $1 - \dfrac{u_T}{2(1-2\alpha u_T)} < 1 + \dfrac{1}{2\alpha}$ as long as $\alpha u_T > 1$. Combining this with the two conditions derived from $u^0 > 0$, there exists a constant solution when $\alpha u_T > 1$ and $1 - \dfrac{u_T}{2(1-2\alpha u_T)} < t < \dfrac{1}{2\alpha} + 1$. $\Diamond$

The non-trivial constant solution is stable. It is bistable with the stable zero constant solution.

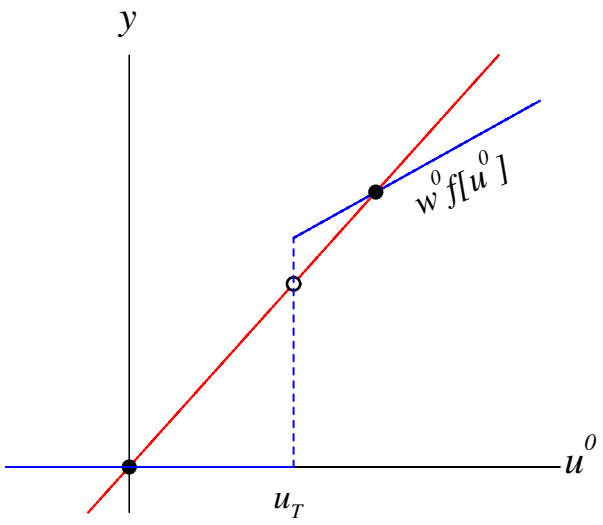

Figure 2.3. Bistability of constant solutions. The solid circles are the two stable constant solutions. w^0 is the integral of $w(x)$ on its domain .

2.3 Single-pulse solutions

The main goal to study equation (2.2) is to find a stationary single-pulse solution that satisfies the following:

Definition 2.1. Single-pulse solution*:*

$$u(x) \begin{cases} > u_T & \text{if } x \in (-x_T, x_T),\ x_T > 0 \\ = u_T & \text{if } x = -x_T, x = x_T \\ < u_T & \text{otherwise} \end{cases}$$

such that $(u, u', u'', u''') \to (0,0,0,0)$ *exponentially fast as* $x \to \pm\infty$ *and* $u, u' \in L^1(R)$. *Here* u, u' *are bounded and continuous on* $\Re$. u'', u''' *and* u'''' *are continuous everywhere for* $x \in \Re$ *except* $x = \pm x_T$ *and bounded everywhere on* $\Re$, *and.* $u(x)$ *is symmetric with* $u''(0) < 0$; $u(0)$ *is the maximum between* $-x_T$ *and* x_T *(* figure2.4.)

I also observed a pulse where $u''(0)$ has opposite sign, *i.e.* $u''(0) > 0$, which implies $u(0)$ is no longer the maximum of the pulse. I call this solution a $dimple - pulse$. I also observe that the threshold u_T is the controlling factor for the transition between a single-pulse and a dimple-pulse. For fixed parameters a, A, α, there is a transition threshold. Above the transition threshold, there are single-pulses. If u_T is lower than the transition threshold, there exist dimple-pulses, instead of single-pulses. Examples are shown in later sections.

I find that there exists a single-pulse solution not only when $A > a$, but also when $A \leq a$. Before I demonstrate the strategy of finding the single-pulse solution, I estimate a broad range on which there is no single-pulse solution merely by studying the integral equation (2.2).

Theorem 2.1. *For fixed* a, A *and* $\beta = 1$, *there is no single-pulse solution if both* $\alpha < \dfrac{a}{2A}$ *and* $u_T > \dfrac{2A}{a}$ *are true.*

Proof of theorem 2.1: Substituting the exponential connection function (2.3) and firing rate function (2.5) into the integral equation (2.2),

$$u(x) = \int_{\infty}^{\infty} (Ae^{-a|x-y|} - e^{-|x-y|})[\alpha(u(y) - u_T) + 1]\Theta(u - u_T)dy$$

Suppose there is a single-pulse solution as defined above when both $\alpha < \dfrac{a}{2A}$ and $u_T > \dfrac{2A}{a}$ are satisfied. Then

$$\begin{aligned} u(0) &= \int_{-\infty}^{\infty} (Ae^{-a|y|} - e^{-|y|})[\alpha(u(y) - u_T) + 1]\Theta(u - u_T)dy \\ &= \int_{-x_T}^{x_T} (Ae^{-a|y|} - e^{-|y|})[\alpha(u(y) - u_T) + 1]dy \\ &\leq \int_{-x_T}^{x_T} Ae^{-a|y|}[\alpha(u(y) - u_T) + 1]dy \\ &= \int_{-x_T}^{x_T} Ae^{-a|y|}\alpha u(y)dy + \int_{-x_T}^{x_T} Ae^{-a|y|}(1 - \alpha u_T)dy \end{aligned} \tag{2.12}$$

Let $I := [-x_T, x_T]$. $u(x)$ is continuous on I. $Ae^{-a|y|}$ is integrable on I and such that $Ae^{-a|y|} \geq 0$ for all $x \in I$. By Mean Value Theorem for Integrals, $\exists\ c^0 \in I$ s. t.

$$\begin{aligned} (2.12) \quad &= \alpha u(c^0) \int_{-x_T}^{x_T} Ae^{-a|y|}dy + (1-\alpha u_T) \int_{-x_T}^{x_T} Ae^{-a|y|}dy \\ &\leq \alpha u(c^0) \int_{-\infty}^{\infty} Ae^{-a|y|}dy + (1-\alpha u_T) \int_{-\infty}^{\infty} Ae^{-a|y|}dy \\ &= \alpha P u(c^0) + (1-\alpha u_T)P \qquad (2.13) \end{aligned}$$

where $P = \int_{-\infty}^{\infty} Ae^{-a|y|}dy = \dfrac{2A}{a}$.

If $\alpha P < 1$ and $(1-\alpha u_T) \leq 0$ are both true, $u(0) < u(c^0)$, $c \in I$, which can not be true because $u(0)$ is the maximum of $u(x)$ on $\Re$.

From $\alpha P < 1$, $\alpha < \dfrac{a}{2A}$. From $(1-\alpha u_T) \leq 0$, $u_T \geq \dfrac{1}{\alpha}$, *i.e.*, $u_T \geq \dfrac{1}{\alpha} > \dfrac{1}{\frac{a}{2A}} = \dfrac{2A}{a}$. Therefore, there is no single-pulse when both $\alpha < \dfrac{a}{2A}$ and $u_T > \dfrac{2A}{a}$ are both true. $\Diamond$

Theorem 2.1 is useful in indicating where a pulse cannot exist but it does not say how to find a single-pulse.

2.4 Strategy to construct a single-pulse solution

The general approach to study the integral equation (2.2) is to derive an associated differential equation whose solutions are also solutions of the integral equation (2.2). Then I study the associated differential equation.

I derive the differential equation by using Fourier transform

$$F[g(x)] = \int_{-\infty}^{\infty} g(x)e^{isx}dx$$

where $g \in L^1(R)$ and $s \in R$

and inverse Fourier transform

$$g(x) = \frac{1}{2\pi} \int_{-\infty}^{\infty} F[g(x)]e^{-isx}ds$$

Under all conditions of $u(x)$ of equation (2.2), an application of Fourier transform to (2.2) is

well-defined and turns the convolution into point-wise product

$$F[u] = F[w]F[f[u]]. \tag{2.14}$$

Computing $F[w]$, (2.14) gives

$$F[u] = \frac{(2aA + 2as^2A - 2a^2 - 2s^2)F[f]}{(a^2 + a^2s^2 + s^2 + s^4)}. \tag{2.15}$$

Multiply both sides of (2.15) by the denominator of the right hand side and use the linear property of the Fourier Transform and the identities

$$F[u''] = -s^2F[u]; F[u''''] = s^4F[u]$$

to obtain

$$F[u'''' - (a^2 + 1)u'' + a^2u] = F[2(aA - a^2)f] + 2(aA - 1)F[s^2f] \tag{2.16}$$

By the definitions of $u(x)$ and $f(u)$,

$$F[u'''' - (a^2 + 1)u'' + a^2u]$$

and

$$F[2(aA - a^2)f]$$

are in $L^1(R)$.

Integrate $F[s^2f]$ by parts to yield

$$\begin{aligned}
&F[s^2f] \\
&= \int_{-\infty}^{\infty} s^2e^{isx}f[u(x)]dx \\
&= \int_{-x_T}^{x_T} s^2e^{isx}f[u(x)]dx \\
&= f[u(x_T)](-ise^{isx_T} + ise^{-isx_T}) + f'[u(x_T^-)]u'(x_T)(e^{isx_T} + e^{-isx_T}) - \int_{-x_T}^{x_T} e^{isx}\frac{d^2f[u(x)]}{dx^2}dx
\end{aligned}$$

note that $f[u(x)] \equiv 0$ outside of $(-x_T, x_T)$. Obviously, $F[s^2 f] \in L^1(R)$.

Applying Inverse Fourier Transformation, (2.16) gives a fourth order ordinary differential equation

$$u'''' - (a^2+1)u'' + a^2 u = 2(aA - a^2)f[u(x)] + \\ 2(aA-1)\left\{ f[u(x_T)]\Delta'(x) + f'[u(x_T^-)]u'(x_T)\Delta(x) - \frac{d^2 f[u(x)]}{dx^2} \right\} \tag{2.17}$$

where

$$\Delta'(x) = \delta'(x - x_T) + \delta'(x + x_T)$$

$$\Delta(x) = \delta(x - x_T) + \delta(x + x_T)$$

Here $\delta(x)$ and $\delta'(x)$ are defined as

$$\delta(x) = \int_{-\infty}^{\infty} e^{isx} dx, \qquad \delta'(x) = is \int_{-\infty}^{\infty} e^{isx} dx \qquad \text{respectively.}$$

If $u(x)$ is a solution of (2.17) that satisfies all its properties as defined, (2.14)-(2.16) all hold, then it follows that $u(x)$ is also a solution of (2.2). So it suffices to find a single-pulse solution of (2.17).

To show the existence of a single-pulse solution of (2.17), I construct such a solution (figure(2.4)) by decomposing ODE (2.17) into two linear differential equations (2.18) and (2.19).

$$u'''' - (a^2+1)u'' + a^2 u = 2 \quad a(A-a)f(u) - 2(aA-1)\tfrac{d^2 f(u)}{dx^2} \quad \text{if } u > u_T \text{ (region I)} \tag{2.18}$$

$$u'''' - (a^2+1)u'' + a^2 u = 0 \qquad \text{if } u < u_T \text{ (region II)} \tag{2.19}$$

The solution of (2.18) on region I, the solution of (2.19) on region II and the solution of (2.19) on region III are called $u_{\mathrm{I}}(x)$, $u_{\mathrm{II}}(x)$ and $u_{\mathrm{III}}(x)$, respectively. Then $u_{\mathrm{I}}(x)$, $u_{\mathrm{II}}(x)$ and $u_{\mathrm{III}}(x)$ must be connected together at $-x_T$ and x_T to get a continuous and smooth $u(x)$ on $\Re$. To do so, I match $u_{\mathrm{I}}(x)$ and $u_{\mathrm{II}}(x)$ at x_T by the five matching conditions (2.20)-(2.24). Since $u(x)$ is symmetric,

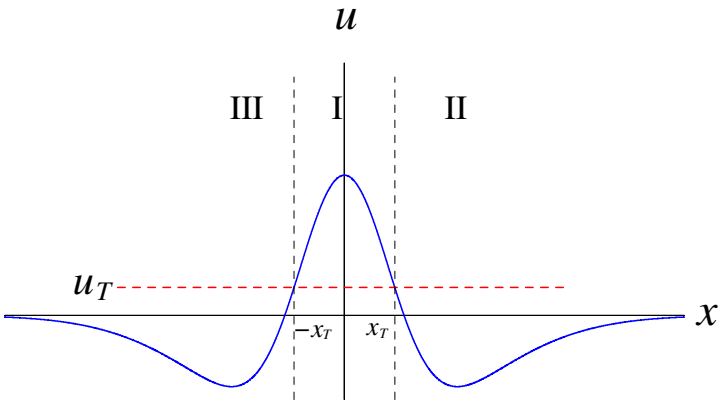

Figure 2.4. Single-pulse solution.

---

similar matching conditions apply to $u_{\mathrm{I}}(x)$ and $u_{\mathrm{III}}(x)$ at $-x_T$:

$$u_{\mathrm{I}}(x_T) = u_T \tag{2.20}$$

$$u_{\mathrm{II}}(x_T) = u_T \tag{2.21}$$

$$u'_{\mathrm{I}}(x_T) = u'_{\mathrm{II}}(x_T) \tag{2.22}$$

$$u''_{\mathrm{I}}(x_T) = u''_{\mathrm{II}}(x_T) - 2(aA-1)f(u(x_T)) \tag{2.23}$$

$$u'''_{\mathrm{I}}(x_T) = u'''_{\mathrm{II}}(x_T) - 2(aA-1)f'(u(x_T))u'(x_T) \tag{2.24}$$

(2.20)-(2.22) are obvious by the continuity of $u(x)$ and $u'(x)$. To get (2.23), integrate ODE (2.17) on a small neighborhood of x_T. Integrating ODE (2.17) twice, first with respect to x, second over a small neighborhood of x_T, (2.24) is obtained. Notice that $u''(x)$ and $u'''(x)$ are discontinuous at x_T, *i.e.* there are jumps in $u''(x_T)$ and $u'''(x_T)$.

ODE (2.19) in region II is rather simple. Only the family of solutions

$$u_{\mathrm{II}}(x) = Ee^{-ax} + Fe^{-x} \qquad E, F \in R \tag{2.25}$$

satisfies the definition of single-pulse solution. Note that in region III, by symmetry,

$$u_{\mathrm{III}}(x) = Ee^{ax} + Fe^{x} \qquad E, F \in R \tag{2.26}$$

Substituting $f[u(x)] = \alpha(u - u_T) + 1$ on (x_T, x_T) and $\frac{d^2 f[u(x)]}{dx^2} = \alpha u''(x)$, ODE (2.18) becomes

$$u'''' - (a^2 + 1 - 2\alpha(aA - 1))u'' + (a^2 - 2a\alpha(A - a))u = 2a(A - a)(1 - \alpha u_T) \tag{2.27}$$

The eigenvalues of ODE (2.27) are ω_1, $-\omega_1$, ω_2, $-\omega_2$ such that

$$\begin{aligned} \omega_1^2 &= R + S \\ \omega_2^2 &= R - S \end{aligned}$$

where

$$\Delta = (a^2 + 1 - 2\alpha(aA - 1))^2 - 4(a^2 - 2a\alpha(A - a))$$

$$R = \frac{(a^2 + 1 - 2\alpha(aA - 1))}{2}$$

$$S = \frac{\sqrt{\Delta}}{2} = \frac{\sqrt{(a^2 + 1 - 2\alpha(aA - 1))^2 - 4(a^2 - 2a\alpha(A - a))}}{2}$$

Imposing symmetry and $u'(0) = 0$, the general solution of ODE(2.27) can be written in the form

$$u_{\mathrm{I}}(x) = C(e^{\omega_1 x} + e^{-\omega_1 x}) + D(e^{\omega_2 x} + e^{-\omega_2 x}) + \frac{2(A - a)(\beta - \alpha u_T)}{a - 2\alpha(A - a)} \tag{2.28}$$

for $x \in (-x_T, x_T)$. $x_T \in R$. $C, D \in \mathbf{C}$. C, D could be real or complex, but overall $u_{\mathrm{I}}(x)$ must be real.

One of my goals is to find out how the shape of the single-pulse changes in terms of width and height according to the connectivity and gain. For simplicity, I call x_T the width of a pulse even though it is actually the half width. The height of a single-pulse is $u(0)$.

2.5 Amari case ($\alpha = 0$)

Amari generates a condition on which single-pulse solutions exist for the same network with a general Gaussian like connection [3]. In this section, I will reevaluate the Amari case ($\alpha = 0$) for the exponential connection function, and I will show a quantitative condition of the existence of the single-pulse solution on the parameters A and a. When $\alpha = 0$, the gain function becomes the Heaviside function $\Theta(u)$. The term $2(aA-1)\dfrac{d^2 f[u]}{dx^2}$ is no longer in ODE (2.18). The two ODEs in region I and region II are simplified as follows:

$$u'''' - (a^2+1)u'' + a^2 u = \quad 2a(A-a)f[u] \quad \text{if } u > u_T \text{ (region I)} \tag{2.29}$$

$$u'''' - (a^2+1)u'' + a^2 u = \quad 0 \quad \text{if } u < u_T \text{ (region II)} \tag{2.30}$$

The solutions for (2.29) and (2.30) are

$$u_{\mathrm{I}}(x) = C(e^{ax} + e^{-ax}) + D(e^{x} + e^{-x}) + \frac{2(A-a)(\beta - \alpha u_T)}{a - 2\alpha(A-a)} \tag{2.31}$$

$$u_{\mathrm{II}}(x) = Ee^{-ax} + Fe^{-x} \tag{2.32}$$

respectively. Applying condition (2.20)-(2.24), I obtain a five equation system

$$Ee^{-ax_T} + Fe^{-x_T} = u_T \tag{2.33}$$

$$C(e^{ax_T} + e^{-ax_T}) + D(e^{x_T} + e^{-x_T}) + \frac{2(A-a)\beta}{a} = u_T \tag{2.34}$$

$$aC(e^{ax_T} - e^{-ax_T}) + D(e^{x_T} - e^{-x_T}) = -aEe^{-ax_T} - Fe^{-x_T} \tag{2.35}$$

$$a^2C(e^{ax_T} + e^{-ax_T}) + D(e^{x_T} + e^{-x_T}) = a^2Ee^{-ax_T} + Fe^{-x_T} - 2(aA-1)\beta \tag{2.36}$$

$$a^3C(e^{ax_T} - e^{-ax_T}) + D(e^{x_T} - e^{-x_T}) = -a^3Ee^{-ax_T} - Fe^{-x_T} \tag{2.37}$$

Set the left-hand side of (2.33) and (2.34) equal to each other. Solve four algebraic equations for C, D, E, F in terms of x_T

$$\begin{cases} C = -\dfrac{A}{a}e^{-ax_T} \\ D = e^{-x_T} \\ E = \dfrac{A}{a}(e^{ax_T} - e^{-ax_T}) \\ F = -(e^{x_T} - e^{-x_T}) \end{cases}$$

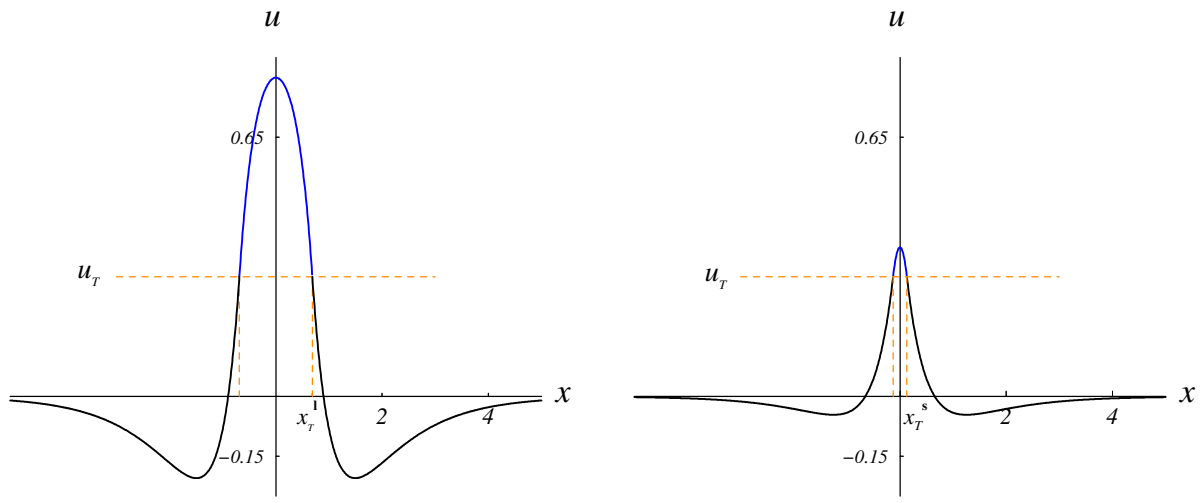

Figure 2.5. Large single-pulse **l** and small single-pulse **s**. $A = 2.8$, $a = 2.6$, $\alpha = 0$, $u_T = 0.3$. (Left) Single-pulse **l**: $x_T^{\mathbf{l}} = 0.68633$, height=$u(0) = 0.79991$. (Right) Single-pulse **s**: $x_T^{\mathbf{s}} = 0.12985$, height=$u(0) = 0.37358$.

Proposition 2.3. *There are two pulse solutions when* $u_T \leq \int_0^{\frac{\ln A}{a-1}} w(x)dx$ *and* $(\frac{A}{a} - 1) < u_T$ *for* $A > a$ *and* $0 \leq u_T$ *for* $A < a$.

Proof of proposition 2.3 Substitute E, F into (2.33) or C, D into (2.34), I have the existence function $\Phi(x)$

$$\Phi(x) = \frac{A}{a}(1 - e^{-2ax}) - (1 - e^{-2x}) \tag{2.38}$$

$\Phi(x_T) = u_T$ must be satisfied for a single-pulse. I can represent this in a figure 2.6 and 2.7. If $\Phi(x)$ crosses the line $y = u_T$ twice, there are two single-pulse solutions (figure 2.6 ($A < a$) and 2.7 ($A > a$)). Since

$$\lim_{x\to\infty} \Phi(x) = \frac{A}{a} - 1 = \begin{cases} < 0 & \text{if } A < a \quad \text{figure 2.6} \\ \geq 0 & \text{if } A \geq a \quad \text{figure 2.7} \end{cases}$$

the lower limit of the threshold u_T that supports two pulses is 0 if$A < a$; the lower limit of the threshold u_T that guarantees two pulses is $\frac{A}{a} - 1$ when $A > a$.

The upper limit on threshold u_T that supports two pulse solutions is the maximum of $\Phi(x)$. Solving

$$\frac{d\Phi}{dx} = Ae^{-2ax} - 2e^{-2x} = 0$$

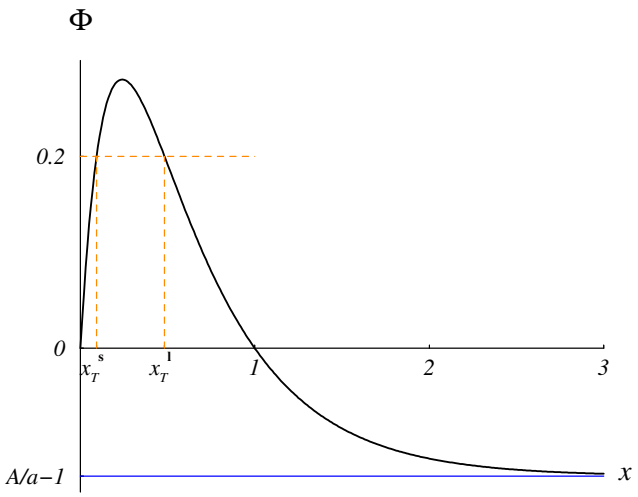

Figure 2.6. Existence function $\Phi(x)$ when $A < a$. $\alpha = 0$, $A = 2.6$, $a = 3$. $\lim_{x\to\infty} \Phi(x) = \dfrac{A}{a} - 1 = -0.1333$. $\Phi(x)$ gives the range of threshold u_T that supports two single-pulse solutions. Example: At $u_T = 0.2$, $\Phi(x)$ shows that we have a single-pulse solution **l** (**l**=large) which is wider and has width $x_T^{\mathbf{l}}$; the second single-pulse solution is narrower and has width $x_T^{\mathbf{s}}$ (**s**=small) .

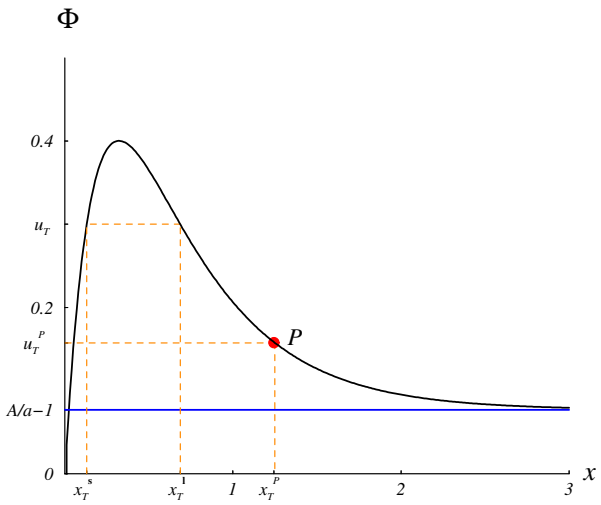

Figure 2.7. Existence function $\Phi(x)$ when $A > a$. $\alpha = 0$, $A = 2.8$, $a = 2.6$, $\lim_{x\to\infty} \Phi(x) = \dfrac{A}{a} - 1 = 0.07692$. Example: At $u_T = 0.3$, $\Phi(x)$ shows that there is a single-pulse solution **l** (**l**=large) which is wider and has width $x_T^{\mathbf{l}} = 0.68633$; the second single-pulse solution is narrower and has width $x_T^{\mathbf{s}} = 0.12985$ (**s**=small). P is the transition point where single-pulse **l** changes into a dimple-pulse **d**. The transition threshold u_T^P=0.15672. $x_T^P = 1.24379$.

---

finds $x = \dfrac{\ln A}{2(a-1)}$. Thus Φ reaches its maximum at

$$\Phi(x) = \frac{A}{a}(1 - e^{-\frac{a \ln A}{a-1}}) - (1 - e^{-\frac{\ln A}{a-1}}) = \int_0^{\frac{\ln A}{a-1}} w(x)dx \tag{2.39}$$

This proves the proposition. $\Diamond$

Proposition 2.3 does not immediately imply that there are two-single pulses. This is because sometimes for a small threshold there can be a dimple-pulse. For example, in figure 2.7, P is the transition point where the single-pulse **l** transforms into a dimple-pulse **d**. At threshold u_T^P, there is a pulse solution $u(x)$ such that $u''(0) = 0$. When the threshold is between $\frac{A}{a} - 1 \geq 0$ and u_T^P, the large single-pulse **l** becomes a dimple-pulse **d**, but small single-pulses remain as single-pulses. The transition point P is identified numerically using AUTO. I continue $u''(0)$ with a initial value of $u''(0)$ calculated from a known pulse solution while changing threshold u_T. The threshold value where $u''(x)$ crosses zero is the transition point P.

2.6 Eigenvalue structure

For the case of $\alpha \neq 0$, once a, and A are fixed, the eigenvalues $\omega_1, -\omega_1, \omega_2, -\omega_2$ change only while α changes. All possible eigenvalue structures must be discussed. The following tables enumerate all the possible forms of ω_1 and ω_2.

	E1	E2	E3	E4	E5	E6
	$\triangle > 0$ $R < 0 < \lvert R\rvert$ $\lvert R\rvert < S$	$\triangle > 0$ $0 < S < R$	$\triangle > 0$ $R < 0 < S$ $S < \lvert R\rvert$	$\triangle = 0$	$\triangle < 0$	$\Delta > 0$ $R < 0 < \lvert R\rvert$ $\lvert R\rvert = S$
ω_1	real	real	imaginary	$= \omega_2$	$= \omega_2^*$, complex	$= \sqrt{2R}$
ω_2	imaginary	real	imaginary	$= \omega_1$	$= \omega_1^*$, complex	0
α	(α_4, ∞)	$(-\infty, \alpha_1)$	(α_3, α_4)	α_1, α_3	(α_1, α_3)	α_4

Table 2.1. Eigenvalue chart when $A > a$.

	E1	E2	E3	E4	E5	E6
	$\triangle > 0$ $0 < R < S$	$\triangle > 0$ $0 < S < R$	$\triangle > 0$ $R < 0 < S < \lvert R\rvert$	$\triangle = 0$	$\triangle < 0$	$\Delta > 0$ $0 < R = S$
ω_1	real	real	imaginary	$= \omega_2$	$= \omega_2^*$, complex	$= \sqrt{2R}$
ω_2	imaginary	real	imaginary	$= \omega_1$	$= \omega_1^*$, complex	0
α	$(-\infty, \alpha_0)$	(α_0, α_1)	(α_3, ∞)	α_1, α_3	(α_1, α_3)	α_0

Table 2.2. Eigenvalue chart when $A < a$.

Here α_0, α_1, α_2, α_3, α_4 are in the order shown in figure (2.8). α_1 and α_3 are given by solving

	E1	E2	E3	E4	E5	E6
	$\triangle > 0$ $0 < R < S$	$\triangle > 0$ $0 < S < R$	$\triangle > 0$ $R < 0 < S < \lvert R \rvert$	$\triangle = 0$	$\triangle < 0$	$R = S$
ω_1	$\emptyset$	real	imaginary	$= \omega_2$	$= \omega_2^*$, complex	$\emptyset$
ω_1		real	imaginary	$= \omega_2$	$= \omega_1^*$, complex	
α		$(-\infty, \alpha_1)$	(α_3, ∞)	α_1, α_3	(α_1, α_3)	

Table 2.3. Eigenvalue chart when $A = a$.

equation

$$\Delta = (a^2 + 1 - 2\alpha(aA - 1))^2 - 4(a^2 - 2a\alpha(A - a)) \tag{2.40}$$

for α. When $R > 0$ and $\Delta > 0$, solving $R - S = 0$ gives $\alpha_0 = \dfrac{a}{2(A-a)}$. When $R < 0$ and $\Delta > 0$, solving $R + S = 0$ gives $\alpha_4 = \dfrac{a}{2(A-a)}$.

Remark 2.1. *Although both α_0 and α_4 have the same expression, they do not co-exist. When $A < a$, $\alpha_0 = \dfrac{a}{2(A-a)} < 0$ and when $A > a$, $\alpha_4 = \dfrac{a}{2(A-a)} > 0$.*

There are three common cases: both eigenvalues $\omega_{1,2}$ are real, both are complex and both are imaginary. α_1 and α_3 are decided by Δ, which is a quadratic form in α, given by

$$\Delta = 4(aA - 1)^2\alpha^2 + [4(aA - 1)(a^2 + 1) + 8a(A - a)]\alpha + (a^2 - 1)^2$$

I will start from the case in which both ω_1 and ω_2 are real.

Even though from table 2.1 to 2.3, $\alpha < 0$ are taken into account for possible eigenvalue structures, I only consider the case of firing rate with a positive slope, *i.e.*, $\alpha > 0$. $\alpha = 0$ with the general coupling weight function is fully treated in [3] and reevaluated in section 2.5.

Remark 2.2. *For all values of ω_1 and ω_2, $u_{\mathrm{II}}(x)$ and $u_{\mathrm{III}}(x)$ always have the form (2.25) and (2.26) respectively.*

2.7 Real ω_1 and ω_2

2.7.1 Construction of single-pulse solutions

When $\alpha \in (0, \alpha_1)$, both Δ and R are positive, so ω_1 and ω_2 are real (figure 2.9.) $u_{\mathrm{I}}(x)$ and

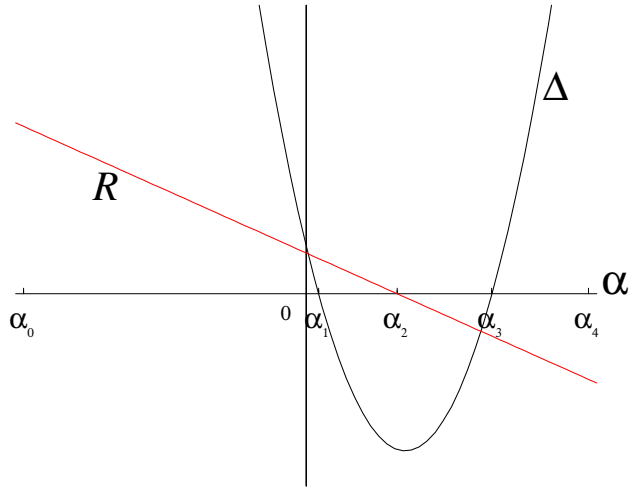

Figure 2.8. Plots of Δ and R.

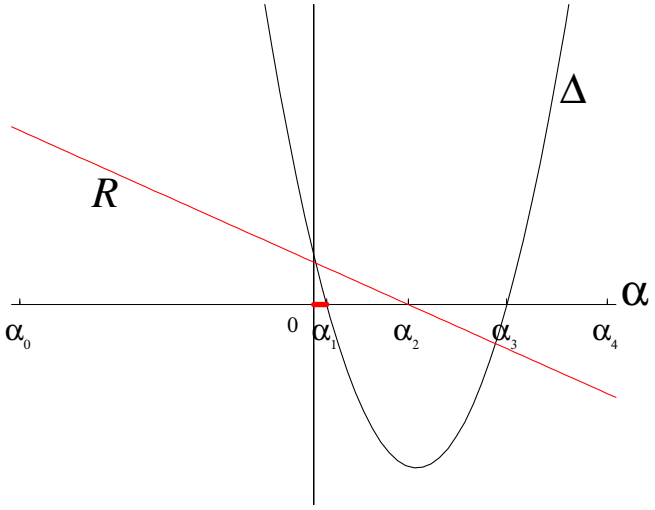

Figure 2.9. Real eigenvalue range (the segment in red color on the x-axis).

$u_{\mathrm{II}}(x)$ have the following form.

$$u_{\mathrm{I}}(x) = C(e^{\omega_1 x} + e^{-\omega_1 x}) + D(e^{\omega_2 x} + e^{-\omega_2 x}) + \frac{2(A-a)(\beta - \alpha u_T)}{a - 2\alpha(A-a)} \tag{2.41}$$

$$u_{\mathrm{II}}(x) = Ee^{-ax} + Fe^{-x} \tag{2.42}$$

When eigenvalues ω_1 and ω_2 are real, C and D must be real to have real $u_{\mathrm{I}}(x)$. Applying $u_{\mathrm{I}}(x)$ and $u_{\mathrm{II}}(x)$ in the forms of (2.41) and (2.42), to the matching condition (2.20)-(2.24).

$$Ee^{-ax_T} + Fe^{-x_T} = u_T \tag{2.43}$$

$$C(e^{\omega_1 x_T} + e^{-\omega_1 x_T}) + D(e^{\omega_2 x_T} + e^{-\omega_2 x_T}) + \frac{2(A-a)(\beta - \alpha u_T)}{a - 2\alpha(A-a)} = u_T \tag{2.44}$$

$$\omega_1 C(e^{\omega_1 x_T} - e^{-\omega_1 x_T}) + \omega_2 D(e^{\omega_2 x_T} - e^{-\omega_2 x_T}) = -aEe^{-ax_T} - Fe^{-x_T} \tag{2.45}$$

$$\omega_1^2 C(e^{\omega_1 x_T} + e^{-\omega_1 x_T}) + \omega_2^2 D(e^{\omega_2 x_T} + e^{-\omega_2 x_T}) = a^2 Ee^{-ax_T} + Fe^{-x_T} - 2(aA-1)\beta \tag{2.46}$$

$$\omega_1^3 C(e^{\omega_1 x_T} - e^{-\omega_1 x_T}) + \omega_2^3 D(e^{\omega_2 x_T} - e^{-\omega_2 x_T}) = (-a^3 + 2a\alpha(aA-1))Ee^{-ax_T} + (-1 + 2\alpha(aA-1))Fe^{-x_T} \tag{2.47}$$

For appropriate parameter values, using Mathematica [67], I am able to solve this five equation system from (2.43) to (2.47) for five unknowns C, D, E, F and x_T, which give me the explicit formula of $u_{\rm I}(x)$ and $u_{\rm II}(x)$. To get a whole picture of a single-pulse, I plot $u_{\rm I}(x)$ on $(-x_T, x_T)$, $u_{\rm II}(x)$ on (x_T, ∞) and $u_{\rm III}(x)$ on $(-\infty, x_T)$. Figure (2.10) shows a graph of single-pulse obtained in this fashion by Mathematica [67] when the parameter set $(a, A, \alpha, \beta, u_T)$ is $(2.6, 2.8, 0.15, 1, 0.400273)$. The solution is $(C, D, E, F, x_T) = (-0.8532, 1.16865, 2.94108, -0.89571, 0.41902)$. The height $u_{\rm I}(0)$ of the pulse is 0.77892. Its width is $x_T^{\rm l} = 0.41902$. Another solution of system (2.43)-(2.47) given by Mathematica [67] shows that there exists a small (in amplitude) and narrow single-pulse solution (right panel of figure 2.11) for the same set of parameters. The height and the width of this pulse are $u_{\rm I}(0) = 0.6123$ and $x_T^{\rm s} = 0.2582$ respectively.

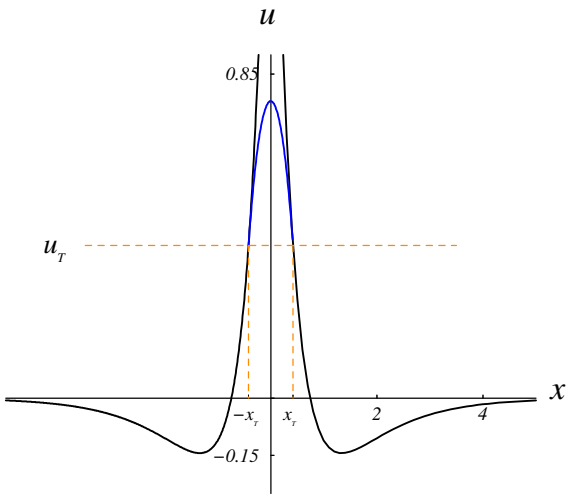

Figure 2.10. Construction of large single-pulse **l**.

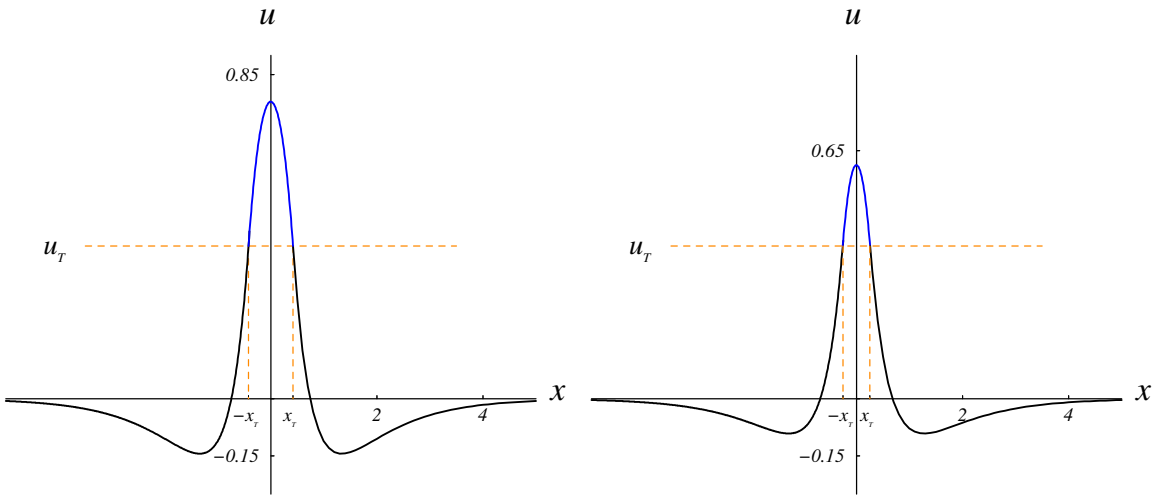

Figure 2.11. Large single-pulse **l** and small single-pulse **s**. $A = 2.8$, $a = 2.6$, $\alpha = 0.15$, $u_T = 0.3$. (Left) Single-pulse **l**: $x_T^{\mathbf{l}} = 0.41092$, height=$u(0) = 0.77892$. (Right) Single-pulse **s**: $x_T^{\mathbf{s}} = 0.2582$, height=$u(0) = 0.6123$.

2.7.2 Existence function $\Phi(x)$ for real ω_1 and ω_2

Eliminate the threshold u_T, which only appears in (2.43) and (2.44) from system (2.43)-(2.47) to get an equivalent four-equation system

$$\begin{aligned}
C(e^{\omega_1 x_T} + e^{-\omega_1 x_T}) + D(e^{\omega_2 x_T} + e^{-\omega_2 x_T}) + \frac{2(A-a)\beta}{a - 2\alpha(A-a)} &= \\
\frac{a}{a - 2\alpha(A-a)}(Ee^{-ax_T} + Fe^{-x_T}) & \quad (2.48)\\
\omega_1 C(e^{\omega_1 x_T} - e^{-\omega_1 x_T}) + \omega_2 D(e^{\omega_2 x_T} - e^{-\omega_2 x_T}) &= -aEe^{-ax_T} - Fe^{-x_T} \quad (2.49)\\
\omega_1^2 C(e^{\omega_1 x_T} + e^{-\omega_1 x_T}) + \omega_2^2 D(e^{\omega_2 x_T} + e^{-\omega_2 x_T}) &= a^2 Ee^{-ax_T} + Fe^{-x_T} \\
& \quad -2(aA-1)\beta \quad (2.50)\\
\omega_1^3 C(e^{\omega_1 x_T} - e^{-\omega_1 x_T}) + \omega_2^3 D(e^{\omega_2 x_T} - e^{-\omega_2 x_T}) &= (-a^3 + 2a\alpha(aA-1))Ee^{-ax_T} + \\
& \quad (-1 + 2\alpha(aA-1))Fe^{-x_T} \quad (2.51)
\end{aligned}$$

Equations (2.48)-(2.51) form a linear system in C, D, E, F. To obtain an existence function $\Phi(x)$, I construct coefficient vectors

$$m_1 = \begin{pmatrix} e^{\omega_1 x_T} + e^{-\omega_1 x_T} \\ \omega_1(e^{\omega_1 x_T} - e^{-\omega_1 x_T}) \\ \omega_1^2(e^{\omega_1 x_T} + e^{-\omega_1 x_T}) \\ \omega_1^3(e^{\omega_1 x_T} - e^{-\omega_1 x_T}) \end{pmatrix}, m_2 = \begin{pmatrix} e^{\omega_2 x_T} + e^{-\omega_2 x_T} \\ \omega_2(e^{\omega_2 x_T} - e^{-\omega_2 x_T}) \\ \omega_2^2(e^{\omega_2 x_T} + e^{-\omega_2 x_T}) \\ \omega_2^3(e^{\omega_2 x_T} - e^{-\omega_2 x_T}) \end{pmatrix},$$

$$m_3 = \begin{pmatrix} \frac{a}{a-2\alpha(A-a)} \\ a \\ -a^2 \\ a^3 - 2a\alpha(aA-1) \end{pmatrix}, m_4 = \begin{pmatrix} \frac{a}{a-2\alpha(A-a)} \\ 1 \\ -1 \\ 1 - 2\alpha(aA-1) \end{pmatrix}, m_0 = \begin{pmatrix} \frac{(A-a)\beta}{a-2\alpha(A-a)} \\ 0 \\ -2(aA-1)\beta \\ 0 \end{pmatrix}.$$

Let $DET_{x_T}(\alpha) = \begin{vmatrix} m_1 & m_2 & m_3 & m_4 \end{vmatrix}$, where $|.|$ is the determinant. For a fixed set of parameters $(a, A, \alpha, \beta, u_T) = (2.6, 2.8, 0.15, 1, 0.400273)$, the solution $(C, D, E, F, x_T) = (-0.8532, 1.16865, 2.94108, -0.89571, 0.41902)$ is given by Mathematica with$DET_{x_T}(\alpha)$ equal to -243.2415568475316. I use this solution as an initial guess to continue system (2.43)-(2.47) using AUTO while following $DET_{x_T}(\alpha)$ as α decreases to 0 and then increases to α_1. The value of $DET_{x_T}(\alpha)$ is recorded and plotted in figure 2.12. It shows that $DET_{x_T}(\alpha) \neq 0$ as $\alpha < \alpha_1$. Therefore I can always solve the linear system (2.48)-(2.49) for C, D, E, F by Cramer's rule.

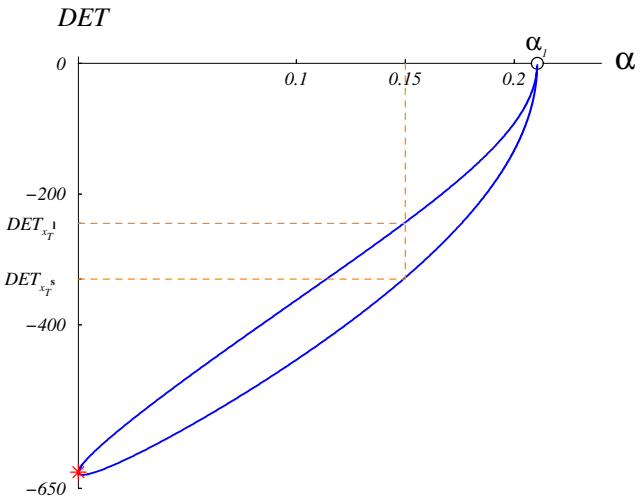

Figure 2.12. DET with real ω_1 and ω_2. Example: $a = 2.6$, $A = 2.8$, $\alpha = 0.15$, $u_T = 0.400273$. $DET_{x_T^s} = -327.6453262677492$, $DET_{x_T^1} = -243.2415568475316$. Saddle node $\star = (0, -624.918866676)$. Remark: $\omega_1 \neq \omega_2$. At $\alpha = \alpha_1$, $\omega_1 = \omega_2$, this will be discussed in Section (2.10).

Now I demonstrate that this is not only true on the DET curve in Figure 2.12 but also true in an open set W of (α, a, A, x_T). For fixed $\alpha = 0.15$ and $u_T = 0.400273$, one can define system (2.48)-(2.51) as a map $\mathbf{f}(C, D, E, F, a, A, x_T)$ from an open set $U \subset \Re^7$ to $\Re^4$ such that $\mathbf{f}(C, D, E, F, a, A, x_T) = 0$ at the point

$$(C^0, D^0, E^0, F^0, a^0, A^0, x_T^0) = (-0.8532, 1.16865, 2.94108, -0.89571, 2.6, 2.8, 0.41902).$$

Let $\mathbf{x} = (C, D, E, F)$ and $\mathbf{y} = (a, A, x_T)$. Obviously, $\mathbf{f_x} = DET_{x_T^1}(\alpha) \neq 0$ (on the upper branch of DET in Figure 2.12), then by the Implicit Function Theorem, there exist open sets $V^{\mathbf{l}} \subset \Re^7$ and $W^{\mathbf{l}} \subset \Re^3$ with $(C^0, D^0, E^0, F^0, a^0, A^0, x_T^0) \in V^{\mathbf{l}}$ and $(a^0, A^0, x_T^0) \in W^{\mathbf{l}}$, having the following property: to every $\mathbf{y} \in W^{\mathbf{l}}$ there corresponds a unique $\mathbf{x}$ such that $\mathbf{f}(\mathbf{x}, \mathbf{y}) = \mathbf{0}$, *i.e.* $(C, D, E, F) = \mathbf{g}(a, A, x_T)$, where $\mathbf{g}$ is a differentiable mapping of $W^{\mathbf{l}}$ into $\Re^4$. Similarly, for the same α and u_T on the lower branch of DET curve in Figure 2.12, there is an open set $V^{\mathbf{s}}$ and $W^{\mathbf{s}}$. Generally, for fixed threshold, for any $\alpha \in (0, \alpha_1)$, there are open sets $W^{\mathbf{l}}$ or $W^{\mathbf{s}} \subset \Re^3$. The union of them is an open set W' of (a, A, x_T). Then there is an open set $W = (0, \alpha_1) \times W' \subset \Re^4$.

For any $(\alpha, a, A, x_T) \in W$, solve E and F by Cramer's Rule.

$$E = \frac{\begin{vmatrix} m_1 & m_2 & m_0 & m_4 \end{vmatrix}}{\begin{vmatrix} m_1 & m_2 & m_3 & m_4 \end{vmatrix}} \begin{matrix} \\ \\ \\ e^{-ax_T} \end{matrix},$$

$$F = \frac{\begin{vmatrix} m_1 & m_2 & m_3 & m_0 \end{vmatrix}}{\begin{vmatrix} m_1 & m_2 & m_3 & m_4 \end{vmatrix}} \begin{matrix} \\ \\ \\ e^{-x_T} \end{matrix}.$$

Substitute $E(x)$ and $F(x)$ back into $\Phi(x) = E(x)e^{-ax} + F(x)e^{-x}$

$$\Phi(x) = Ee^{-ax} + Fe^{-x} = \frac{\begin{vmatrix} m_1 & m_2 & m_0 & (m_3 - m_4) \end{vmatrix}}{\begin{vmatrix} m_1 & m_2 & m_3 & m_4 \end{vmatrix}}.$$

Plotting $\Phi(x)$ gives figure 2.13.

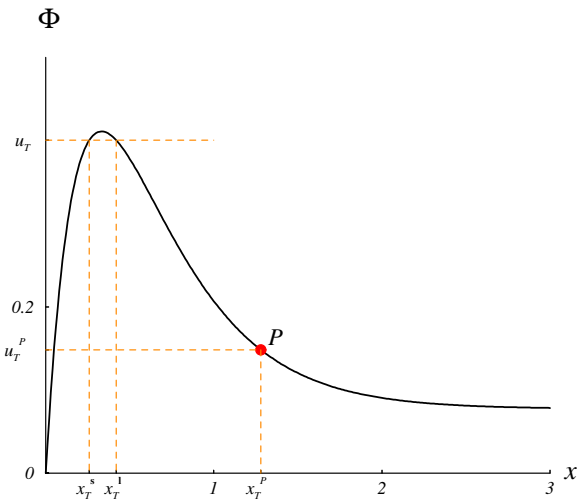

Figure 2.13. Existence function $\Phi(x)$. $\alpha = 0.15$, $A = 2.8$, $a = 2.6$. At $u_T = 0.400273$, $\Phi(x)$ has a single-pulse **l** which has width $x_T^{\mathbf{l}} = 0.4109$; the second single-pulse **s** is narrower with width $x_T^{\mathbf{s}} = 0.2582$. At P, threshold $u_T^P = 0.1489$, $u''(0)$ of the pulse at P is 0.

2.7.3 Transition point P between single-pulses and dimple-pulses

$\Phi(x)$ gives us the range of thresholds u_T on which there exist two pulse solutions; a large pulse **l** (or dimple-pulse **d**) and a small pulse **s**, or only one small single-pulse solution. The x-value of

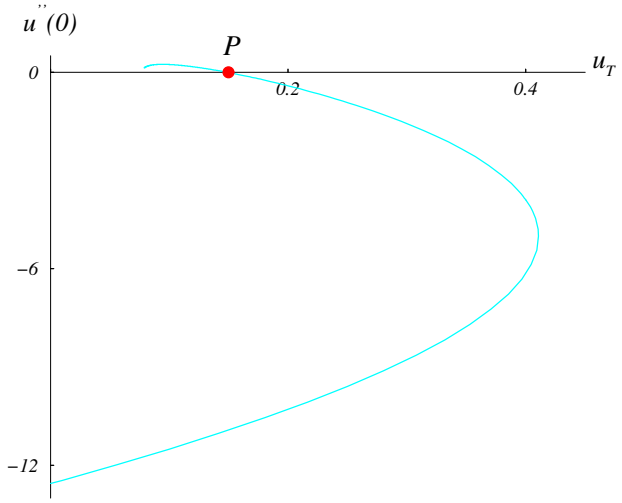

Figure 2.14. Plot of $u''(0)$ when $\alpha = 0.15$,$A = 2.8$,$a = 2.6$. P is the transition point between single-pulse **l** and dimple-pulse **d**. When threshold $u_T^P = 0.1489$, $u''(0)$ of the pulse $= 0$.

---

the intersection of u_T and $\Phi(x)$ is the width of a pulse. In figure 2.13, $x_T^{\mathbf{s}}$ is the width of the small single-pulse **s**, and $x_T^{\mathbf{l}}$ is the width of the large single-pulse **l**. At P, the threshold is $u_T^P = 0.14838$, and $u''(0) = 0$ for the pulse solution in figure 2.15. Dimple-pulses appear if the threshold is between $u_T^P = 0.1489$ and the limit of $\Phi(x)$ as $x \to \infty$ (figure 2.13.) Figure 2.14 is the AUTO plot of $u''(0)$. The threshold when $u''(0)$ crosses zero is the transition threshold u_T^P.

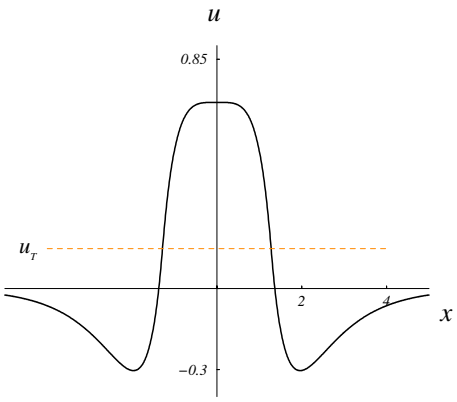

Figure 2.15. Example of P-pulse: $a = 2.6$, $A = 2.8$, $\alpha = 0.15$, $u_T^P = 0.14838$. The width of this pulse $x_T^P = 1.27978$. And $u''(0) = 0$.

2.7.4 Loss of pulse with too much excitation or inhibition in the network

After introducing function $\Phi(x)$, I can explain why too much excitation in the network can eliminate a single-pulse. More excitation in the network means the ratio $A/a > 1$. If this ratio is too big, the following example illustrates what can happen. When $A = 5$, $a = 1.5$ and $\alpha = 0.04$. Function $\Phi(x)$ looks like figure 2.16. There is no longer a big single-pulse (or a dimple-pulse.)

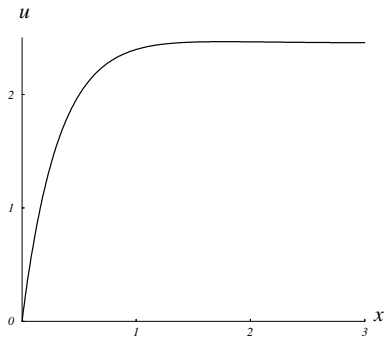

Figure 2.16. $\Phi(x)$ with too much excitation: $A = 5$, $a = 1.5$, $\alpha = 0.04$. There is only pulse **s**, no pulse **l**.

When the ratio $A/a < 1$, more inhibition than excitation is in the network. If there is too much inhibition in the network, say $A/a = 0.1$ and $A = 1.1$, the positive part of $\Phi(x)$ almost disappears (figure 2.17). Obviously, single-pulse solution no longer exist for positive threshold.

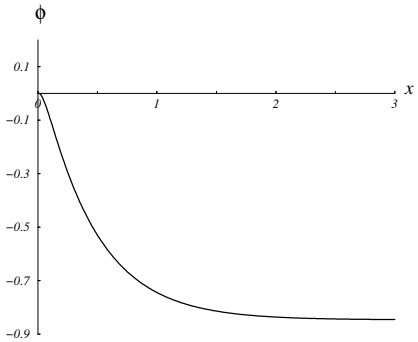

Figure 2.17. $\Phi(x)$ with too much inhibition: $A = 1.1$, $a = 11$, $\alpha = 0.15$. There is neither pulse **s** nor pulse **l**.

2.8 Complex ω_1 and ω_2 with nonzero real part

As shown in figure 2.9, ω_1 and ω_2 are both real only when α is in the interval $(0, \alpha_1)$. Sometimes, this interval can be very small. For instance, when $A = 2.5$ and $a = 1.5$, by solving the equation $\Delta = 0$ for α, $\alpha_1 = 0.0725$, $\alpha_3 = 0.7126$. Both eigenvalues are real only in a tiny range $(0, 0.0725)$. I must go beyond that range $(0, \alpha_1)$. In this section I will check if there exists a single-pulse solution when $\alpha > \alpha_1$. In between α_1 and α_3, $\Delta < 0$, therefore both ω_1 and ω_2 are complex (figure 2.18.) It can be proved that α_1 and α_3 are both positive (See A.1 in Appendix).

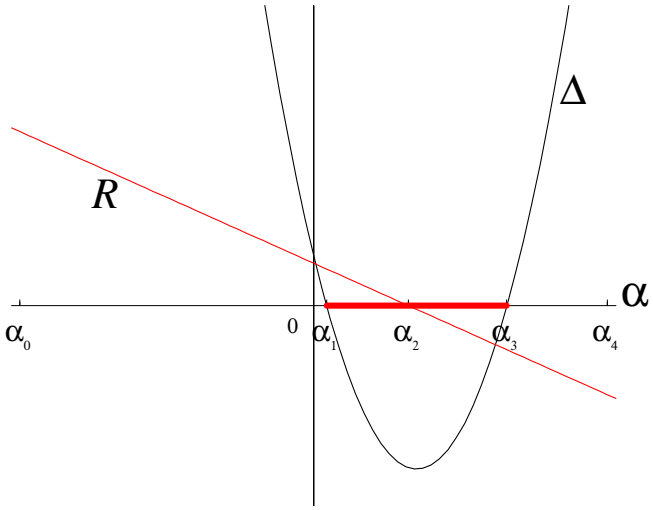

Figure 2.18. Complex eigenvalue range.

Proposition 2.4. *Both α_1 and α_3 are positive and they are never equal to each other, i.e. $\Delta(\alpha) = 0$ always has two different roots. (See proof A.1 in Appendix).*

Proposition 2.5. *For the balanced case in which $A = a$, $\alpha_1 < 1/2$, $\alpha_3 > 1/2$. When A becomes larger, α_1 moves closer to α_3, but never reaches it. (See proof A.2 in Appendix).*

For fixed A and a, by Proposition 2.4 and Proposition 2.5, there is always an interval of α in which both eigenvalues are complex. When $\Delta < 0$, ω_1 and ω_2 are complex conjugate to each other and they have non-trivial real parts. Let $w_1 = p + iq$, $w_2 = p - iq$ with $p \neq 0$ and $p, q \in \Re$.

2.8.1 Construction of a single-pulse with complex ω_1 and ω_2

To guarantee a real $u_{\mathrm{I}}(x)$, C and D must be complex. Imposing symmetry, one can have $C = D^*$. Suppose $C = C_R + iC_I$, then $D = C_R - iC_I$. Substituting C, D, ω_1 and ω_2 into general form (2.28) for $u_{\mathrm{I}}(x)$ to yield

$$u_{\mathrm{I}}(x) = 4C_R \cos(qx)\cosh(px) - 4C_I \sin(qx)\sinh(px) + \frac{2(A-a)(\beta - \alpha u_T)}{a - 2\alpha(A-a)}$$

Now write the solution in a real form as

$$J\cos(qx)\cosh(px) + K\sin(qx)\sinh(px) + \frac{2(A-a)(\beta - \alpha u_T)}{a - 2\alpha(A-a)}$$

where $J = 4C_R$ and $K = -4C_I$. Applying the same boundary conditions (2.20)- (2.24), obtain the following 5 equations:

$$Ee^{-ax_T} + Fe^{-bx_T} = u_T \tag{2.52}$$

$$J\cos(qx_T)\cosh(px_T) + K\sin(qx_T)\sinh(px_T) + \frac{2(A-a)(\beta - \alpha u_T)}{a - 2\alpha(A-a)} = u_T \tag{2.53}$$

$$(Kp - Jq)\cosh(px_T)\sin(qx_T) + (Jp + Kq)\cos(qx_T)\sinh(px_T) = -aEe^{-ax_T} - Fe^{-x_T} \tag{2.54}$$

$$(Jp^2 + 2Kpq - Jq^2)\cosh(px_T)\cos(qx_T) + (Kp^2 - 2Jpq - Kq^2)\sinh(px_T)\sin(qx_T) = a^2Ee^{-ax_T} + Fe^{-x_T} - 2\beta(aA-1) \tag{2.55}$$

$$(Kp^3 - 3Jp^2q - 3Kpq^2 + Jq^3)\cosh(px_T)\sin(qx_T) + (Jp^3 - 3Kp^2q - 3Jpq^2 - Kq^3)\sinh(px_T)\cos(qx_T) = (-a^3 + 2a\alpha(aA-1))Ee^{-ax_T} + (-1 + 2\alpha(aA-1))Fe^{-x_T} \tag{2.56}$$

Numerically solving J, K, E, F, x_T in these five equations using Mathematica [67], one can obtain the explicit form of $u_{\mathrm{I}}(x)$. The plots of pulse **l** and **s** are shown in figure 2.20

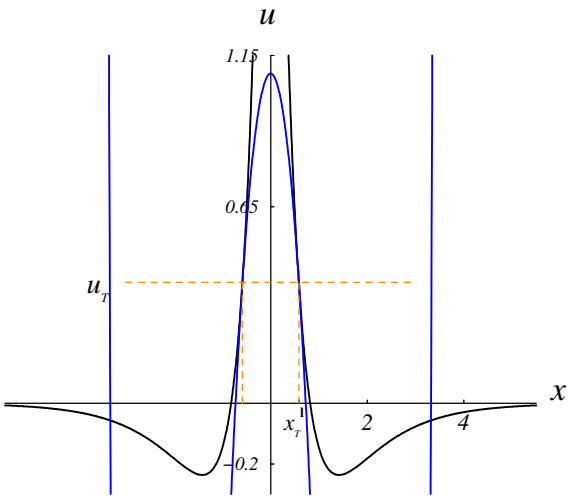

Figure 2.19. Big single-bump.

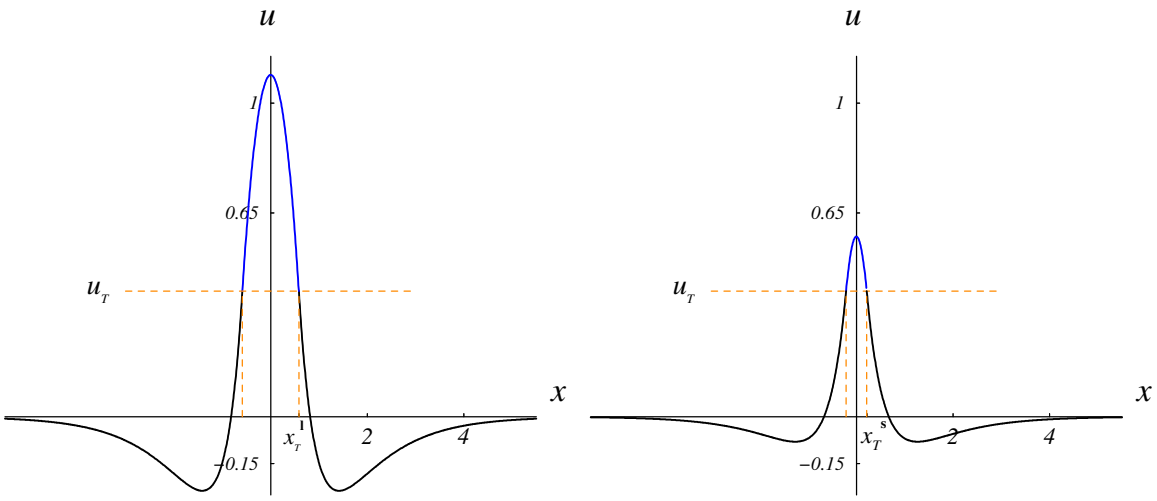

Figure 2.20. Two single-pulses: $A = 2.8$, $a = 2.6$, $\alpha = 0.6178$, $u_T = 0.3$. (Left) Single-pulse **l**: $x_T^{\mathrm{l}} = 0.58384$, height=$u(0) = 1.0901$. (Right) Single-pulse **s**: $x_T^{\mathrm{s}} = 0.21317$, height=$u(0) = 0.5744$.

2.8.2 Existence function $\Phi(x)$

Eliminate the threshold $-u_T$ from (2.52) and (2.53) and rearrange terms.

$$J\cos(qx_T)\cosh(px_T) + K\sin(qx_T)\sinh(px_T) + \frac{2(A-a)\beta}{a-2\alpha(A-a)} = \frac{a}{a-2\alpha(A-a)}(Ee^{-ax_T} + Fe^{-x_T}) \qquad (2.57)$$

$$-J[q\sin(qx_T\cosh(px_T) - p\cos(qx_T)\sinh(px_T)] + K[p\cosh(p\sin(qx_T\cosh(px_T)) + q\cos(qx_T)\sinh(px_T)]$$
$$= -aEe^{-ax_T} - Fe^{-x_T} \qquad (2.58)$$

$$J[(p^2-q^2)\cos(qx_T)\cosh(px_T) - 2pq\sin(qx_T)\sinh(px_T)] +$$
$$K[(p^2-q^2)\sin(qx_T)\sinh(px_T) + 2pq\cos(qx_T)\cosh(px_T)] = a^2Ee^{-ax_T} + Fe^{-x_T} - 2\beta(aA-1) \qquad (2.59)$$

$$J[(q^3 - 3p^2q)q\sin(qx_T)\cosh(px_T) + (p^3 - 3pq^2)\cos(qx_T)\sinh(px_T)] +$$
$$K[(p^3 - 3pq^2)\sin(qx_T)\cosh(px_T) - (q^3 + 3p^2q)\cos(qx_T)\sinh(px_T)] = (-a^3 + 2a\alpha(aA - 1))Ee^{-ax_T} +$$
$$(-1 + 2\alpha(aA - 1))Fe^{-x_T} \qquad (2.60)$$

Fix parameters $(a, A) = (2.6, 2.8)$ and $u_T = 0.400273$. Starting from the small single-pulse solution **s**, $(J, K, E, F, x_T) = (0.44644, -3.09450, 1.344130, -0.460306, 0.213173)$, I follow $DET_{x_T}(\alpha)$, the value of the coefficient matrix of system (2.57)-(2.60) on the interval (α_1, α_3) in AUTO. This is the upper curve in figure (2.21). Repeat the same procedure to obtain the lower curve in figure (2.21) using solution (0.962175, -1.57206, 5.85067, -1.58116, 0.58385) for a large single-pulse as starting point.

Remark 2.3. *$DET \neq 0$ except at $\alpha = \alpha_1$ and $\alpha = \alpha_3$, which will be discussed in section (2.10).*

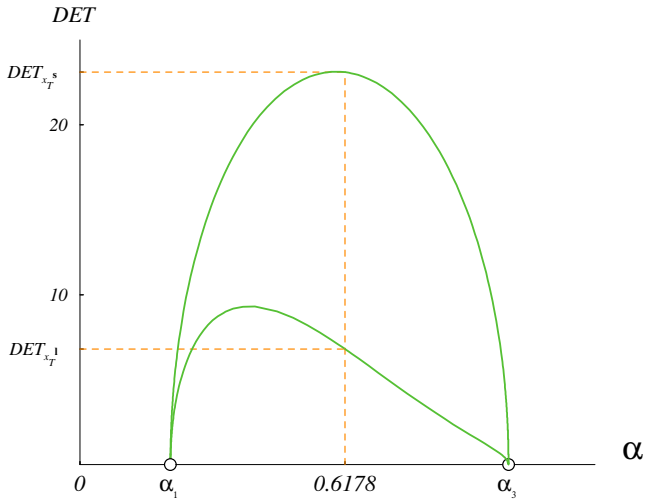

Figure 2.21. DET with complex ω_1 and ω_2. Example: $a = 2.6$, $A = 2.8$, $\alpha = 0.6178$, $u_T = 0.400273$. $DET_{x_T^{\mathbf{s}}} = 23.09342539459342$, $DET_{x_T^{\mathbf{1}}} = 6.7982341398391818$. Remark: $\omega_1 \neq \omega_2$. At $\alpha = \alpha_1$ and $\alpha = \alpha_3$, $\omega_1 = \omega_2$, this will be discussed in Section (2.10).

Since $DET \neq 0$ for fixed a, A and u_T, The linear system (2.57)-(2.60) can be solved for J, K, E, F. Then the existence function $\Phi(x)$ (figure (2.22)) is obtained in the analogous fashion explained in section (2.7.2).

However, $\Phi(x)$ for complex $\omega_{1,2}$ has major differences from the $\Phi(x)$ for real ω in section (2.7.2). Here, $\Phi(x)$ oscillates. After its first local minimum between P_1 and P_2 (figure 2.22,) it keeps oscillating (sometimes the amplitude of the oscillations is too small to see.) Additionally,

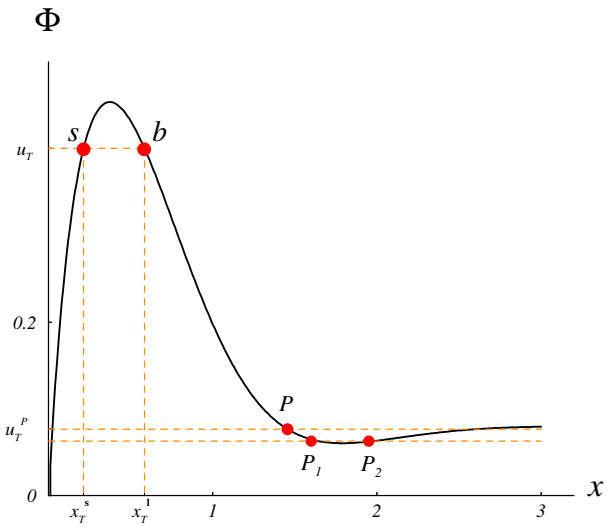

Figure 2.22. Existence function $\Phi(x)$. $\alpha = 0.6178$, $A = 2.8$, $a = 2.6$. At $u_T = 0.400273$, $\Phi(x)$ shows that there is a single-pulse **l** which is wider and has width $x_T^{\mathbf{l}} = 0.58385$; the second single-pulse **s** is narrower and has width $x_T^{\mathbf{s}} = 0.21317$. As we increase u_T to the maximum of $\Phi(x)$, pulse **s** and **l** become one. At P, $u_T^P = 0.0767$, $x_T^P = 1.454$, $u''(0) = 0$. At both P_1 and P_2, threshold is 0.063, $u''(0) > 0$, and widths are 1.6 and 1.9 respectively. See figure 2.23.

---

when the threshold is between the first local minimum and the next local maximum, there are more than two pulse solutions. For example, from the existence function $\Phi(x)$ with complex $\omega_{1,2}$, I identify one small single-pulse **s**, and two dimple-pulses (figure 2.23.) The phenomenon of three pulses coexisting cannot be observed for Amari's model or for section 2.7.2 because in those cases the existence function $\Phi(x)$ always approaches an asymptote without any oscillations as x increases. Oscillations only occur when ω_1 or ω_2 are complex.

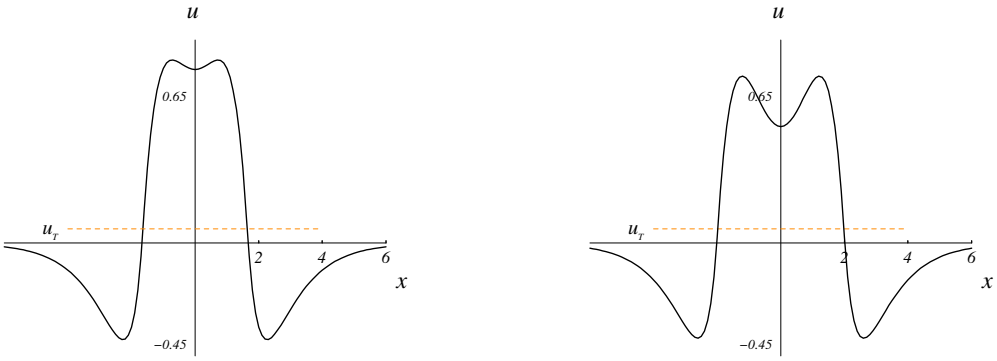

Figure 2.23. Dimple-pulses. $A = 2.8$, $a = 2.6$, $\alpha = 0.6178$, $u_T = 0.063$. (Left) Dimple-pulse at P_1: $x_T^{\mathbf{d}} = 1.6$. (Right) Dimple-pulse at P_2: $x_T^{\mathbf{d}} = 1.9$.

2.9 Imaginary ω_1 and ω_2

Here there are at least two single-pulse solutions if α is not bigger than a critical value, and I lose the large single-pulse **l** as soon as α reached that value.

When $\alpha > \alpha_3$, $\Delta > 0$, $R < 0$ and $S = \dfrac{\sqrt{\Delta}}{2} < |R|$. The real parts of ω_1 and ω_2 are both zero. Suppose that $w_1 = iq_1$, $w_2 = iq_2$ with $q_1, q_2 \in \Re$. According to Table 2.1, Table 2.2 and Table 2.3, when $A \leq a$, both ω_1 and ω_2 are imaginary if $\alpha > \alpha_3$ (Figure 2.24.) When $A > a$, both ω_1 and ω_2 are imaginary if $\alpha_3 < \alpha < \alpha_4 = \dfrac{a}{2(A-a)}$ (Figure 2.25.) Notice that $\alpha \neq \dfrac{a}{2(A-a)}$. Otherwise the constant term in $u_{\mathrm{I}}(x)$ becomes ∞. Thus

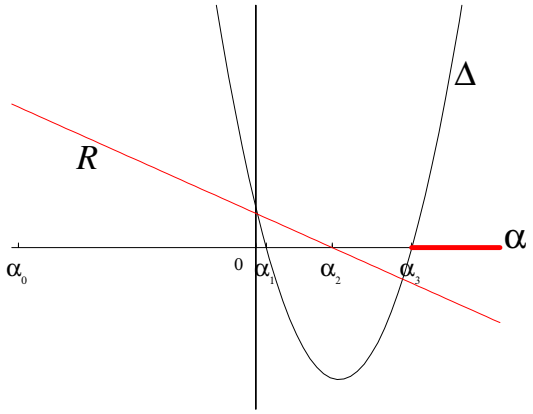

Figure 2.24. Imaginary eigenvalue ($A \leq a$).

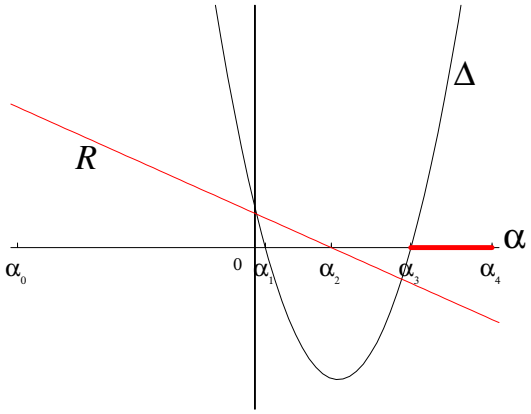

Figure 2.25. Imaginary eigenvalue ($A > a$).

$$u_{\mathrm{I}}(x) = J\cos(q_1 x_T) + K\cos(q_2 x_T) + \frac{2(A-a)(\beta - \alpha u_T)}{a - 2\alpha(A-a)}$$

Applying the boundary condition to $u_{\mathrm{I}}(x)$ and $u_{\mathrm{II}}(x)$ yields

$$J\cos(q_1 x_T) + K\cos(q_2 x_T) + \frac{2(A-a)(\beta - \alpha u_T)}{(a - 2\alpha(A-a))} = u_T \tag{2.61}$$

$$Ee^{-ax_T} + Fe^{-x_T} = u_T \tag{2.62}$$

$$-q_1 J\sin(q_1 x_T) - q_2 K\sin(q_2 x_T) = -aEe^{-ax_T} - Fe^{-x_T} = 0 \tag{2.63}$$

$$-q_1^2 J\cos(q_1 x_T) - q_2^2 K\cos(q_2 x_T) = a^2 Ee^{-ax_T} + Fe^{-x_T} - 2(aA-1)\beta \tag{2.64}$$

$$q_1^3 J\sin(q_1 x_T) + q_2^3 K\sin(q_2 x_T) = (-a^3 + 2a\alpha(aA-1))Ee^{-ax_T} + (-1 + 2\alpha(aA-1))Fe^{-x_T} \tag{2.65}$$

Both single-pulses **s** and **l** exist. (See figure 2.26.)

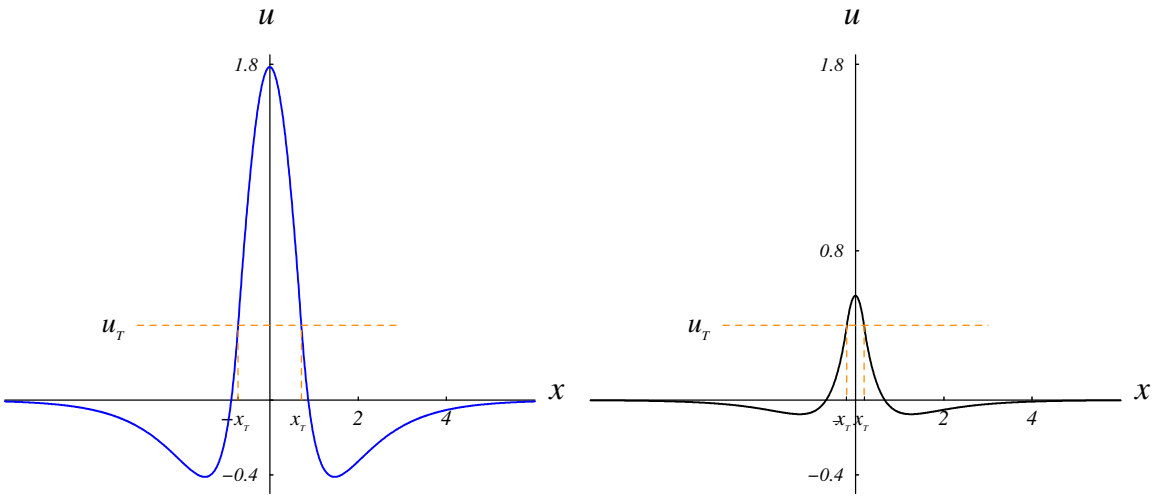

Figure 2.26. Single-pulses. $A = 2.8$, $a = 2.6$, $\alpha = 0.999$, $u_T = 0.400273$. (Left) Single-pulse **l**: $x_T^{\mathrm{l}} = 0.7160624397376277$, height=$u(0) = 1.784986781128356$. (Right) Single-pulse **s**: $x_T^{\mathrm{s}} = 0.1946261544329597$, height=$u(0) = 0.5593035435768856$.

2.9.1 $\Phi(x)$ and a critical value of α

After I eliminate threshold u_T from the above system, I have the following linear system in J, K, E, F.

$$
\begin{aligned}
J\cos(q_1x_T) + K\cos(q_2x_T) + \frac{2(A-a)\beta}{(a-2\alpha(A-a))} &= \frac{a}{(a-2\alpha(A-a))}(Ee^{-ax_T} + Fe^{-x_T}) && (2.66)\\
-q_1J\sin(q_1x_T) - q_2K\sin(q_2x_T) &= -aEe^{-ax_T} - Fe^{-x_T} && (2.67)\\
-q_1^2J\cos(q_1x_T) - q_2^2K\cos(q_2x_T) &= a^2Ee^{-ax_T} + Fe^{-x_T} - 2(aA-1)\beta && (2.68)\\
q_1^3J\sin(q_1x_T) + q_2^3K\sin(q_2x_T) &= (-a^3 + 2a\alpha(aA-1))Ee^{-ax_T} + \\
&\quad (-1 + 2\alpha(aA-1))Fe^{-x_T} && (2.69)
\end{aligned}
$$

$$
\text{Let } m_1 = \begin{pmatrix} \cos(q_1x_T) \\ -q_1\sin(q_1x_T) \\ -q_1^2\cos(q_1x_T) \\ q_1^3\sin(q_1x_T) \end{pmatrix},\ m_2 = \begin{pmatrix} \cos(q_2x_T) \\ -q_2\sin(q_2x_T) \\ -q_2^2\cos(q_2x_T) \\ q_2^3\sin(q_2x_T) \end{pmatrix},
$$

$$m_3 = \begin{pmatrix} \frac{a}{a-2\alpha(A-a)} \\ a \\ -a^2 \\ a^3 - 2a\alpha(aA-1) \end{pmatrix}, m_4 = \begin{pmatrix} \frac{a}{a-2\alpha(A-a)} \\ 1 \\ -1 \\ 1 - 2\alpha(aA-1) \end{pmatrix}, m_0 = \begin{pmatrix} \frac{(A-a)\beta}{a-2\alpha(A-a)} \\ 0 \\ -2(aA-1)\beta \\ 0 \end{pmatrix}.$$

Then, by Cramer's Rule,

$$J = \frac{\begin{vmatrix} m_0 & m_2 & m_3 & m_4 \end{vmatrix}}{\begin{vmatrix} m_1 & m_2 & m_3 & m_4 \end{vmatrix}}, \qquad K = \frac{\begin{vmatrix} m_1 & m_0 & m_3 & m_4 \end{vmatrix}}{\begin{vmatrix} m_1 & m_2 & m_3 & m_4 \end{vmatrix}},$$

$$E = \frac{\begin{vmatrix} m_1 & m_2 & m_0 & m_4 \end{vmatrix}}{\begin{vmatrix} m_1 & m_2 & m_3 & m_4 \end{vmatrix} e^{-ax_T}}, \qquad F = \frac{\begin{vmatrix} m_1 & m_2 & m_3 & m_0 \end{vmatrix}}{\begin{vmatrix} m_1 & m_2 & m_3 & m_4 \end{vmatrix} e^{-x_T}},$$

where $|.|$ is determinant. The determinant $DET_{x_T}(\alpha) = \begin{vmatrix} m_1 & m_2 & m_3 & m_4 \end{vmatrix}$. For the parameter set $(a, A, u_T, \beta) = (2.6, 2.8, 0.400273, 1)$, $DET_{x_T^{\mathbf{s}}}(0.9987153) = -0.0876436218375472$ for the single-pulse $\mathbf{s}$, and $DET_{x_T^{\mathbf{l}}}(0.9987153) = -0.1467101420392571$ for pulse $\mathbf{l}$. Using them as initial points, I obtain two branches of $DET_{x_T}(\alpha)$ by AUTO as α value is gradually increased (figure 2.27.) The red one is the DET value for single-pulse $\mathbf{l}$. The black one is the DET value for single-pulse $\mathbf{s}$. In the branch of pulse $\mathbf{s}$, $DET_{x_T}(\alpha)$ has no zero, so pulse $\mathbf{s}$ is always there. But in the other branch for the large $\mathbf{l}$, $DET_{x_T}(\alpha)$ is zero as α approaches a critical value α^0. For example, with the given parameter set and the help of AUTO, I find that as $\alpha = 1.403937241$, DET is very small number $6.81111707640769736 \times e^{-7}$. The height of pulse $\mathbf{l}$ is

$$\begin{aligned} u(0) &= J + K + \frac{2(A-a)(\beta - \alpha u_T)}{a - 2\alpha(A-a)} \\ &= \frac{\begin{vmatrix} (m_1 - m_2) & m_0 & m_3 & m_4 \end{vmatrix}}{\begin{vmatrix} m_1 & m_2 & m_3 & m_4 \end{vmatrix}} \end{aligned}$$

As α approaches the critical value α^0, the numerator $\begin{vmatrix} (m_1 - m_2) & m_0 & m_3 & m_4 \end{vmatrix}$ is a continuous function in α, and it is a finite number as $\alpha = \alpha^0$. But the denominator $\begin{vmatrix} m_1 & m_2 & m_3 & m_4 \end{vmatrix}$ is zero as $\alpha = \alpha^0$. Therefore, the height $u(0)$ of the large pulse goes to infinity. Therefore, I lose the

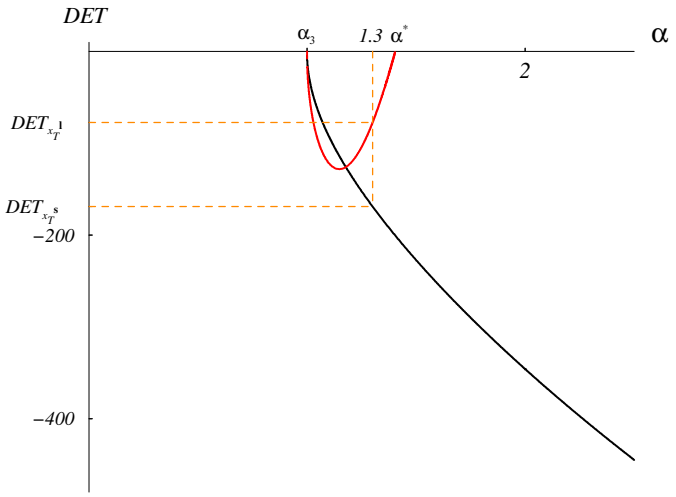

Figure 2.27. DET with imaginary ω_1 and ω_2. Example: $a = 2.6$, $A = 2.8$, $\alpha = 1.3$, $u_T = 0.400273$. $DET_{x_T^{\mathbf{s}}} = -169.031206395783$, $DET_{x_T^{\mathbf{l}}} = -77.27219862125841$. Remark: $\omega_1 \neq \omega_2$. At $\alpha = \alpha_1$ and $\alpha = \alpha_3$, $\omega_1 = \omega_2$, this will be discussed in Section (2.10).

---

large pulse.

Further studying the existence function I draw the same conclusion that I lose the single-pulse **l** if $\alpha \geq \alpha^0$ (see figure 2.28.)

$$\Phi(x) = Ee^{-ax} + Fe^{-x} = \frac{\begin{vmatrix} m_1 & m_2 & m_0 & (m_3 - m_4) \end{vmatrix}}{\begin{vmatrix} m_1 & m_2 & m_3 & m_4 \end{vmatrix}},$$

When both ω_1 and ω_2 are imaginary, there is always the small single-pulse **s** but there is no single-pulse **l** if $\alpha \geq \alpha^0$ at which determinant $\begin{vmatrix} m_1 & m_2 & m_3 & m_4 \end{vmatrix}$ is zero. A third solution (the third intersection of u_T and $\Phi(x)$) could also exist. I have not studied the properties of the third solution.

2.9.2 Theoretical reasons for the existence of α^0

There are theoretical reasons for the existence of α^0 where the large pulse runs off to infinity. As the height of the large pulse becomes very big, the width of the large pulse is still finite. This can be observed both from the existence function $\Phi(x)$ and the continuation picture in section 2.11. I must go back to the integral equation (2.2) to explain why there is such a phenomenon. (2.2) can

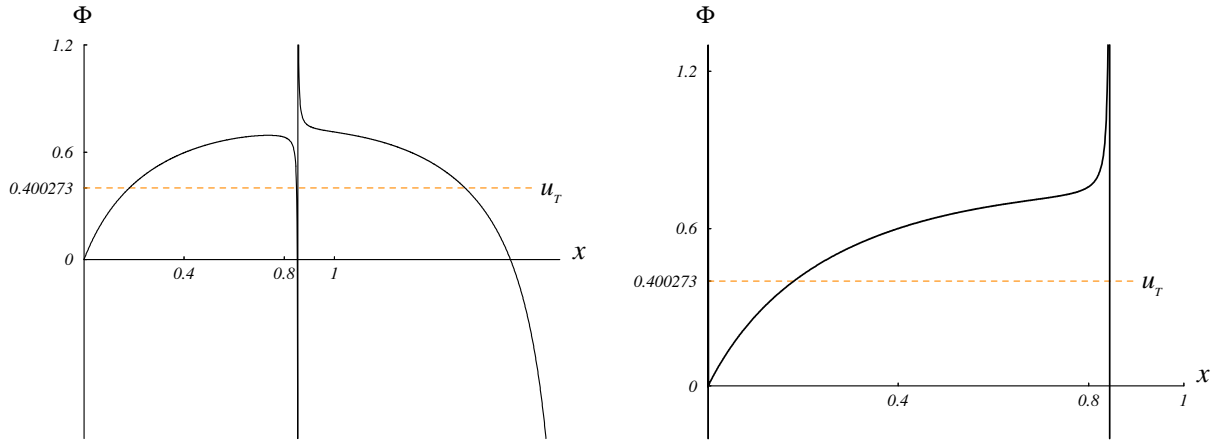

Figure 2.28. Existence function Φ for imaginary $\omega_{1,2}$. $A = 2.8$, $a = 2.6$, $u_T = 0.400273$. (Left) $\alpha = 1.4$. There is a single-pulse **l**, and $x_T^1 = 0.8491539857774331$, height=$u(0) = 146.2227855915919$, which is big because $\alpha = 1.4$ is close to α^0 where $DET = 0$. (Right) $\alpha = 1.41 > \alpha^0$. Single-pulse **l** no longer exist. The vertical line in both pictures is an asymptote of $\Phi(x)$ because at that point the denominator of $\Phi(x)$ is zero.

---

be rewritten as

$$\begin{aligned} u(x) &= (\beta - \alpha u_T)\int_{-x_T}^{x_T} w(x-y)dy + \alpha\int_{-x_T}^{x_T} w(x-y)u(y)dy \\ \frac{1}{\alpha}u(x) &= \frac{1}{\alpha}(\beta - \alpha u_T)\int_{-x_T}^{x_T} w(x-y)dy + \int_{-x_T}^{x_T} w(x-y)u(y)dy \end{aligned}$$

Let $h(x) = \dfrac{1}{\alpha}(\beta - \alpha u_T)\displaystyle\int_{-x_T}^{x_T} w(x-y)dy$ and $\mu = \dfrac{1}{\alpha}$.

Equation (2.2) becomes

$$\mu u(x) = h(x) + \int_{-x_T}^{x_T} w(x-y)u(y)dy \tag{2.70}$$

Define a linear operator T: $C[-x_T, x_T] \to C[-x_T, x_T]$ such that $Tu = \displaystyle\int_{-x_T}^{x_T} w(x-y)u(y)dy$, where $C[-x_T, x_T]$ is a normed space.

I have shown many examples that the operator equation (2.70) has solutions $u(x)$ on $C[-x_T, x_T]$. By the Fredholm Alternative theorem [35], equation (2.70) has a solution for $h(x) \in C[-x_T, x_T]$ if and only if the homogeneous equation

$$\mu u(x) = \int_{-x_T}^{x_T} w(x-y)u(y)dy$$

has only the trivial solution $u(x) \equiv 0$.

The homogeneous equation is $\mu u = Tu$. When it has only the trivial solution, μ is not an eigenvalue of operator T. If μ is an eigenvalue of T, *i.e.*, equation $\mu u = Tu$ has a non-trivial solution, then equation (2.70) does not have a solution.

T is a compact operator on normed space $C[-x_T, x_T]$ [36]. There are some nice properties about eigenvalues of a compact operator.

Theorem 2.2. *The set of eigenvalues of a compact linear operator on a normed space is countable (perhaps finite or even empty), and the only possible point of accumulation is $\mu = 0$.*

Theorem 2.2 is proven in [37]. From this theorem, it is known that all the eigenvalues of T (could be infinitely many) can be arranged in a sequence converging to zero. It is also known that each of the countable many eigenvalues is finite. Thus, there is the largest positive eigenvalue, say μ_1. When α happens to be the reciprocal of this largest positive eigenvalue, *i.e.*, $\alpha = \dfrac{1}{\mu_1}$, equation (2.70) has no solution. This value of α is the critical value $\alpha^0 = \dfrac{1}{\mu_1}$ where the large pulse solution is lost.

Remark 2.4. *The small single-pulse solution still exists at $\alpha = \alpha^0 = \dfrac{1}{\mu_1}$. This is because for the small single-pulse the value of x_T is different. There is a different operator equation on a different normed space.*

2.10 Equal eigenvalues

As mentioned in previous sections, there are two special points, α_1 and α_3. At these two points, $\Delta = 0$ implying $\omega_1 = \omega_2$. If $R > 0$, $\omega_1 = \omega_2 \in \Re$. If $R < 0$, $\omega_1 = \omega_2 = i\sqrt{|R|} \in \Im$.

Remark 2.5. *α_2, at which $R = 0$, is not always between α_1 and α_3.*

2.10.1 Real $\omega_1 = \omega_2$

First, I look at the case $R > 0$. Four eigenvalues are ω_1, ω_1, $-\omega_1$ and $-\omega_1$. $\omega_1 = \sqrt{R}$ repeats twice, so does $-\omega_1 = -\sqrt{R}$. Following is the general form for $u_{\rm I}(x)$

$$u_{\rm I}(x) = C1e^{\omega_1 x} + C2xe^{\omega_1 x} + D1e^{-\omega_1 x} + D2xe^{-\omega_1 x} + \frac{2(A-a)(\beta - \alpha u_T)}{a - 2\alpha(A-a)}$$

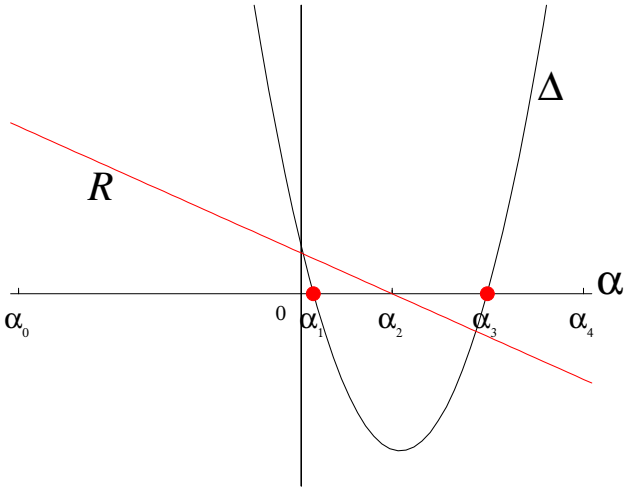

Figure 2.29. equal eigenvalues $\alpha = \alpha_1$ or $\alpha = \alpha_3$.

Because of the symmetry of $u_{\rm I}(x)$, $C1 = D1$ and $C2 = D2$. $u_{\rm I}(x)$ can be written as

$$u_{\rm I}(x) = C(e^{\omega_1 x} + e^{-\omega_1 x}) + Dx(e^{\omega_1 x} + e^{-\omega_1 x}) + \frac{2(A-a)(\beta - \alpha u_T)}{a - 2\alpha(A-a)}$$

Applying matching conditions (2.20)-(2.24) gives

$$C(e^{\omega_1 x_T} + e^{-\omega_1 x_T}) + Dx_T(e^{\omega_1 x_T} + e^{-\omega_1 x_T}) + \frac{2(A-a)(\beta - \alpha u_T)}{a - 2\alpha(A-a)} = u_T \quad (2.71)$$

$$Ee^{-ax_T} + Fe^{-x_T} = u_T \quad (2.72)$$

$$(C\omega_1 + D)(e^{\omega_1 x_T} - e^{-\omega_1 x_T}) + D\omega_1 x_T(e^{\omega_1 x_T} + e^{\omega_1 x_T}) = -aEe^{-ax_T} - Fe^{-x_T} \quad (2.73)$$

$$(C\omega_1^2 + 2D\omega_1)(e^{\omega_1 x_T} + e^{-\omega_1 x_T}) + D\omega_1^2 x_T(e^{\omega_1 x_T} - e^{\omega_1 x_T}) = a^2 Ee^{-ax_T} + Fe^{-x_T} - 2(aA-1)\beta \quad (2.74)$$

$$(C\omega_1^3 + 3D\omega_1^2)(e^{\omega_1 x_T} - e^{-\omega_1 x_T}) + D\omega_1^3 x_T(e^{\omega_1 x_T} + e^{\omega_1 x_T}) = (-a^3 + 2a\alpha(aA-1))Ee^{-ax_T} + (-1 + 2\alpha(aA-1))Fe^{-x_T} \quad (2.75)$$

Since all four eigenvalues are real, there are no oscillations in the existence function $\Phi(x)$. Therefore there are only two pulse solutions. One is a small single-pulse, and the other one is either a large single-pulse or a dimple-pulse depending on the threshold u_T.

2.10.2 Imaginary $\omega_1 = \omega_2$

When $\alpha = \alpha_3$, $R < 0$, then $\omega_1 = \omega_2 = \sqrt{R} = i\sqrt{-R}$. Let $\omega = \sqrt{-R}$, where $\omega \in \Re$.

The general solution $u_{\mathrm{I}}(x)$ is

$$u_{\mathrm{I}}(x) = C_1 \cos \omega x + C_2 \sin \omega x + D_1 x \cos \omega x + D_2 x \sin \omega x + \frac{2(A-a)(\beta - \alpha u_T)}{a - 2\alpha(A-a)}$$

Since $u_{\mathrm{I}}(x) = u_{\mathrm{I}}(-x)$, we have $C_2 = D_1 = 0$. $u_{\mathrm{I}}(x)$ can be written as

$$u_{\mathrm{I}}(x) = C \cos \omega x + D x \sin \omega x + \frac{2(A-a)(\beta - \alpha u_T)}{a - 2\alpha(A-a)}$$

Applying matching conditions (2.20)-(2.24) gives

$$\begin{aligned}
C \cos \omega x_T + D_2 x_T \sin \omega x_T + \frac{2(A-a)(\beta - \alpha u_T)}{a - 2\alpha(A-a)} &= u_T && (2.76)\\
E e^{-a x_T} + F e^{-x_T} &= u_T && (2.77)\\
(D - C\omega) \sin \omega x_T + D\omega x_T \cos \omega x_T &= -aE e^{-a x_T} - F e^{-x_T} && (2.78)\\
(2D\omega - C\omega^2) \cos \omega x_T - D\omega^2 x_T \sin \omega x_T &= a^2 E e^{-a x_T} + F e^{-x_T} - \\
& \quad 2(aA - 1)\beta && (2.79)\\
(C\omega^3 - 3D\omega^2) \sin \omega x_T - D\omega^3 x_T \cos \omega x_T &= (-a^3 + 2a\alpha(aA-1)) E e^{-a x_T} + \\
& \quad (-1 + 2\alpha(aA-1)) F e^{-x_T} && (2.80)
\end{aligned}$$

There are oscillations in the existence function $\Phi(x)$ because all the eigenvalues are imaginary. Therefore, more than two pulses can coexist (figure 2.30) depending on the threshold u_T.

2.11 Continuation

I have covered all the different situations. Now I consider general images on how parameters a, A, α affect localized excitations, i.e stationary pulses. I first fix the connectivity and threshold to study the relation between stationary pulses and the slope α in the gain function. In figure 2.32 and 2.33, the x-axis is α. The y-axes are width and height of the single-pulse, respectively.

Note the large pulse **l** and the small pulse **s** collide into a saddle node bifurcation. I can always

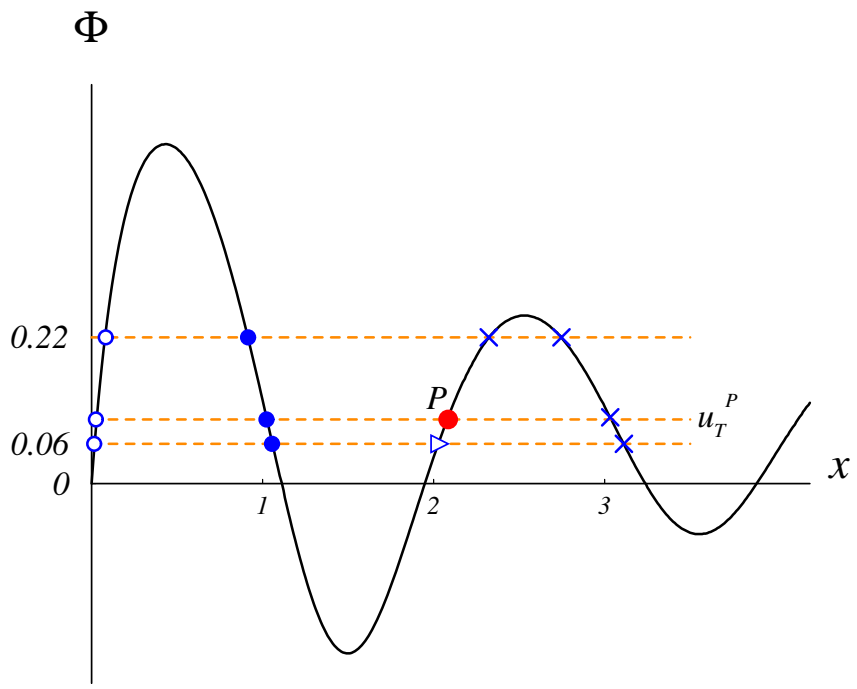

Figure 2.30. Existence function $\Phi(x)$ with imaginary $\omega_1 = \omega_2$. $A = 2.8$, $a = 2.6$, $\alpha = \alpha_3$, $u_T^P = 0.0967003$. The three empty circles are small single-pulses. The three solid circles are large single-pulses. The triangle is a dimple-pulse. Point P is where the dimple-pulse (figure 2.31) breaks into a double-pulse (Chapter 4). The $\times$s are neither single-pulses nor a dimple-pulses, and they are not valid solutions.

---

give a lower bound u_T^- for threshold u_T so that the saddle node is exactly at $\alpha = 0$:

$$u_T^- = \int_0^{\frac{\ln A}{a-1}} w(x)dx$$

If I set threshold $u_T = \int_0^{\frac{\ln A}{a-1}} w(x)dx$, I obtain figure 2.34 and 2.35.

2.12 Conclusions

The eigenvalue structure is important for determining how many pulses exist. For real ω_1 and ω_2, there is no oscillation in the existence function $\Phi(x)$. There are at most two pulses, a small single-pulse and a large one. Amari's case ($\alpha = 0$) belongs to this regime. The large single-pulse can transform to a dimple-pulse depending on the threshold value (figure 2.15.) If ω_1 and ω_2 are complex, there are oscillations in the existence function $\Phi(x)$ (figure 2.22, figure 2.30) There could be a small single-pulse and two large pulses. The two large ones could be dimple-pulses depending

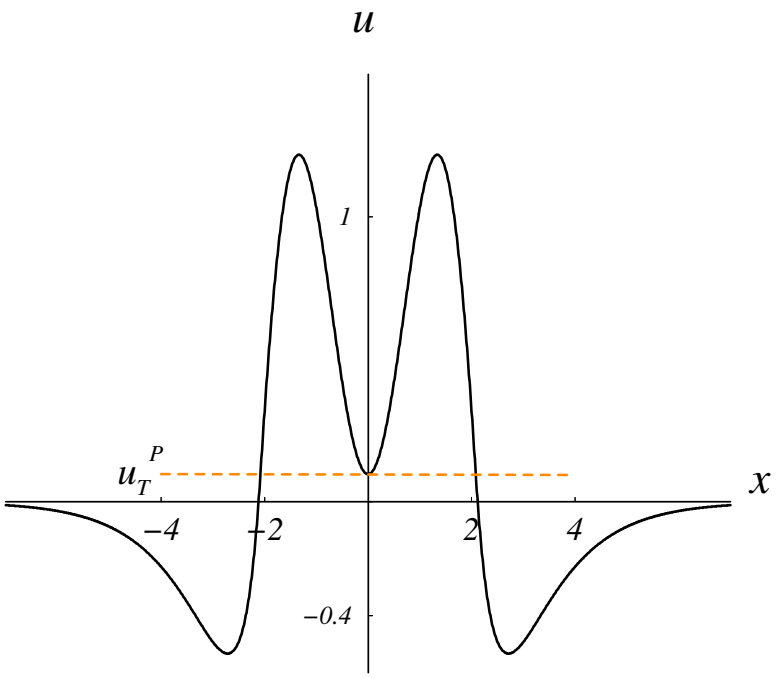

Figure 2.31. The transition from a dimple-pulse to a double-pulse at P. The threshold is $u_T^P = 0.0967003$, and $u(0) = 0.0967003$.

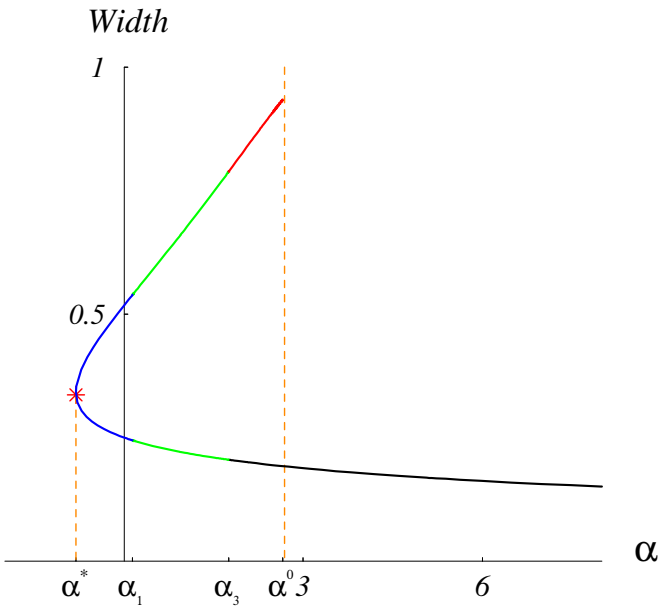

Figure 2.32. Widths of single-pulse **l** (upper branch) and **s** (lower branch). $a = 2.6$, $A = 2.8$, $u_T = 0.400273$.$\alpha \in [\alpha^*, \alpha^0)$, there are two single-pulses. $\alpha \in [\alpha^0, \infty)$, there is only one single-pulse solution. Saddle node $\alpha = \alpha^*$ is where the large single-pulse **l** and the small single-pulse **s** become one. α^0 is where the large pulse **l** runs off to infinity.

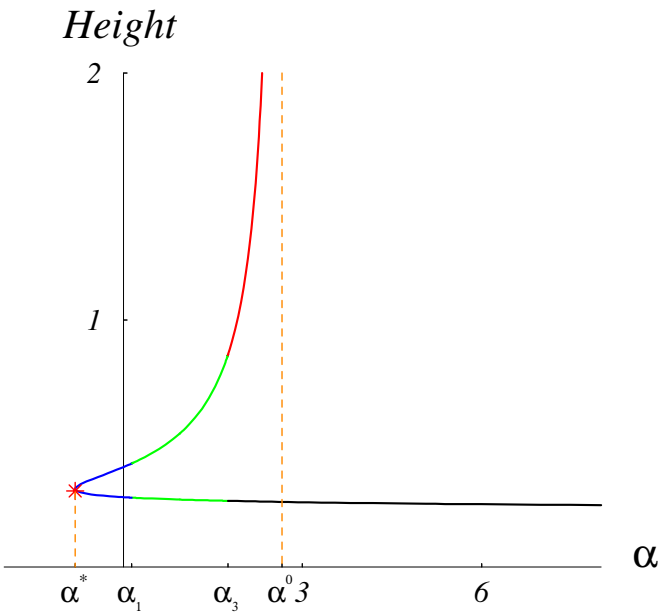

Figure 2.33. Heights of single-pulse **l** (upper branch) and **s** (lower branch). $a = 2.6$, $A = 2.8$, $u_T = 0.3$. $\alpha \in [\alpha^*, \alpha^0)$, there are two single-pulses. $\alpha \in [\alpha^0, \infty)$, there is only one single-pulse solution. Saddle node $\alpha = \alpha^*$ is where the large single-pulse **l** and the small single-pulse **s** become one. α^0 is where the large single-pulse **l** runs off to infinity.

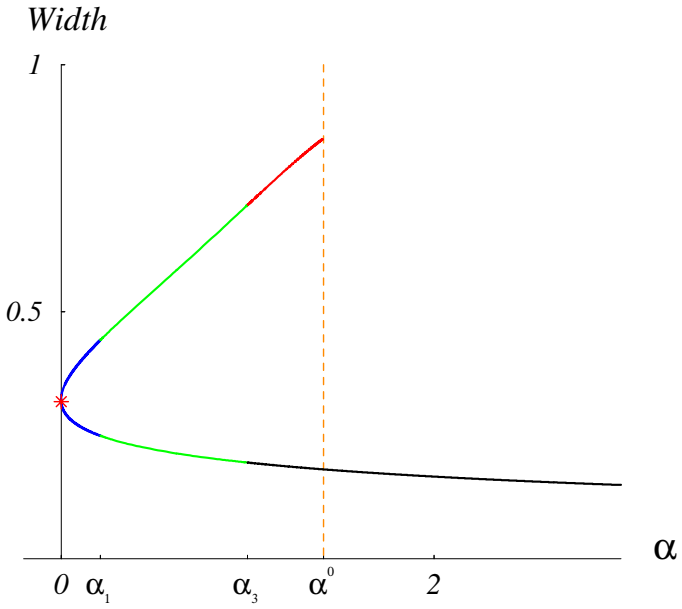

Figure 2.34. Widths of single-pulse **l** (upper branch) and **s** (lower branch). $a = 2.6$, $A = 2.8$, $u_T = 0.3$. $\alpha \in [\alpha^*, \alpha^0)$, there are two single-pulses. $\alpha \in [\alpha^0, \infty)$, there is only one single-pulse solution. Saddle node $\alpha = 0$ is where the large single-pulse **l** and the small single-pulse **s** become one. α^0 is where the large single-pulse **l** runs off to infinity.

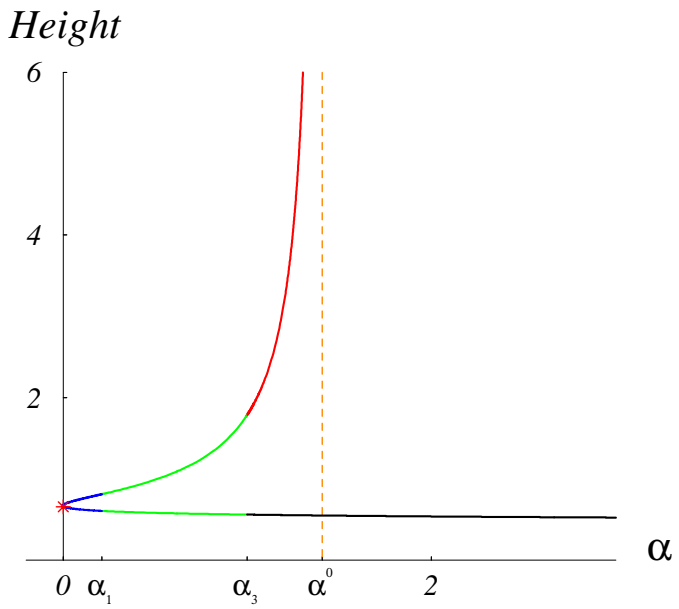

Figure 2.35. Heights of single-pulse **l** (upper branch) and **s** (lower branch). $a = 2.6$, $A = 2.8$, $u_T = 0.400273$. $\alpha \in [\alpha^*, \alpha^0)$, there are two single-pulses. $\alpha \in [\alpha^0, \infty)$, there is only one single-pulse solution. Saddle node $\alpha = 0$ is where the large single-pulse **l** and the small single-pulse **s** become one. α^0 is where the large single-pulse **l** runs off to infinity.

---

on the threshold (figure 2.23.) There also exists a transition point where a dimple-pulse breaks into a double-pulse (defined in Chapter 4). Examples are in section 2.10.2: figure 2.30 and figure 2.31.

The slope α governs the eigenvalue structure once a and A are fixed. When α is in the regime where $\omega_{1,2}$ are real, there are at most two single-pulses solutions. When α is in the regime that $\omega_{1,2}$ are complex, there are oscillations in the existence function. Oscillations sometimes result in the coexistence of more than two single-pulses depending on the threshold u_T. This implies that the gain function plays a role equally important as connection function. As α increases, single-pulses exist continuously until α reaches the critical value α^0. Once α reaches α^0, pulse **s** is still there, but pulse **l** runs off to infinity.

There are three ways that the large pulse **l** can disappear. First, for fixed α and u_T, if the excitation is too much, *i.e.*, ration A/a grows bigger and bigger, the width of the large pulse becomes wider and eventually the pulse breaks off (see section 2.7.4.) Secondly, with fixed excitation, *i.e.*, fixed a and A, if the gain is too big, *i.e.*, α is big, the large pulse eventually runs off to infinity. This is fully demonstrated in section 2.9. The third way is that the stable large pulse coalesces with the unstable small pulse and form a saddle node bifurcation. This is demonstrated in section

2.11. The stability of the large pulse and the instability of the small pulse will be shown in chapter 3.

2.13 Behavior in 4-parameter space

There are four parameters I want to vary. But it is not possible to plot a 4-D picture including all the parameters. I reduce the 4-D parameter space to 3-D by using α as $x-$axis, a/A as $y-$axis and u_T as $z-$axis.

From section (2.7.2), (2.8) and (2.9), for a fixed set (a, A, α), the first local maximum of $\Phi(x)$ is the maximum threshold that a pulse solution exists. I identify this maximum at which the large single-pulse **l** and the small single-pulse **s** coalesce into one pulse in a saddle node bifurcation. I first set $A = 1.5$, then vary the ratio a/A and α to identify the maximum u_T that supports single-pulse solutions. I then calculate the firing rate f_{max}, which is the maximum of the firing rate function with the single-pulse solution supported by the maximum threshold. Then I plot the maximum u_T and f_{max} to obtain two surfaces for maximum u_T vs a/A and α and f_{max} vs a/A and α. Below the surface of maximum u_T vs a/A and α, and above surface $u_T = 0$, there could be only one single-pulse **s**, coexistence of a single-pulse **s** and a single-pulse **l** (or a dimple-pulse **d** but in a smaller global range), or coexistence of more than two pulses. Next I increase A by step size 0.5 and repeat the above procedure to generate many surfaces described above. Globally I have a general idea of where there are pulse solutions (figure 2.36 and 2.37.) Notice that there are edges where the surfaces tends not to converge. That is where the large single-pulse runs off to infinity, and the corresponding α is the α^0 that is introduced in section (2.9.1). In general, if there is not too much excitation or inhibition and the firing rate is low, there are single-pulse solutions.

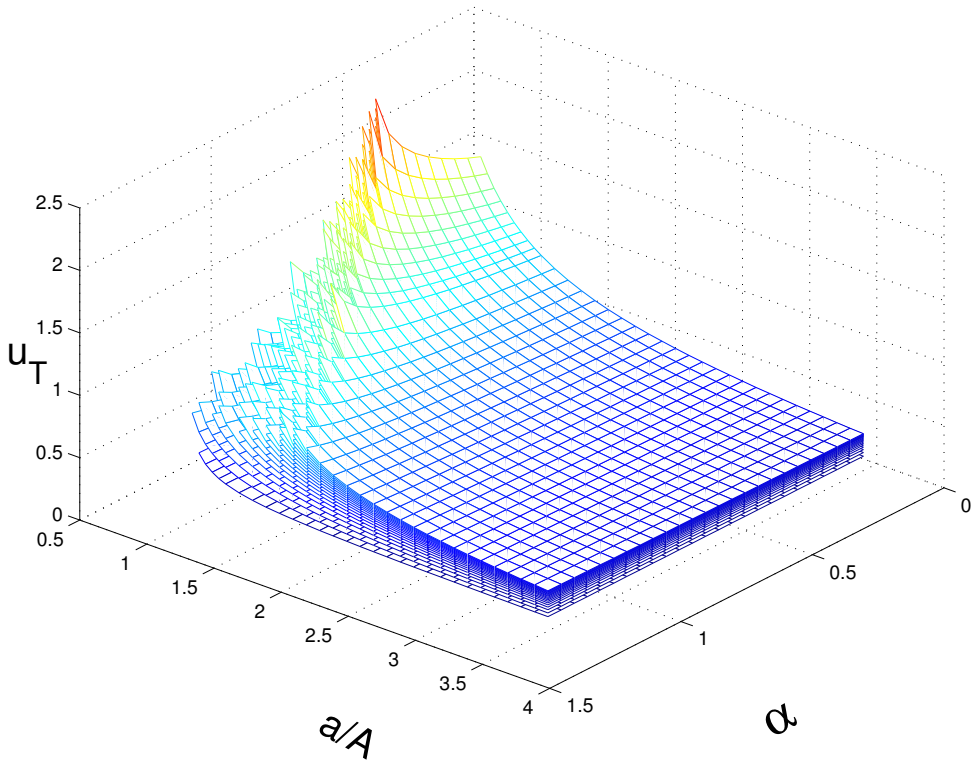

Figure 2.36. Global picture 1: Maximum threshold vs α and a/A.

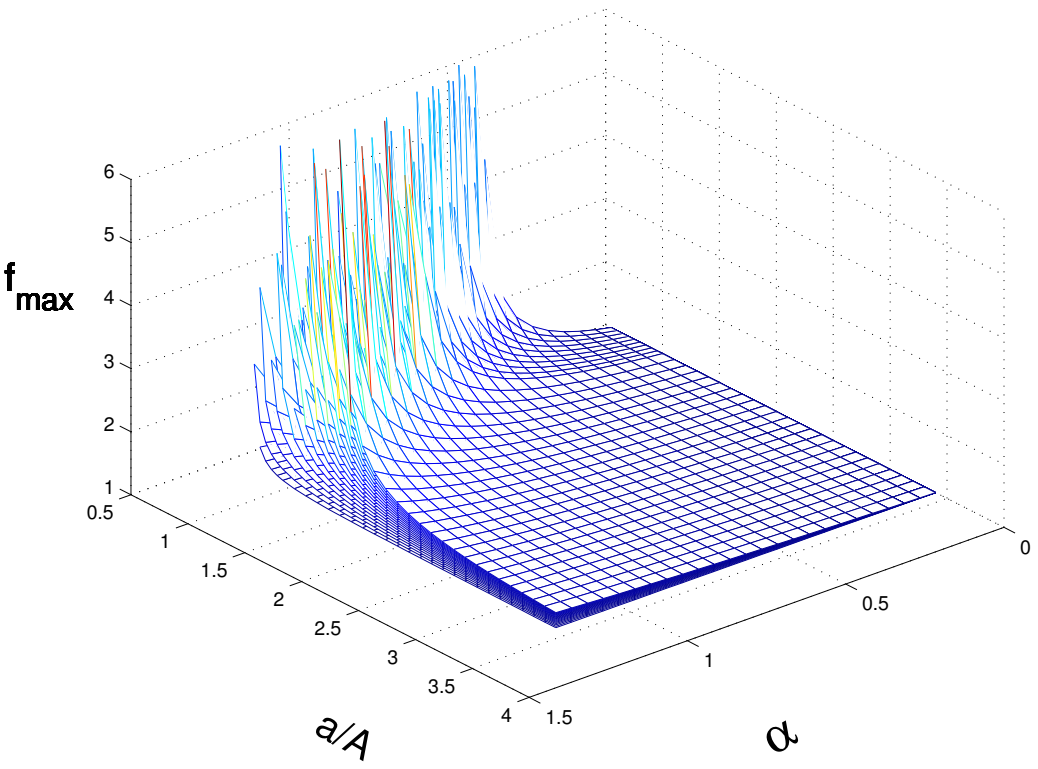

Figure 2.37. Global picture 2: Maximum point of firing rate vs α and a/A .

Chapter 3

Linear stability of standing pulses

In order for persistent activity to serve as a working memory, standing pulses must be stable to small perturbations. The goal is to examine the stability of

$$\frac{\partial u(x,t)}{\partial t} = -u(x,t) + \int_{-\infty}^{\infty} w(x-y) f[u(y,t)] dy. \tag{3.1}$$

to small perturbations. In this chapter, I will first review Amari's techniques of analyzing linear stability [3]. Since the firing rate function I adopt does not saturate, these techniques do not apply to the work in this thesis. I will examine the stability of the stationary pulse solution of (3.1) by adding a small perturbation and linearizing around the stationary solution. I derive an eigenvalue problem with two boundary (threshold points) terms which again comes from the discontinuity in the piece-wise linear firing rate function. It is difficult to analyze the eigenvalue system because of the boundary terms. A combination of analytical and numerical methods is used to fulfill this task. This stability analysis generalizes Amari's.

3.1 Amari's analysis for standing pulse stability

I first introduce Amari's techniques [3] to analyze the linear stability. Amari uses a Heaviside firing rate function $\Theta(u)$ in (3.1). Let $u(x,t)$ be a standing single-pulse solution at time t. The excited region for $u(x,t)$ is $R[u(x,t)] = (x_1, x_2)$. And let

$$c_1 = \frac{\partial u(x_1,t)}{\partial x} \qquad c_1 > 0$$

$$c_2 = -\frac{\partial u(x_2,t)}{\partial x} \qquad c_2 > 0$$

After a short time dt, $u(x,t)$ changes to $u(x,t+dt)$. The excited region at time $t+dt$ is

$$R[u(x,t+dt)] = (x_1(t+dt), x_2(t+dt)).$$

Then the boundary of the excited region satisfies

$$\begin{aligned} u(x_i(t),t) &= u_T \\ u(x_i+dx_i,t+dt) &= u_T \end{aligned}$$

where $x_i + dx_i = x_i(t+dt)$ $(i = 1, 2)$. A Taylor expansion of (3.2) around $u(x_i, t)$ gives

$$u(x_i,t) + \frac{\partial u(x_i,t)}{\partial x}dx_i + \frac{\partial u(x_i,t)}{\partial t}dt = u_T.$$

Thus

$$\frac{\partial u(x_i,t)}{\partial x}dx_i + \frac{\partial u(x_i,t)}{\partial t}dt = 0,$$
$$\frac{dx_i}{dt} = -\frac{\partial u(x_i,t)/\partial t}{\partial u(x_i,t)/\partial x}$$

From (3.1), $\frac{\partial u(x_i,t)}{\partial t} = -u(x_i,t) + \int_{x_1(t)}^{x_2(t)} w(x_i - y)\Theta[u(y,t)]dy$. Thus

$$\frac{dx_1}{dt} = -\frac{1}{c_1}[-u(x_1,t) + \int_{x_1}^{x_2} w(x_1-y)dy] = \frac{1}{c_1}[u_T - W(x_2-x_1)] \quad (3.2)$$

$$\frac{dx_2}{dt} = \frac{1}{c_2}[-u(x_2,t) + \int_{x_1}^{x_2} w(x_2-y)dy] = \frac{1}{c_2}[-u_T + W(x_2-x_1)] \quad (3.3)$$

Here $W(x) = \int_0^x w(y)dy$ and $W(x)$ is an odd function.

Let $\Delta(t) = x_2(t) - x_1(t)$. $\Delta(t)$ is the width of a single-pulse solution at time t. (3.3)-(3.2) yields

$$\frac{d\Delta}{dt} = (\frac{1}{c_1} + \frac{1}{c_2})[W(\Delta) - u_T] \quad (3.4)$$

Equation (3.4) can be further simplified to the following if the single-pulse is symmetric, *i.e.* $c_1 = c_2$.

$$\frac{d\Delta}{dt} = \frac{2}{c}[W(\Delta) - u_T] \quad (3.5)$$

This simple equation gives the condition for stability. The equilibrium of equation (3.5) is given by

$$W(\Delta) - u_T = 0.$$

The condition $W(\Delta) = u_T$ gives two single-pulse solutions (figure 3.1.) When $\Delta = \Delta_T^{\mathbf{l}}$, $\frac{dW(\Delta)}{d\Delta}|_{\Delta=\Delta_T^{\mathbf{l}}} < 0$, which means the width Δ of the single-pulse always is attracted toward the equilibrium. Therefore, this single-pulse solution is stable. When $\Delta = \Delta_T^{\mathbf{s}}$, $\frac{dW(\Delta)}{d\Delta}|_{\Delta=\Delta_T^{\mathbf{s}}} > 0$. This means the width Δ of the single-pulse is repelled from the equilibrium $\Delta_T^{\mathbf{s}}$. This single-pulse solution is unstable.

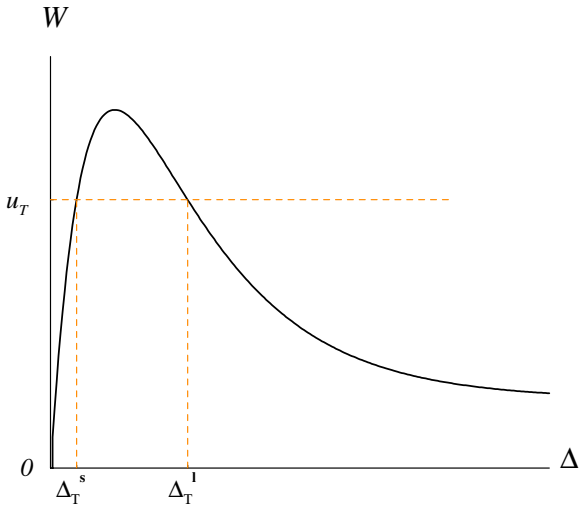

Figure 3.1. Function $W(\Delta) = \int_0^x w(y)dy$. At u_T, $W(\Delta)$ shows that we have a single-pulse solution that is wider and has width $\Delta_T^{\mathbf{l}}$ (**l**=large;) the second single-pulse solution is narrower and has width $\Delta_T^{\mathbf{s}}$ (**s**=small).

3.2 Eigenvalue problem

In this section, I derive the eigenvalue problem by linearizing the dynamical system around a stationary solution. Let $u(x)$ be the stationary standing pulse at time $t = 0$. After a short time period t, $u(x)$ evolves into $u(x,t) = u(x)+v(x,t)$, where $v(x,t) = \epsilon v(x)e^{\lambda t}$ is the small perturbation. $\epsilon > 0$ is small and $v(x)$ is a bounded and continuous function. The boundaries $-x_T$ and x_T of $u(x)$ change to $x_1(t)$, $x_2(t)$ respectively. x_1 and x_2 are functions of time t. Let $x_1(t) = -x_T + \Delta_1(t)$, $x_2(t) = x_T + \Delta_2(t)$, and $c = \frac{du(x)}{dx}\,|_{x=-x_T}$ where $\Delta_1(t)$ and $\Delta_2(t)$ are the changes of the boundaries $-x_T$ and x_T respectively, and $c > 0$.

Lemma 3.1. *Under the above assumption,*

$$\Delta_1(t) = -\frac{v(-x_T)e^{\lambda t}}{c}, \qquad \Delta_2(t) = \frac{v(x_T)e^{\lambda t}}{c}.$$

Proof of Lemma 3.1: By the definition of $x_1(t)$ and $u(x_1, t)$,

$$u(x_1, t) = u(-x_T + \Delta_1(t), t) = u_T,$$

where u_T is the threshold. Linearize $u(x, t)$ around $x = -x_T$ to get

$$\begin{aligned} u(-x_T, t) + u_x(-x_T, t)\Delta_1(t) &= u_T \\ u(-x_T) + v(-x_T, t) + u_x(-x_T, t)\Delta_1(t) &= u_T \\ v(-x_T, t) + \frac{\partial}{\partial x}[u(-x_T) + v(x_T, t)]\Delta_1(t) &= 0 \end{aligned}$$

Ignoring high order terms,

$$\begin{aligned} v(-x_T, t) + u'(-x_T)\Delta_1(t) &= 0 \\ \Delta_1(t) = -\frac{v(-x_T, t)}{c} &= -\frac{v(-x_T)e^{\lambda t}}{c} \end{aligned}$$

where c is the slope of $u(x)$ at x_T, *i.e.* $c = u'(-x_T)$ and $c > 0$.

Similarly,

$$v(x_T, t) + u'(x_T)\Delta_2(t) = 0$$

therefore,

$$\Delta_2 = \frac{v(x_T, t)}{c} = \frac{v(x_T)e^{\lambda t}}{c} \qquad \Diamond$$

Theorem 3.1. *Linearizing (3.1) around stationary solution $u(x)$, one can obtain the eigenvalue problem*

$$(1 + \lambda)v(x) = w(x - x_T)\frac{v(x_T)}{c} + w(x + x_T)\frac{v(-x_T)}{c} + \alpha \int_{-x_T}^{x_T} w(x - y)v(y)dy \qquad (3.6)$$

Proof of theorem 3.1: From (3.1)

$$\begin{aligned} \frac{\partial u(x,t)}{\partial t} + u(x,t) &= \int_{-\infty}^{\infty} w(x-y)[\alpha(u(y,t)-u_T)+1]\Theta(u-u_T)dy \\ \frac{\partial v(x,t)}{\partial t} + u(x) + v(x,t) &= \int_{x_1}^{x_2} w(x-y)[\alpha(u(y,t)-u_T)+1]dy \end{aligned} \tag{3.7}$$

Right-hand side of (3.7) is

$$\int_{-x_T}^{x_T} w(x-y)[\alpha(u(y)-u_T)+1]dy + \alpha\int_{-x_T}^{x_T} w(x-y)v(y,t)dy + I_1 + I_2$$

where

$$\begin{aligned} I_1 &= \int_{x_1}^{-x_T} w(x-y)[\alpha(u(y)+v(y,t)-u_T)+1]dy \\ I_2 &= \int_{x_T}^{x_2} w(x-y)[\alpha(u(y)+v(y,t)-u_T)+1]dy \end{aligned}$$

Since $u(x)$ is the stationary solution, it satisfies

$$u(x) = \int_{-x_T}^{x_T} w(x-y)[\alpha(u(y)-u_T)+1]dy$$

(3.7) becomes

$$v_t(x,t) + v(x,y) = \alpha\int_{-x_T}^{x_T} w(x-y)v(y,t)dy + I_1 + I_2 \tag{3.8}$$

Now let

$$F(x,y,t) = \int_0^y w(x-s)[\alpha(u(s)+v(s,t)-u_T)+1]ds.$$

Obviously,

$$\frac{\partial F}{\partial y} = w(x-y)[\alpha(u(y)+v(y,t)-u_T)+1]$$

$$F(x,x_1,t) = F(x,-x_T+\Delta_1,t)$$

$$
\begin{aligned}
&= F(x,-x_T,t) + \frac{\partial F}{\partial y}|_{y=-x_T}\Delta_1 + h.o.t. \\
&= F(x,-x_T,t) + w(x+x_T)[\alpha(u(-x_T)+v(-x_T,t)-u_T)+1]\Delta_1 + h.o.t.
\end{aligned}
$$

One can ignore all the high order terms including $v(-x_T,t)\Delta_1$, which is $-c\Delta_1^2$. Then

$$F(x,x_1,t) = F(x,-x_T,t) + w(x+x_T)\Delta_1$$

Similarly,

$$F(x,x_2,t) = F(x,x_T,t) + w(x-x_T)\Delta_2.$$

I_1 and I_2 can be written as

$$
\begin{aligned}
I_1 &= F(x,-x_T,t) - F(x,x_1,t) = w(x+x_T)\Delta_1 \\
I_2 &= F(x,x_2,t) - F(x,-x_T,t) = w(x-x_T)\Delta_2
\end{aligned}
$$

Now (3.8) becomes

$$v_t(x,t) + v(x,t) = \alpha\int_{-x_T}^{x_T} w(x-y)v(y,t)dy + w(x+x_T)\Delta_1 + w(x-x_T)\Delta_2 \tag{3.9}$$

Substitute Δ_1, Δ_2 derived in **Lemma 3.1** and $v(x,t) = \epsilon v(x)e^{\lambda t}$ into (3.9), to obtain

$$(1+\lambda)v(x) = w(x-x_T)\frac{v(x_T)}{c} + w(x+x_T)\frac{v(-x_T)}{c} + \int_{-x_T}^{x_T} w(x-y)v(y)dy \qquad \Diamond$$

If the real parts of all the eigenvalues λ are negative, the stationary solution $u(x)$ is stable. If the real part of one of the eigenvalues is positive, $u(x)$ is unstable. The two terms $w(x-x_T)\frac{v(x_T)}{c}$ and $w(x+x_T)\frac{v(-x_T)}{c}$ in (3.10) result from the boundary $-x_T$ and x_T where the jump occurs in the gain function. These two terms do not have any contribution both within the boundary, *i.e.* $(-x_T,x_T)$ and outside the boundary *i.e.* $(-\infty,-x_T)\cup(x_T,\infty)$.

3.3 Linear stability analysis of Amari's case

In the case of $\alpha = 0$, (3.1) has the form

$$\frac{\partial u(x,t)}{\partial t} = -u(x,t) + \int_{-\infty}^{\infty} w(x-y)\Theta[u(y,t)]dy \tag{3.10}$$

where $\Theta(u)$ is the Heaviside function. Applying the eigenvalue equation (3.6) to (3.10) yields

$$(1+\lambda)v(x) = w(x-x_T)\frac{v(x_T)}{c} + w(x+x_T)\frac{v(-x_T)}{c}$$

Substitute boundaries $-x_T$ and x_T to the above equation

$$\left(1+\lambda-\frac{w(0)}{c}\right)v(x_T) - \frac{w(2x_T)}{c}v(-x_T) = 0$$
$$-\frac{w(2x_T)}{c}v(x_T) + \left(1+\lambda-\frac{w(0)}{c}\right)v(-x_T) = 0$$

This system has non-trivial solution only when the determinant of the coefficient matrix is equal to 0. Set the determinant of the following matrix equal to 0 and solve for λ.

$$\begin{bmatrix} 1+\lambda-\frac{w(0)}{c} & -w(2x_T) \\ -w(2x_T) & 1+\lambda-\frac{w(0)}{c} \end{bmatrix}$$

Then

$$\lambda = \frac{w(0) \pm w(2x_T)}{c} - 1$$

When $\alpha = 0$, one can explicitly solve for λ upon the existence of the single-pulse solution that gives us the width x_T. And the value of λ is in agreement with Ref. [53].

Lemma 3.2. *When $\alpha = 0$, $u'(-x_T) = w(0) - w(2x_T)$ and $u'(-x_T) = -u'(x_T)$, where $u(x)$ is the stationary single-pulse solution.*

Proof of lemma 3.2: The stationary single-pulse solution of (3.10) satisfies

$$u(x) = \int_{-x_T}^{x_T} w(x-y)dy \tag{3.11}$$

Changing variables, (3.11) becomes

$$u(x) = \int_{x+x_T}^{x-x_T} w(y)dy \tag{3.12}$$

Differentiating $u(x)$ yields

$$u'(x) = w(x+x_T) - w(x-x_T)$$

Therefore $u'(-x_T) = w(0) - w(2x_T)$, and $u'(x_T) = w(2x_T) - w(0) = -u'(-x_T)$ $\Diamond$

Consider the example: $a = 2.4$, $A = 2.8$, $u_T = 0,400273$, $\alpha = 0$. There exist two single-pulses. From lemma 3.2, one of the eigenvalues is $\lambda = \dfrac{w(0) - w(2x_T)}{w(0) - w(2x_T)} - 1 = 0$. For the pulse **l**, $x_T^{\mathbf{l}} = 0.607255$ and $c = 1.94506$ gives $\lambda = \dfrac{w(0) + w(2x_T)}{c} - 1 = -0.165986 < 0$. Pulse **l** is stable. For pulse **s** $x_T^{\mathbf{s}} = 0.21325$, $c = 1.44675$ gives $\lambda = \dfrac{w(0) + w(2x_T)}{c} - 1 = 0.488339 > 0$. Thus, the small single-pulse is unstable.

3.4 Properties of the eigenvalue problem

In this section, I prove a number of properties of the eigenvalue problem. These properties are critical to the stability analysis of standing pulses.

Lemma 3.3. *The gain function* $f[u] = [\alpha(u-u_T)+1]]\,\Theta(u-u_T)$ *can be written as* $f[u] = F[u] + \Theta(u-u_T)$, *where* $F[u] = \alpha(u-u_T)\Theta(u-u_T)$.

Proof of lemma 3.3

It is obvious by distributing $\Theta(u-u_T)$ into the parenthesis (see figure 3.4.) $\Diamond$

Suppose

$$\phi_1(x) = \frac{1}{2a}\int_{-\infty}^{\infty} e^{-a|x-y|}(F_u + \Theta_u)v(y)dy$$

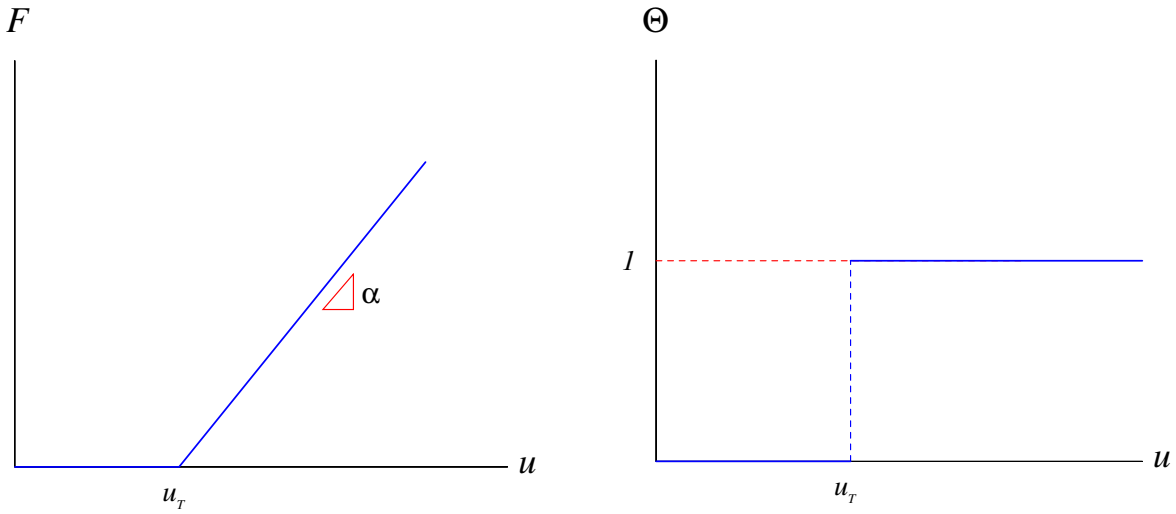

Figure 3.2. Function $F[u]$ and the Heaviside function $\Theta(u - u_T)$.

$$\phi_2(x) = \frac{1}{2}\int_{-\infty}^{\infty} e^{-|x-y|}(F_u + \Theta_u)v(y)dy$$

Lemma 3.4. *The RHS of (3.6) can be written as* $2(aA\phi_1 - \phi_2)$*, i.e.*

$$(1+\lambda)v = 2(aA\phi_1 - \phi_2)$$

Proof of lemma 3.4:

$$\begin{aligned}
(1+\lambda)v &= w(x-x_T)\frac{v(x_T)}{c} + w(x+x_T)\frac{v(-x_T)}{c} + \alpha\int_{-x_T}^{x_T} w(x-y)v(y)dy \\
&= \int_{-\infty}^{\infty} w(x-y)\frac{\delta(x-x_T)+\delta(x+x_T)}{c}v(y)dy + \int_{-\infty}^{\infty} w(x-y)F_u v(y)dy \\
&= \int_{-\infty}^{\infty} w(x-y)\Theta_u v(y)dy + \int_{-\infty}^{\infty} w(x-y)F_u v(y)dy \\
&= A\int_{-\infty}^{\infty} e^{-a|x-y|}(F_u+\Theta_u)v(y)dy - \int_{-\infty}^{\infty} e^{-|x-y|}(F_u+\Theta_u)v(y)dy \\
&= 2(aA\phi_1 - \phi_2) \qquad \Diamond
\end{aligned}$$

Lemma 3.5. *ϕ_1 and ϕ_2 satisfy the following ODEs respectively*

$$-\phi_1'' + a^2\phi_1 = (F_u + \Theta_u)v \tag{3.13}$$

$$-\phi_2'' + a^2\phi_2 = (F_u + \Theta_u)v \tag{3.14}$$

Proof of lemma 3.5: Differentiate ϕ_1 once and twice.

$$\phi_1' = \frac{1}{2}\left[\int_{-\infty}^{x} e^{-a(x-y)}(F_u+\Theta_u)v dy + \int_{x}^{\infty} e^{a(x-y)}(F_u+\Theta_u)v dy\right] \quad (3.15)$$

$$\phi_1'' = \frac{a}{2}\left[\int_{-\infty}^{x} e^{-a(x-y)}(F_u+\Theta_u)v dy + \int_{x}^{\infty} e^{a(x-y)}(F_u+\Theta_u)v dy - 2(F_u+\Theta_u)v\right] \quad (3.16)$$

$-(3.15)+a^2(3.16)$ yields

$$-\phi_1'' + a^2\phi_1 = (F_u+\Theta_u)v$$

$-\phi_2'' + a^2\phi_2 = (F_u+\Theta_u)v$ can be obtained in the same fashion. $\Diamond$

Lemma 3.6. $\lim_{x\to\pm\infty}\phi_{1,2}=0$ *and* $\lim_{x\to\pm\infty}\phi_{1,2}'=0$ *provided that* $v(x)$ *is bounded on* $(-\infty,\infty)$ *and exponentially decays to zero as* $x\to\pm\infty$

Proof of lemma 3.6: When $x >> x_T$

$$\begin{aligned}
\phi_1(x) &= \frac{1}{2a}\int_{-\infty}^{\infty} e^{-a|x-y|}(F_u+\Theta_u)v(y) \\
&= \frac{1}{2a}\left[\alpha\int_{-x_T}^{x_T} e^{-a|x-y|}v(y)dy + \int_{-x_T}^{x_T} e^{-a|x-y|}\frac{(\delta(x-x_T)+\delta(x+x_T))}{c}v(y)dy\right] \\
&= \frac{1}{2a}\left[\alpha\int_{-x_T}^{x_T} e^{-a(x-y)}v(y)dy + e^{-a|x-x_T|}\frac{v(x_T)}{c} + e^{-a|x+x_T|}\frac{v(-x_T)}{c}\right] \\
&= \frac{1}{2a}\left[\alpha e^{-ax}\int_{-x_T}^{x_T} e^{ay}v(y)dy + e^{-a(x-x_T)}\frac{v(x_T)}{c} + e^{-a(x+x_T)}\frac{v(-x_T)}{c}\right]
\end{aligned}$$

It is clear that $\lim_{x\to\infty}\phi_1=0$ provided that $v(x)$ is bounded on $[-x_T,x_T]$.

When $x << -x_T < 0$,

$$\phi_1(x) = \frac{1}{2a}\left[\alpha e^{ax}\int_{-x_T}^{x_T} e^{-ay}v(y)dy + e^{a(x-x_T)}\frac{v(x_T)}{c} + e^{a(x+x_T)}\frac{v(-x_T)}{c}\right]$$

Hence $\lim_{x\to-\infty}\phi_1=0$.

$$\phi_1' = \frac{1}{2}\left[-\int_{-\infty}^{x} e^{-a(x-y)}(F_u+\Theta_u)v dy + \int_{x}^{\infty} e^{a(x-y)}(F_u+\Theta_u)v dy\right]$$

As $x \to \infty$,

$$\begin{aligned}\lim_{x\to\infty}\phi_1' &= \lim_{x\to\infty}\left\{-\frac{1}{2}\int_{-\infty}^{x} e^{-a(x-y)}(F_u+\Theta_u)v dy\right\} \\ &= \lim_{x\to\infty}\left\{-\frac{e^{-ax}}{2}\left[\alpha\int_{-x_T}^{x_T} e^{ay}dy + e^{ay}\frac{v(x_T)}{c}\right]\right\}\end{aligned}$$

As $x \to -\infty$

$$\begin{aligned}\lim_{x\to\infty}\phi_1' &= \lim_{x\to-\infty}\left\{-\frac{1}{2}\int_{x}^{\infty} e^{a(x-y)}(F_u+\Theta_u)v dy\right\} \\ &= \lim_{x\to\infty}\left\{-\frac{e^{ax}}{2}\left[\alpha\int_{-x_T}^{x_T} e^{ay}dy + e^{ax_T}\frac{v(x_T)}{c}\right]\right\}\end{aligned}$$

Similarly, one can prove that $\lim_{x\to\pm\infty}\phi_2 = 0$ and $\lim_{x\to\pm\infty}\phi_2' = 0$.

Therefore, $\lim_{x\to\pm\infty}\phi_{1,2} = 0$, $\lim_{x\to\pm\infty}\phi_{1,2}' = 0$. $\Diamond$

Theorem 3.2. *Eigenvalue λ in (3.10) is real.*

Proof of Theorem 3.2: $aA\bar{\phi_1}(3.13) - \bar{\phi_2}(3.14)$ gives

$$aA\bar{\phi_1}(-\phi_1'' + a^2\phi_1) - \bar{\phi_2}(-\phi_2'' + \phi_2) = (F_u+\Theta_u)v(aA\bar{\phi_1} - \bar{\phi_2}) \tag{3.17}$$

where $\bar{\phi}_{1,2}$ are the complex conjugates of $\phi_{1,2}$. Integration by parts gives

$$\int_{-\infty}^{\infty}\bar{\phi_1}\phi_1'' dx = \bar{\phi_1}\phi_1'|_{-\infty}^{\infty} - \int_{-\infty}^{\infty}\bar{\phi_1'}\phi_1' dx = \int_{-\infty}^{\infty}\left|\phi_1'\right|^2 dx$$

and similarly $\int_{-\infty}^{\infty}\bar{\phi_2}\phi_2'' dx = \int_{-\infty}^{\infty}\left|\phi_2'\right|^2 dx$. From lemma 3.4

$$\begin{aligned}\frac{1}{2}(1+\lambda)v &= aA\phi_1 - \phi_2 \\ \frac{1}{2}(1+\bar{\lambda})\bar{v} &= aA\bar{\phi_1} - \bar{\phi_2}\end{aligned}$$

Integrating both sides of (3.17) gives

$$aA\left(\int_{-\infty}^{\infty}|\phi_1'|^2 dx + a^2\int_{-\infty}^{\infty}|\phi_1|^2 dx\right) - \left(\int_{-\infty}^{\infty}|\phi_2'|^2 dx + \int_{-\infty}^{\infty}|\phi_2|^2 dx\right) = \frac{1}{2}(1+\bar{\lambda})\int_{-\infty}^{\infty}|v|^2(F_u+\Theta_u)dx$$

$\int_{-\infty}^{\infty} |v|^2 \Theta_u dx = \frac{1}{c}\int_{-\infty}^{\infty} |v|^2 (\delta(x-x_T)+\delta(x+x_T))\,dx = \frac{1}{c}\left(|v(x_T)|^2 + |v(-x_T)|^2\right)$ Hence

$$\frac{1}{2}(1+\bar{\lambda}) = \frac{aA\left(\int_{-\infty}^{\infty}|\phi_1'|^2\,dx + a^2\int_{-\infty}^{\infty}|\phi_1|^2\,dx\right) - \left(\int_{-\infty}^{\infty}|\phi_2'|^2\,dx + \int_{-\infty}^{\infty}|\phi_2|^2\,dx\right)}{\int_{-\infty}^{\infty} F_u|v|^2 + \frac{1}{c}\left(|v(x_T)|^2 + |v(-x_T)|^2\right)} \tag{3.18}$$

The right-hand side of (3.18) is real, therefore λ has to be real. $\Diamond$

Theorem 3.3. *Eigenvalue λ in (3.10) is bounded by $\lambda_b \equiv \frac{2k_0}{c} + 2\alpha k_1 x_T - 1$ where k_0 is the maximum of $|w(x)|$ on $[0, 2x_T]$ and $|w(x-y)| \le k_1$ for all $(x,y) \in J \times J$, $J = [-x_T, x_T]$.*

Proof of theorem 3.3: Define a linear operator L: $C[-x_T, x_T] \to C[-x_T, x_T]$ such that

$$Lv(x) = w(x-x_T)\frac{v(x_T)}{c} + w(x+x_T)\frac{v(-x_T)}{c} + \alpha\int_{-x_T}^{x_T} w(x-y)v(y)dy$$

The norm on $C[-x_T, x_T]$ is defined as

$$\|.\| = \max_{x\in J}|v(x)|$$

Function $w(x-y)$ is continuous on square $J \times J$. The eigenvalue problem derived in section 3.2 gives

$$(1+\lambda)v = Lv \tag{3.19}$$

Taking the norm of both sides of (3.19),

$$(1+\lambda)\|v\| = \|Lv\|$$

$$\begin{aligned}
\|Lv\| &= \left\| w(x-x_T)\frac{v(x_T)}{c} + w(x+x_T)\frac{v(-x_T)}{c} + \alpha\int_{-x_T}^{x_T} w(x-y)v(y)dy \right\| \\
&= \max_{x\in J}\left| w(x-x_T)\frac{v(x_T)}{c} + w(x+x_T)\frac{v(-x_T)}{c} + \alpha\int_{-x_T}^{x_T} w(x-y)v(y)dy \right| \\
&\le \max_{x\in J}\left| w(x-x_T)\frac{v(x_T)}{c}\right| + \max_{x\in J}\left| w(x+x_T)\frac{v(-x_T)}{c}\right| + \max_{x\in J}\left|\alpha\int_{-x_T}^{x_T} w(x-y)v(y)dy\right|
\end{aligned}$$

$$
\begin{aligned}
&\leq |w(x-x_T)|\,\frac{\|v(x)\|}{c} + |w(x+x_T)|\,\frac{\|v(x)\|}{c} + \alpha\int_{-x_T}^{x_T}\max_{x\in J}\{|w(x-y)|\}\,\|v(y)\|\,dy \\
&\leq 2k_0\frac{\|v(x)\|}{c} + 2\alpha k_1 x_T\|v(x)\|
\end{aligned}
$$

where

$$
k_0 = \max_{x\in J}|w(x-x_T)| = \max_{x\in J}|w(x+x_T)|
$$

since $w(x)$ is symmetric. And $|w(x-y)| \leq k_1$ for all $(x,y) \in J \times J$. Therefore

$$
\begin{aligned}
(1+\lambda)\|v(x)\| = \|Lv(x)\| &\leq 2k_0\frac{\|v(x)\|}{c} + 2\alpha k_1 x_T\|v(x)\| \\
\lambda &\leq \frac{2k_0}{c} + 2\alpha k_1 x_T - 1 \equiv \lambda_b. \qquad \Diamond
\end{aligned}
$$

Theorem 3.4. *Define operator L: $C[-x_T, x_T] \to C[-x_T, x_T]$ such that*

$$
Lv(x) = w(x-x_T)\frac{v(x_T)}{c} + w(x+x_T)\frac{v(-x_T)}{c} + \alpha\int_{-x_T}^{x_T} w(x-y)v(y)dy
$$

Then L is a compact operator on $C[-x_T, x_T]$

Proof of theorem 3.4: Operator

$$
T_1(v(x)) = w(x-x_T)\frac{v(x_T)}{c} + w(x+x_T)\frac{v(-x_T)}{c}: \qquad C[-x_T, x_T] \to C[-x_T, x_T]
$$

is linear. The bound of T_1 follows from

$$
\begin{aligned}
\|T_1 v\| &= \max_{x\in J}\left|w(x-x_T)\frac{v(x_T)}{c} + w(x+x_T)\frac{v(-x_T)}{c}\right| \\
&\leq |w(x-x_T)|\frac{\|v(x)\|}{c} + |w(x+x_T)|\,\frac{\|v(x)\|}{c} \\
&\leq 2k_0\frac{\|v\|}{c}
\end{aligned}
$$

Let v_n be any bounded sequence in $C[-x_T, x_T]$ and $\|v_n\| \leq c_0$ for all n. Let $y_n = T_1 v_n$. Then $\|y_n\| \leq \|T_1\|\|v_n\|$. Hence sequence y_n is bounded and equicontinuous. Since $w(x,t) = w(x-t)$ is continuous on $J \times J$ and $J \times J$ is compact, w is uniformly continuous on $J \times J$. Hence, for any

given $\epsilon > 0$, there is a $\delta > 0$ such that for $t = x_T$ and all $x_1, x_2 \in J$ satisfying $|x_1 - x_2| < \delta$

$$|w(x_1 - x_T) - w(x_2 - x_T)| < \frac{c}{2c_0}\epsilon.$$

Consequently, for x_1, x_2 as before and every n, one can obtain

$$\begin{aligned} |y_n(x_1) - y_n(x_2)| &= \left| [w(x_1 - x_T) - |w(x_2 - x_T)] \frac{v_n(x_T)}{c} + [w(x_1 + x_T) - w(x_2 + x_T)] \frac{v_n(-x_T)}{c} \right| \\ &< |w(x_1 - x_T) - |w(x_2 - x_T)| \frac{c_0}{c} + |w(x_1 + x_T) - w(x_2 + x_T)| \frac{c_0}{c} \\ &< \frac{c}{2c_0}\epsilon\frac{c_0}{c} + \frac{c}{2c_0}\epsilon\frac{c_0}{c} = \epsilon \end{aligned}$$

This proves the equicontinuity of y_n. By Ascoli's theorem, y_n has a convergent subsequence. v_n is a arbitrary bounded sequence and $y_n = T_1 v_n$. By the compactness criterion: an operator is compact if and only if it maps every bounded sequence x_n in X onto a sequence Tx_n in Y which has a convergent subsequence. The compactness of T_1 follows from this criterion.

Using similar technique, one can prove the integral linear operator

$$T_2(v(x)) = \alpha \int_{-x_T}^{x_T} w(x - y)v(y)dy$$

is compact. The proof is given in [38]. The sum of two compact linear operators, $T_1 + T_2$, is compact. $\Diamond$

Theorem 3.5. *$\lambda = -1$ is the only possible accumulation point of the set of all λ values in the eigenvalue problem. And every spectral value $\lambda \neq -1$ of L is an eigenvalue of L.*

Proof of theorem 3.5: Let $\gamma = (1 + \lambda)$, the eigenvalue problem becomes

$$\gamma v(x) = Lv(x),$$

and the linear operator L is compact on the normed space $C[-x_T, x_T]$. γ is the eigenvalue of operator L. By theorem 2.2 proved in [37]: the only possible point of accumulation is $\gamma = 0$, *i.e.*, $\lambda = -1$.

The second part of the theorem can be easily derived from the following property of eigenvalues

of compact operators proven in [39]. Let $T : X \to X$ be a compact linear operator on a Banach space X. Then every spectral value $\gamma \neq 0$ of T (if it exists) is an eigenvalue of T. $\gamma \neq 0$ corresponds to $\lambda \neq -1$ for compact operator L. Therefore, every spectral value $\lambda \neq -1$ of L is an eigenvalue of L. $\Diamond$

Remark 3.1. *This theorem shows that if the compact operator L has infinitely many eigenvalues, on can arrange them in a sequence converging to* -1. *Theorem 3.5 also implies that the only possible continuous spectrum is* -1. *There is no continuous spectrum when* $\lambda > -1$. *Therefore, all the spectral values* λ *such that* $\lambda > -1$ *are eigenvalues.*

Theorem 3.6. 0 *is an eigenvalue.*

Proof of theorem 3.6: Consider the equilibrium equation

$$\begin{aligned} u(x) &= \int_{-\infty}^{\infty} w(x-y) f[u(y)] dy \\ &= \int_{-x_T}^{x_T} w(x-y) \left\{ \alpha \left[u(y) - u_T \right] + 1 \right\} dy \end{aligned} \tag{3.20}$$

where $u(x)$ is a stationary standing pulse solution. After a change of variables $p = x - y$, (3.20) becomes

$$u(x) = \int_{x+x_T}^{x-x_T} w(p) \left\{ \alpha \left[u(x-p) - u_T \right] + 1 \right\} dy \tag{3.21}$$

Differentiating (3.21) with respect to x yields

$$\begin{aligned} u'(x) &= w(x+x_T) \left[\alpha(u(-x_T) - u_T) + 1 \right] - w(x-x_T) \left[\alpha(u(x_T) - u_T) + 1 \right] \\ &\quad + \alpha \int_{x-x_T}^{x+x_T} w(p) u'(x-p) dp \end{aligned} \tag{3.22}$$

Since $u(-x_T) = u(x_T) = u_T$ and $u'(-x_T) = c = -u'(x_T)$,

$$\begin{aligned} u'(x) &= w(x+x_T) \frac{u'(-x_T)}{c} - w(x-x_T) \frac{-u'(x_T)}{c} + \alpha \int_{x-x_T}^{x+x_T} w(p) u'(x-p) dp \\ &= w(x-x_T) \frac{u'(x_T)}{c} + w(x+x_T) \frac{u'(-x_T)}{c} + \alpha \int_{-x_T}^{x_T} w(x-y) u'(y) dy \end{aligned} \tag{3.23}$$

(3.23) is the eigenvalue problem (3.10) with eigenvalue satisfying $1+\lambda = 1$, resulting in $\lambda = 0$. The corresponding eigenfunction is $u'(x)$.Therefore, $\lambda = 0$ is an eigenvalue of (3.10) corresponding to eigenfunction $u'(x)$. $\Diamond$

3.4.1 The discontinuity of the eigenfunctions at the boundaries

Consider the following eigenvalue equation

$$(1+\lambda)v(x) = w(x-x_T)\frac{v(x_T)}{c} + w(x+x_T)\frac{v(-x_T)}{c} + \alpha\int_{-x_T}^{x_T} w(x-y)v(y)dy \tag{3.24}$$

where $v'(x)$, $v''(x)$ and $v'''(x)$ are continuous on $(-\infty,-x_T)$, $(-x_T,x_T)$ and (x_T,∞). They have discontinuities at $-x_T$ and x_T because $w'(x)$ is discontinuous at 0. In order to know the jumps of $v'(x)$, $v''(x)$ and $v'''(x)$ at the boundaries $-x_T$ and x_T, I first prove proposition 3.1.

Proposition 3.1. *If* $W(x) = \int_{-x_T}^{x_T} w(x-y)v(y)dy$ *with* $x \in (-\infty,\infty)$. *Then* $W(x)$ *and* $W'(x)$ *are continuous at the boundaries* $-x_T$ *and* x_T. *But* $W''(x)$ *and* $W'''(x)$ *are discontinuous at* $-x_T$ *and* x_T.

Proof of proposition 3.1:

It is obvious that $W(x)$ is continuous on $(-\infty,\infty)$ by the continuity of $v(x)$ and $w(x)$ on $(-\infty,\infty)$. By change of variable,

$$W(x) = \int_{-x_T}^{x_T} w(x-y)v(y)dy = \int_{x+x_T}^{x-x_T} w(z)v(x-z)dz.$$

$$W'(x) = w(x+x_T)v(-x_T) - w(x-x_T)v(x_T) - \int_{x+x_T}^{x-x_T} w(z)v'(x-z)dz$$

$W'(x)$ is continuous on $(-\infty,\infty)$.

For $x \in (-\infty,\infty)$, and $x \neq -x_T, x_T$,

$$\begin{aligned} W''(x) &= w'(x+x_T)v(-x_T) - w'(x-x_T)v(x_T) + w(x+x_T)v'(-x_T^+) - w(x-x_T)v'(x_T^-) \\ &- \int_{x+x_T}^{x-x_T} w(z)v''(x-z)dz \end{aligned}$$

Since $w'(x \pm x_T)$ appears in $W''(x)$ and $w'(x \pm x_T)$ are discontinuous at the boundaries $x = x_T$, $W''(x)$ is discontinuous at the boundaries. I use the notation $[\cdot]$ to represent the jump at the boundary, *i.e.*, $[W''(x_T)]$ is the jump of $W''(x)$ at x_T. Then

$$\begin{aligned} \left[W''(x_T)\right] &= -\left[w'(0)\right] v(x_T) \\ \left[W''(-x_T)\right] &= \left[w'(0)\right] v(-x_T) \end{aligned}$$

When $x \neq -x_T, x_T$,

$$\begin{aligned} W'''(x) &= w''(x+x_T)v(-x_T) - w''(x-x_T)v(x_T) + w'(x+x_T)v'(-x_T^+) - w'(x-x_T)v'(x_T^-) \\ &+ w(x+x_T)v''(-x_T^+) - w(x-x_T)v''(x_T^-) - \int_{x+x_T}^{x-x_T} w(z)v'''(x-z)dz \end{aligned}$$

$$\begin{aligned} \left[W'''(x_T)\right] &= -\left[w''(0)\right] v(x_T) - \left[w'(0)\right] v'(x_T^-) \\ \left[W'''(-x_T)\right] &= \left[w''(0)\right] v(-x_T) + \left[w'(0)\right] v'(-x_T^+) \qquad \Diamond \end{aligned}$$

The eigenvalue problem (3.24) can be written as

$$c(1+\lambda)v(x) = w(x-x_T)v(x_T) + w(x+x_T)v(-x_T) + c\alpha W(x) \tag{3.25}$$

$v(x)$ is continuous on $(-\infty, \infty)$. $v(x)$ has no jumps at $-x_T$ and x_T.

$$[v(-x_T)] = [v(x_T)] = 0$$

Differentiating (3.25) once for $x \neq -x_T$ and $x \neq x_T$, I obtain

$$c(1+\lambda)v'(x) = w'(x-x_T)v(x_T) + w'(x+x_T)v(-x_T) + c\alpha W'(x)$$

$v'(x)$ is discontinuous at the boundaries because of the discontinuity of $w'(x)$ at the boundaries

and the jumps of $v'(x)$ at the boundaries come from $w'(0)$. Therefore

$$\begin{aligned}\left[v'(x_T)\right] &= \frac{1}{c(1+\lambda)}\left[w'(0)\right]v(x_T),\\ \left[v'(-x_T)\right] &= \frac{1}{c(1+\lambda)}\left[w'(0)\right]v(-x_T).\end{aligned}$$

Differentiating (3.25) twice to get the jumps of $v(x)$ at $-x_T$ and x_T.

$$c(1+\lambda)v''(x) = w''(x-x_T)v(x_T)+w''(x+x_T)v(-x_T)+c\alpha W''(x) \qquad x\neq -x_T, x_T$$

There are jumps of $v''(x)$ at $-x_T$ and x_T that come from either $W(-x_T)$ or $W(x_T)$. However no jumps come from $w''(0)$ because $w''(0^-)=w''(0^+)$. And the jumps of $v''(x)$ at $-x_T$ and x_T are

$$\begin{aligned}\left[v''(x_T)\right] &= \frac{\alpha}{1+\lambda}\left[W''(x_T)\right] = -\frac{\alpha}{1+\lambda}\left[w'(0)\right]v(x_T),\\ \left[v''(-x_T)\right] &= \frac{\alpha}{1+\lambda}\left[W''(-x_T)\right] = \frac{\alpha}{1+\lambda}\left[w'(0)\right]v(-x_T).\end{aligned}$$

$$c(1+\lambda)v'''(x) = w'''(x-x_T)v(x_T)+w'''(x+x_T)v(-x_T)+c\alpha W'''(x) \qquad x\neq -x_T, x_T.$$

The jumps of $v'''(x)$ at $-x_T$ and x_T are

$$\begin{aligned}\left[v'''(x_T)\right] &= \frac{1}{c(1+\lambda)}\left[w'''(0)\right]v(x_T)+\frac{\alpha}{1+\lambda}\left[W'''(x_T)\right]\\ &= \frac{1}{c(1+\lambda)}\left[w'''(0)\right]v(x_T)-\frac{\alpha}{1+\lambda}\left[w'(0)\right]v'(x_T^-),\\ \left[v'''(-x_T)\right] &= \frac{1}{c(1+\lambda)}\left[w'''(0)\right]v(-x_T)+\frac{\alpha}{1+\lambda}\left[W'''(x_T)\right]\\ &= \frac{1}{c(1+\lambda)}\left[w'''(0)\right]v(-x_T)+\frac{\alpha}{1+\lambda}\left[w'(0)\right]v'(-x_T^+)\end{aligned}$$

To calculate the jumps explicitly, one must know $[w'(0)]$ and $[w'''(0)]$.

$$w(x) = \begin{cases} Ae^{-ax}-e^{-x} & \text{if } x\geq 0\\ Ae^{ax}-e^{x} & \text{if } x<0\end{cases}$$

$$
\begin{aligned}
w'(x) &= \begin{cases} -aAe^{-ax} + e^{-x} & \text{if } x \geq 0 \\ aAe^{ax} - e^{x} & \text{if } x < 0 \end{cases} \\
w''(x) &= \begin{cases} a^2Ae^{-ax} - e^{-x} & \text{if } x \geq 0 \\ -a^2Ae^{ax} - e^{x} & \text{if } x < 0 \end{cases} \\
w'''(x) &= \begin{cases} -a^3Ae^{-ax} + e^{-x} & \text{if } x \geq 0 \\ a^3Ae^{ax} - e^{x} & \text{if } x < 0 \end{cases}
\end{aligned}
$$

$$
\begin{aligned}
w'(0^+) &= 1 - aA, & w'(0^-) &= aA - 1 \\
w''(0^+) &= a^2A - 1, & w''(0^-) &= a^2A - 1 \\
w'''(0^+) &= 1 - a^3A, & w'''(0^-) &= a^3A - 1
\end{aligned}
$$

Hence,

$$
\begin{aligned}
\big[w'(0)\big] &= w'(0^+) - w'(0^-) = -2(aA - 1) \\
\big[w''(0)\big] &= w''(0^+) - w''(0^-) = 0 \\
\big[w'''(0)\big] &= w'''(0^+) - w'''(0^-) = 2(1 - a^3A)
\end{aligned}
$$

These results lead directly to the following theorem.

Theorem 3.7. *The continuous eigenfunction $v(x)$ on $(-\infty, \infty)$ in (3.10) has the following jumps in its first order, second order and third order derivatives at the boundary $-x_T$ and x_T.*

$$
\begin{aligned}
[v(x_T)] &= 0 \\
\big[v'(x_T)\big] &= \frac{2\alpha(1 - aA)}{1 + \lambda} v(x_T) \\
\big[v''(x_T)\big] &= \frac{2(aA - 1)}{c(1 + \lambda)} v(x_T) \\
\big[v'''(x_T)\big] &= \frac{2(1 - a^3A)}{c(1 + \lambda)} v(x_T) + \frac{2\alpha(aA - 1)}{1 + \lambda} v'(x_T^-)
\end{aligned}
$$

$$
[v(-x_T)] = 0
$$

$$
\begin{aligned}
\left[v'(-x_T)\right] &= \frac{2\alpha(1-aA)}{1+\lambda}v(-x_T) \\
\left[v''(-x_T)\right] &= \frac{-2(aA-1)}{c(1+\lambda)}v(-x_T) \\
\left[v'''(-x_T)\right] &= \frac{2(1-a^3A)}{c(1+\lambda)}v(-x_T) - \frac{2\alpha(aA-1)}{1+\lambda}v'(-x_T^+).
\end{aligned}
$$

3.5 Reduction of the eigenvalue problem to ODE

In this section, I reduce the eigenvalue problem to ordinary differential equations. In section 3.4.1, I have shown that $v'(x)$, $v''(x)$ and $v'''(x)$ have discontinuities at the boundaries $-x_T$ and x_T. I will not reduce the eigenvalue problem to a uniform ODE valid on $(-\infty, \infty)$. I first derive the ODE from (3.10) on $[-x_T, x_T]$, then I derive the ODEs for $\Re - J$ where $J = [-x_T, x_T]$.

3.5.1 ODE on $[-x_T, x_T]$

Let $T(x) = w(x - x_T)\dfrac{v(x_T)}{c} + w(x + x_T)\dfrac{v(-x_T)}{c}$. Then

$$
\begin{aligned}
T(x) &= \left[Ae^{-a(x-x_T)} - e^{-(x-x_T)}\right]\frac{v(x_T)}{c} + \left[Ae^{-a(x+x_T)} - e^{-(x+x_T)}\right]\frac{v(-x_T)}{c} \\
T''(x) &= \left[a^2Ae^{-a(x-x_T)} - e^{-(x-x_T)}\right]\frac{v(x_T)}{c} + \left[a^2Ae^{-a(x+x_T)} - e^{-(x+x_T)}\right]\frac{v(-x_T)}{c} \\
T^{(iv)}(x) &= \left[a^4Ae^{-a(x-x_T)} - e^{-(x-x_T)}\right]\frac{v(x_T)}{c} + \left[a^4Ae^{-a(x+x_T)} - e^{-(x+x_T)}\right]\frac{v(-x_T)}{c}
\end{aligned}
$$

It is a simple calculation to show that

$$
T^{(iv)}(x) - (1+a^2)T''(x) + a^2T(x) = 0
$$

Set

$$
\begin{aligned}
I_1(x) &= \alpha\int_{-x_T}^{x} Ae^{-a(x-y)}v(y)dy, & I_2(x) &= \alpha\int_{-x_T}^{x} e^{-(x-y)}v(y)dy \\
I_3(x) &= \alpha\int_{x}^{x_T} Ae^{a(x-y)}v(y)dy, & I_4(x) &= \alpha\int_{x}^{x_T} e^{(x-y)}v(y)dy
\end{aligned}
$$

Then

$$\alpha \int_{-x_T}^{x_T} w(x-y)v(y)dy = I_1 - I_2 + I_3 - I_4$$

$$I_1' = -aI_1 + \alpha A v(x), \qquad I_2' = -I_2 + \alpha v(x)$$
$$I_3' = aI_3 - \alpha A v(x), \qquad I_4' = I_4 - \alpha v(x)$$

The eigenvalue problem (3.10) is

$$(1+\lambda)v(x) = T(x) + I_1 - I_2 + I_3 - I_4 \tag{3.26}$$

Differentiating (3.26) repeatedly gives

$$\begin{aligned}
(1+\lambda)v'(x) &= T'(x) - aI_1 + I_2 + aI_3 - I_4 && (3.27)\\
(1+\lambda)v''(x) &= T''(x) + a^2 I_1 - I_2 + a^2 I_3 - I_4 + 2\alpha(1-aA)v(x) && (3.28)\\
(1+\lambda)v'''(x) &= T'''(x) - a^3 I_1 + I_2 + a^3 I_3 - I_4 + 2\alpha(1-aA)v'(x) && (3.29)\\
(1+\lambda)v''''(x) &= T^{(iv)}(x) + a^4 I_1 - I_2 + a^4 I_3 - I_4 + 2\alpha(1-a^3A)v(x) \\
&\quad +2\alpha(1-aA)v''(x) && (3.30)
\end{aligned}$$

Take (3.26)-(3.29) as a linear system of I_1, I_2, I_3 and I_4.

$$\begin{aligned}
I_1 - I_2 + I_3 - I_4 &= (1+\lambda)v(x) - T(x) && (3.31)\\
-aI_1 + I_2 + aI_3 - I_4 &= (1+\lambda)v'(x) - T'(x) && (3.32)\\
a^2 I_1 - I_2 + a^2 I_3 - I_4 &= (1+\lambda)v''(x) - 2\alpha(1-aA)v(x) - T''(x) && (3.33)\\
-a^3 I_1 + I_2 + a^3 I_3 - I_4 &= (1+\lambda)v'''(x) - 2\alpha(1-aA)v'(x) - T'''(x) && (3.34)
\end{aligned}$$

Taking (3.33) $- a^2$(3.31) gives

$$I_2 + I_4 = \frac{1}{a^2-1}\left[(\lambda+1)v'' + (2\alpha aA - 2\alpha - a^2\lambda - a^2)v + a^2 T - T''\right]$$

Substitute $I_2 + I_4$ into (3.31)

$$\begin{aligned} I_1 + I_3 &= I_2 + I_4 + (\lambda+1)v - T \\ &= \frac{1}{a^2-1}\left[(\lambda+1)v'' + (2\alpha a A - 2\alpha - \lambda - 1)v + T - T''\right] \end{aligned}$$

Substituting both I_1+I_3 and I_2+I_4 into (3.30), one can obtain the fourth order ordinary differential equation for $x \in [-x_T, x_T]$

$$(1+\lambda)v'''' - \left[(1+\lambda)(a^2+1) + 2\alpha(1-aA)\right]v'' + \left[(\lambda+1)a^2 - 2\alpha a(A-a)\right]v = 0 \tag{3.35}$$

3.5.2 ODE on $x \in (-\infty, -x_T]$ and $[x_T, \infty)$.

I first derive the ODE that is valid on $[x_T, \infty)$. When $x \in [x_T, \infty)$,

$$\begin{aligned} T(x) &= w(x-x_T)\frac{v(x_T)}{c} + w(x+x_T)\frac{v(-x_T)}{c} \\ &= \left[Ae^{-a(x-x_T)} - e^{-(x-x_T)}\right]\frac{v(x_T)}{c} + \left[Ae^{-a(x-x_T)} - e^{-(x-x_T)}\right]\frac{v(-x_T)}{c} \end{aligned}$$

It can be shown that $T(x)$ satisfies

$$T'' + (1+a)T' + aT = 0$$

Let $I_1 = \alpha A \int_{-x_T}^{x_T} e^{-a(x-y)}v(y)dy$ and $I_2 = \int_{-x_T}^{x_T} e^{-(x-y)}v(y)dy$, then $I_1' = -aI_1$ and $I_2' = -I_2$. The eigenvalue equation becomes

$$(1+\lambda)v = T + I_1 - I_2 \tag{3.36}$$

Differentiate (3.36) w.r.t x once and twice.

$$(1+\lambda)v'(x) = T' - aI_1 + I_2 \tag{3.37}$$

$$(1+\lambda)v''(x) = T'' + a^2 I_1 - I_2 \tag{3.38}$$

Add a(3.36)+(a+1)(3.37)+(3.38) to obtain

$$\begin{aligned}(1+\lambda)\left[v''+(a+1)v'+av\right] &= \left[T''+(a+1)T'+aT\right]+ \\ &\quad \left[a^2I_1-I_2+(a+1)(-aI_1+I_2)+a(I_1-I_2)\right]=0\end{aligned}$$

Therefore the ODE on $[x_T,\infty)$ is

$$v''+(a+1)v'+av=0$$

The ODE on $(-\infty,-x_T]$ can be derived in the same manner. Consider

$$\begin{aligned}T(x) &= w(x-x_T)\frac{v(x_T)}{c}+w(x+x_T)\frac{v(-x_T)}{c} \\ &= \left[Ae^{a(x-x_T)}-e^{(x-x_T)}\right]\frac{v(x_T)}{c}+\left[Ae^{a(x-x_T)}-e^{(x-x_T)}\right]\frac{v(-x_T)}{c}\end{aligned}$$

$T(x)$ satisfies

$$T''-(1+a)T'+aT=0$$

Let $I_1=\alpha A\displaystyle\int_{-x_T}^{x_T}e^{a(x-y)}v(y)dy$ and $I_2=\displaystyle\int_{-x_T}^{x_T}e^{(x-y)}v(y)dy$, then $I_1'=aI_1$ and $I_2'=I_2$. Then the eigenvalue equation becomes

$$(1+\lambda)v=T+I_1-I_2 \tag{3.39}$$

Differentiate (3.39) w.r.t x once and twice:

$$(1+\lambda)v'(x) = T'+aI_1+I_2 \tag{3.40}$$

$$(1+\lambda)v''(x) = T''+a^2I_1+I_2 \tag{3.41}$$

(3.39), (3.40) and (3.41) can be combined to give

$$(1+\lambda)\left[v''-(a+1)v'+av\right] = \left[T''+(a+1)T'+aT\right]+$$

$$\left[a^2 I_1 + I_2 - (a+1)(aI_1 + I_2) + a(I_1 + I_2)\right] = 0$$

Therefore the ODE on $(-\infty, -x_T]$ is

$$v'' - (a+1)v' + av = 0$$

One can combine the ODE on $(-\infty, -x_T]$ and the one on $[x_T, \infty)$ by using one uniform ODE on $(-\infty, -x_T] \cup [x_T, \infty)$ such that

$$v'''' - (1+a^2)v''(x) + a^2 v(x) = 0$$

Remark 3.2. *As shown in the derivation of the ODEs, the contribution from the two boundary terms are zero both within the boundary and outside the boundary. Thus these boundary terms contribute to the eigenvalue problem only at the boundaries.*

3.6 Properties of the eigenfunction $v(x)$

From section 3.5, the three ODEs on three different intervals are:

$$\begin{cases} v'' - (a+1)v' + av = 0 & \text{ODE I on } (-\infty, -x_T] \\ (1+\lambda)v'''' - Bv'' + Cv = 0 & \text{ODE II on } [-x_T, x_T] \\ v'' + (a+1)v' + av = 0 & \text{ODE III on } [x_T, \infty) \end{cases}$$

Where $B = (1+\lambda)(a^2+1) + 2\alpha(1-aA)$ and $C = (\lambda+1)a^2 - 2\alpha a(A-a)$

Suppose that $v_1(x)$, $v_2(x)$ and $v_3(x)$ are the solutions of ODE I, ODE II and ODE III, respectively (see figure 3.6.) The three ODEs are all linear with constant coefficients. The continuous and bounded solution $v(x)$ is defined as the following

$$v(x) = \begin{cases} v_1(x) & \text{on } (-\infty, -x_T] \\ v_2(x) & \text{on } [-x_T, x_T] \\ v_3(x) & \text{on } [x_T, \infty) \end{cases}$$

$v_1(x)$ matches $v_2(x)$ at $-x_T$ and $v_2(x)$ matches $v_3(x)$ at x_T.

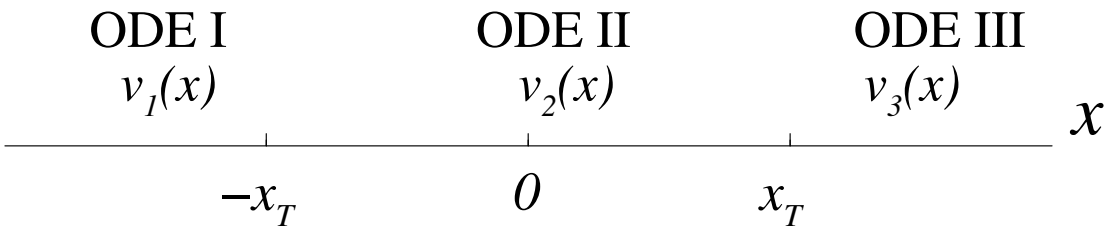

Figure 3.3. Valid ODEs on different sections and their solutions.

Consider ODE II on $[-x_T, x_T]$. If $v_2(x)$ is a solution, then $v_2(-x)$ is also a solution Thus, both the even function $\frac{v_2(x)+v_2(-x)}{2}$ and the odd function $\frac{v_2(x)-v_2(-x)}{2}$ are solutions of ODE II. Therefore, it suffices to consider either even or odd solutions of ODE II separately.

Theorem 3.8. *If $v(x)$ is the eigenfunction corresponding to eigenvalue λ, then $v(x)$ is either even or odd.*

Proof of theorem 3.8: Define a function $T_2(x)$ *s.t.*

$$T_2(x) = \alpha \int_{-x_T}^{x_T} w(x-y)v_2(y)dy$$

When $v_2(x)$ is even, $T_2(x)$ is an even function because

$$\begin{aligned} T_2(-x) &= \alpha \int_{-x_T}^{x_T} w(-x-y)v_2(y)dy = \alpha \int_{-x_T}^{x_T} w(-x+y)v_2(-y)dy \\ &= \alpha \int_{-x_T}^{x_T} w(x-y)v_2(y)dy = T_2(x) \end{aligned}$$

Similarly, for odd $v_2(x)$, $T_2(x)$ is odd because

$$\begin{aligned} T_2(-x) &= \alpha \int_{-x_T}^{x_T} w(-x-y)v_2(y)dy = \alpha \int_{-x_T}^{x_T} w(-x+y)v_2(-y)dy \\ &= -\alpha \int_{-x_T}^{x_T} w(x-y)v_2(y)dy = -T_2(x) \end{aligned}$$

The eigenvalue problem can be written as

$$\begin{aligned}(1+\lambda)v(x) &= w(x-x_T)\frac{v_2(x_T)}{c} + w(x+x_T)\frac{v_2(-x_T)}{c} + \alpha\int_{-x_T}^{x_T} w(x-y)v_2(y)dy \\ &= w(x-x_T)\frac{v_2(x_T)}{c} + w(x+x_T)\frac{v_2(-x_T)}{c} + T_2(x)\end{aligned}$$

Since $v(x)$ is continuous on $\Re$, $v(x_T)$ and $v(-x_T)$ can be replaced by $v_2(x_T)$ and $v_2(-x_T)$, respectively. Then

$$\begin{aligned}(1+\lambda)v(-x) &= w(-x-x_T)\frac{v_2(x_T)}{c} + w(-x+x_T)\frac{v_2(-x_T)}{c} + T_2(-x) \\ &= w(x+x_T)\frac{v_2(x_T)}{c} + w(x-x_T)\frac{v_2(-x_T)}{c} + T_2(-x)\end{aligned}$$

If $v_2(x)$ is even,

$$\begin{aligned}(1+\lambda)v(-x) &= w(x+x_T)\frac{v_2(-x_T)}{c} + w(x-x_T)\frac{v_2(x_T)}{c} + T_2(x) \\ &= (1+\lambda)v(x)\end{aligned}$$

If $v_2(x)$ is odd,

$$\begin{aligned}(1+\lambda)v(-x) &= w(x+x_T)\frac{v_2(x_T)}{c} - w(x-x_T)\frac{v_2(x_T)}{c} - T_2(x) \\ &= -\left[-w(x+x_T)\frac{v_2(x_T)}{c} + w(x-x_T)\frac{v_2(x_T)}{c} + T_2(x)\right] \\ &= -\left[w(x+x_T)\frac{v_2(-x_T)}{c} + w(x-x_T)\frac{v_2(x_T)}{c} + T_2(x)\right] \\ &= -(1+\lambda)v(x) \qquad \Diamond\end{aligned}$$

Theorem 3.9. *The matching conditions at $-x_T$ are identical to those at x_T when $v(x)$ is an odd or an even function.*

Proof of theorem 3.9: This is shown with a direct calculation of the matching conditions of $v'(x)$, $v''(x)$ and $v'''(x)$ at both $-x_T$ and x_T.

Case 1. $v(x)$ is even, *i.e.* $v(-x_T) = v(x_T)$ and $v'(-x_T^+) = -v'(x_T^-)$. Defining the jump of v at

x as $[v(x)] = v(x^+) - v(x^-)$, the follow equalities are derived

$$\begin{aligned}
[v(-x_T)] &= -[v(x_T)] \\
\left[v'(-x_T)\right] &= \left[v'(x_T)\right] \\
\left[v''(-x_T)\right] &= -\left[v''(x_T)\right] \\
\left[v'''(-x_T)\right] &= \left[v'''(x_T)\right]
\end{aligned}$$

From theorem 3.7, the matching conditions at $-x_T$ are

$$\begin{aligned}
[v(-x_T)] &= 0 \\
\left[v'(-x_T)\right] &= \frac{2\alpha(1-aA)}{1+\lambda} v(-x_T) \\
\left[v''(-x_T)\right] &= \frac{-2(aA-1)}{c(1+\lambda)} v(-x_T) \\
\left[v'''(-x_T)\right] &= \frac{2(1-a^3A)}{c(1+\lambda)} v(-x_T) - \frac{2\alpha(aA-1)}{1+\lambda} v'(-x_T^+)
\end{aligned}$$

This can be re-expressed as

$$\begin{aligned}
[v(-x_T)] &= -[v(x_T)] = 0 \\
\left[v'(-x_T)\right] &= \left[v'(x_T)\right] = \frac{2\alpha(1-aA)}{1+\lambda} v(-x_T) \\
\left[v''(-x_T)\right] &= -\left[''v(x_T)\right] = \frac{-2(aA-1)}{c(1+\lambda)} v(-x_T) \\
\left[v'''(-x_T)\right] &= \left[v'''(x_T)\right] = \frac{2(1-a^3A)}{c(1+\lambda)} v(-x_T) - \frac{2\alpha(aA-1)}{1+\lambda} v'(-x_T^+)
\end{aligned}$$

which gives us the matching conditions at x_T

$$\begin{aligned}
[v(x_T)] &= 0 \\
\left[v'(x_T)\right] &= \frac{2\alpha(1-aA)}{1+\lambda} v(x_T) \\
\left[v''(x_T)\right] &= \frac{2(aA-1)}{c(1+\lambda)} v(x_T) \\
\left[v'''(x_T)\right] &= \frac{2(1-a^3A)}{c(1+\lambda)} v(x_T) + \frac{2\alpha(aA-1)}{1+\lambda} v'(x_T^-)
\end{aligned}$$

Now start with the right matching conditions at x_T from theorem 3.7

$$\begin{aligned}
[v(x_T)] &= 0 \\
\left[v'(x_T)\right] &= \frac{2\alpha(1-aA)}{1+\lambda}v(x_T) \\
\left[v''(x_T)\right] &= \frac{2(aA-1)}{c(1+\lambda)}v(x_T) \\
\left[v'''(x_T)\right] &= \frac{2(1-a^3A)}{c(1+\lambda)}v(x_T) + \frac{2\alpha(aA-1)}{1+\lambda}v'(x_T^-)
\end{aligned}$$

and derive the following matching conditions

$$\begin{aligned}
[v(x_T)] &= -[v(-x_T)] = 0 \\
\left[v'(x_T)\right] &= \left[v'(-x_T)\right] = \frac{2\alpha(1-aA)}{1+\lambda}v(x_T) \\
\left[v''(x_T)\right] &= -\left[v''(-x_T)\right] = \frac{2(aA-1)}{c(1+\lambda)}v(x_T) \\
\left[v'''(x_T)\right] &= \left[v'''(-x_T)\right] = \frac{2(1-a^3A)}{c(1+\lambda)}v(x_T) + \frac{2\alpha(aA-1)}{1+\lambda}v'(x_T^-)
\end{aligned}$$

which gives the matching conditions at $-x_T$:

$$\begin{aligned}
[v(-x_T)] &= 0 \\
\left[v'(-x_T)\right] &= \frac{2\alpha(1-aA)}{1+\lambda}v(-x_T) \\
\left[v''(-x_T)\right] &= \frac{-2(aA-1)}{c(1+\lambda)}v(-x_T) \\
\left[v'''(-x_T)\right] &= \frac{2(1-a^3A)}{c(1+\lambda)}v(-x_T) - \frac{2\alpha(aA-1)}{1+\lambda}v'(-x_T^+)
\end{aligned}$$

Therefore the matching conditions at $-x_T$ and x_T are the same.

Case 2: $v(x)$ is odd, *i.e.* $v(-x_T) = -v(x_T)$ and $v'(-x_T^+) = v'(x_T^-)$. Here

$$\begin{aligned}
[v(-x_T)] &= [v(x_T)] \\
\left[v'(-x_T)\right] &= -\left[v'(x_T)\right] \\
\left[v''(-x_T)\right] &= \left[v''(x_T)\right] \\
\left[v'''(-x_T)\right] &= -\left[v'''(x_T)\right]
\end{aligned}$$

Similarly, the matching conditions at $-x_T$ are

$$\begin{aligned}
[v(-x_T)] &= [v(x_T)] = 0 \\
\left[v'(-x_T)\right] &= -\left[v'(x_T)\right] = \frac{2\alpha(1-aA)}{1+\lambda} v(-x_T) \\
\left[v''(-x_T)\right] &= \left[v''(x_T)\right] = \frac{-2(aA-1)}{c(1+\lambda)} v(-x_T) \\
\left[v'''(-x_T)\right] &= -\left[v'''(x_T)\right] = \frac{2(1-a^3A)}{c(1+\lambda)} v(-x_T) - \frac{2\alpha(aA-1)}{1+\lambda} v'(-x_T^+)
\end{aligned}$$

which is the same as the matching conditions at x_T

$$\begin{aligned}
[v(x_T)] &= 0 \\
\left[v'(x_T)\right] &= \frac{2\alpha(1-aA)}{1+\lambda} v(x_T) \\
\left[v''(x_T)\right] &= \frac{2(aA-1)}{c(1+\lambda)} v(x_T) \\
\left[v'''(x_T)\right] &= \frac{2(1-a^3A)}{c(1+\lambda)} v(x_T) + \frac{2\alpha(aA-1)}{1+\lambda} v'(x_T^-).
\end{aligned}$$

To complete the proof, I can derive the matching conditions at $-x_T$ from the matching conditions at x_T. $\Diamond$

3.7 Solutions of ODE II

Assume that A, B, a, α, u_T and x_T are all fixed. The solution structure of ODE II depends on λ. In this section, I give possible solutions for ODE II depending on eigenvalue λ.

ODE II on $[-x_T, x_T]$ is

$$(1+\lambda)v^{(iv)} - Bv'' + Cv = 0$$

The characteristic equation of ODE II is

$$(1+\lambda)\omega^4 - B\omega^2 + C = 0$$

Where

$$B = (1+\lambda)(a^2+1) + 2\alpha(1-aA), \qquad C = (\lambda+1)a^2 - 2\alpha a(A-a).$$

Let

$$\begin{aligned}\Delta &= B^2 - 4BC \\ &= (a^2-1)^2\lambda^2 + 2(a^2-1)(a^2-1-2aA\alpha-2\alpha)\lambda - \\ &\quad (a^2-1)(1-a^2+4\alpha+4aA\alpha) + 4\alpha^2(1-aA)^2\end{aligned}$$

B is a linear function in λ and Δ is a quadratic function in λ. If Δ is negative, there will be complex characteristic values of ODE II. If Δ is positive, I may or may not have complex characteristic values for ODE II. It depends on both B and Δ. For fixed A, a and α. Δ is a parabola with two zeros λ_l and λ_r. λ_l represents the left zero of Δ, and λ_r represents the right zero of Δ. In order to decide the structure of the solution of ODE II, the following lemmas are needed (See proofs in Appendix.)

Lemma 3.7. *λ_B, the zero of B is always between -1 and λ_r. When $a^3 > A$, $\lambda_l < \lambda_B < \lambda_r$. When $a^3 < A$, $\lambda_B < \lambda_l < \lambda_r$.*

By lemma 3.7, there are two possible pictures to describe the relations between λ_l, λ_r and λ_B (see figure 3.4 and 3.5.)

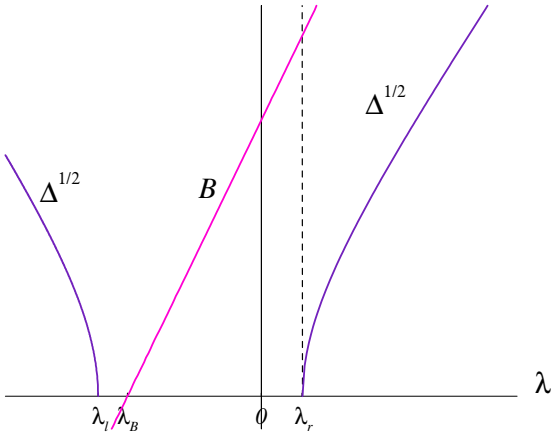

Figure 3.4. Plots of $\sqrt{\Delta}$ and B. When $\lambda_l < \lambda < \lambda_r$, $\sqrt{\Delta}$ is complex. $a = 2.4$, $A = 2.8$, $\alpha = 0.22$.

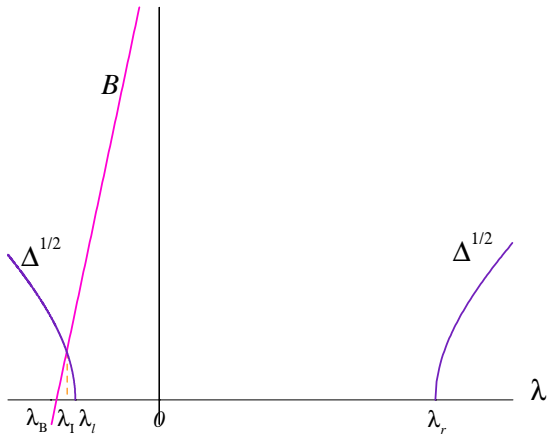

Figure 3.5. Plots of $\sqrt{\Delta}$ and B. When $\lambda_l < \lambda < \lambda_r$, $\sqrt{\Delta}$ is complex. $a = 1.2$, $A = 3.2$, $\alpha = 0.08$.

Lemma 3.8. *(i). When $a^3 > A$, $\lambda_l < \lambda_B < \lambda_r$, B does not intersect the left branch or the right branch of $\sqrt{\Delta}$ (figure 3.4.)*

(ii). When $a^3 < A$, $\lambda_B < \lambda_l < \lambda_r$, B intersects only the left branch of $\sqrt{\Delta}$ once at λ_I (figure 3.5.)

Corollary 3.1. *Suppose ω_1, $-\omega_1$, ω_2 and $-\omega_2$ are the four characteristic values of* ODE II,

(i) When $\lambda_l < \lambda_B < \lambda_r$, table 3.1 shows all the possibilities of ω_1 and ω_2.

(ii) When $\lambda_B < \lambda_l < \lambda_r$, table 3.2 shows all the possibilities of ω_1 and ω_2.

1	2	3	4	5	6
$\lambda = -1$	$-1 < \lambda < \lambda_l$	$\lambda = \lambda_l$	$\lambda_l < \lambda < \lambda_r$	$\lambda = \lambda_r$	$\lambda > \lambda_r$
	$B < 0$	$B < 0$	$B > 0$ or $B < 0$	$B > 0$	$B > 0$
	$\Delta > 0$, $\lvert B\rvert < \sqrt{\Delta}$	$\Delta = 0$	$\Delta < 0$	$\Delta = 0$	$\Delta > 0$
	ω_1 real	ω_1, ω_2 imaginary	ω_1, ω_2 complex	ω_1,ω_2 real	ω_1, ω_2 real
	ω_2 imaginary	$\omega_1 = \omega_2^*$	$\omega_1 = \omega_2^*$	$\omega_1 = \omega_2$	

Table 3.1. Characteristic value chart when $\lambda_l < \lambda_B < \lambda_r$.

Form chart 3.1 and 3.2, there are three possible forms of solution $v_2(x)$: 1) both ω_1 and ω_2 are real; 2) both ω_1 and ω_2 are complex; 3) ω_1 is real and ω_2 is imaginary.

3.7.1 Solution $v_2(x)$ when $\lambda \geq \lambda_r$ and $\lambda_I \leq \lambda < \lambda_l$

The solution $v_2(x)$ of ODE II is either even or odd. Suppose the even $v_2(x)$ is $v_2^{\mathrm{e}}(x)$ and the odd $v_2(x)$ is $v_2^{\mathrm{o}}(x)$.

1	2	3	4	5	6
$-1 < \lambda < \lambda_I$	$\lambda_I \leq \lambda < \lambda_l$	$\lambda = \lambda_l$	$\lambda_l < \lambda < \lambda_r$	$\lambda = \lambda_r$	$\lambda > \lambda_r$
$B < 0$ or $B > 0$	$B > 0$	$B > 0$	$B < 0$	$B > 0$	$B > 0$
$\Delta > 0$, $\lvert B\rvert < \sqrt{\Delta}$	$\Delta > 0$, $\lvert B\rvert > \sqrt{\Delta}$	$\Delta = 0$	$\Delta < 0$	$\Delta = 0$	$\Delta > 0$
ω_1 real	ω_1, ω_2 real	ω_1, ω_2 real	ω_1, ω_2 complex	ω_1,ω_2 real	ω_1, ω_2 real
ω_2 imaginary		$\omega_1 = \omega_2$	$\omega_1 = \omega_2^*$	$\omega_1 = \omega_2$	

Table 3.2. Characteristic value chart when $\lambda_B < \lambda_l < \lambda_r$.

When $\lambda \geq \lambda_r$ and $\lambda_I \leq \lambda \leq \lambda_l$, both ω_1 and ω_2 are real. In general, one can write $v_2^{\rm e}(x)$ of ODE II in the following exponential form

$$v_2^{\rm e}(x) = c_3(e^{\omega_1 x} + e^{-\omega_1 x}) + c_4(e^{\omega_2 x} + e^{-\omega_2 x})$$

Let $\mu_1 = e^{\omega_1 x} + e^{-\omega_1 x}$, $\qquad \mu_2 = e^{\omega_2 x} + e^{-\omega_2 x}$

However, one cannot write $v_2^{\rm e}(x)$ in the above form $c_3\mu_1 + c_4\mu_2$. As $\lambda \to \lambda_r$, λ_l, $\omega_1 \to \omega_2$ and $\mu_1 \to \mu_2$, which means that μ_1 and μ_2 become dependent. μ_1 and μ_2 have to be independent at $\lambda = \lambda_r, \lambda_l, \lambda_I$. Therefore, I adopt the following form for $v_2^{\rm e}(x)$

$$v_2^{\rm e}(x) = c_3(e^{\omega_1 x} + e^{-\omega_1 x}) + c_4\frac{(e^{\omega_1 x} + e^{-\omega_1 x}) - (e^{\omega_2 x} + e^{-\omega_2 x})}{\omega_1 - \omega_2}$$

Let $\epsilon = \omega_1 - \omega_2$, where $\omega_1 > \omega_2$. As $\omega_1 \to \omega_2$, $\epsilon \to 0$. Rewrite $v_2^{\rm e}(x)$ as

$$\begin{aligned} v_2^{\rm e}(x) &= c_3(e^{\omega_1 x} + e^{-\omega_1 x}) + c_4\frac{(e^{\omega_1 x} + e^{-\omega_1 x}) - (e^{(\omega_1-\epsilon) x} + e^{-(\omega_1-\epsilon) x})}{\epsilon} \\ &= c_3(e^{\omega_1 x} + e^{-\omega_1 x}) + c_4\frac{(e^{\omega_1 x} + e^{-\omega_1 x}) - (e^{\omega_1 x}e^{-\epsilon x} + e^{-\omega_1 x}e^{\epsilon x})}{\epsilon} \end{aligned}$$

As $\epsilon \to 0$, replace $e^{\epsilon x}$ by $1 + \epsilon x$, $e^{-\epsilon x}$ by $1 - \epsilon x$, then

$$\begin{aligned} v_2^{\rm e}(x) &= c_3(e^{\omega_1 x} + e^{-\omega_1 x}) + c_4\frac{\epsilon x(e^{\omega_1 x} - e^{-\omega_1 x})}{\epsilon} \\ &= c_3(e^{\omega_1 x} + e^{-\omega_1 x}) + c_4 x(e^{\omega_1 x} - e^{-\omega_1 x}) \\ &= 2c_3\cosh px + 2c_4 x\sinh px \end{aligned}$$

Similarly, $v_2^{\mathrm{o}}(x)$ can be written as

$$v_2^{\mathrm{o}}(x) = c_3(e^{\omega_1 x} - e^{-\omega_1 x}) + c_4 \frac{(e^{\omega_1 x} - e^{-\omega_1 x}) - (e^{\omega_2 x} - e^{-\omega_2 x})}{\omega_1 - \omega_2}$$

3.7.2 Solution $v_2(x)$ when $\lambda_l < \lambda < \lambda_r$

Here both ω_1 and ω_2 are complex. Let $\omega_1 = p + iq$, $\omega_2 = p - iq$. When $v_2(x)$ is even, write $v_2^{\mathrm{e}}(x)$ as

$$v_2^{\mathrm{e}}(x) = 2c_3 \cos qx \cosh px + 2c_4 \frac{\sin qx}{q} \sinh px \tag{3.42}$$

As $\lambda \to \lambda_l$ or λ_r, $q \to 0$,

$$v_2(x) \to 2c_3 \cos qx \cosh px + 2c_4 x \sinh px \tag{3.43}$$

$v_2^{\mathrm{o}}(x)$ can be written as

$$v_2^{\mathrm{o}}(x) = 2c_3 \cos qx \sinh px - 2c_4 \frac{\sin qx}{q} \cosh px$$

where $p = \sqrt{\frac{\sqrt{B^2 + |\Delta|}}{2(1+\lambda)}} \cos\theta$, $p = \sqrt{\frac{\sqrt{B^2 + |\Delta|}}{2(1+\lambda)}} \sin\theta$ and $\theta = \frac{1}{2} \arctan \frac{\sqrt{|\Delta|}}{B}$

3.8 Stability criteria

By theorem 3.7, $v_1(x)$ and $v_2(x)$ must match at $-x_T$, and $v_2(x)$ must match $v_3(x)$ at x_T. By theorem 3.9, no matter if $v_2(x)$ is even or odd, the matching conditions at $-x_T$ are same as the matching conditions at x_T. Therefore, it suffices to apply the matching condition to $v_2(x)$ and $v_3(x)$ at x_T for both even $v_2(x)$ and odd $v_2(x)$. In general, the matching conditions can be written

as

$$T1: \quad \begin{cases} [v(x_T)] = v_3(x_T) - v_2(x_T) & = & 0 \\ [v'(x_T)] = v_3'(x_T) - v_2'(x_T) & = & \dfrac{2\alpha(1-aA)}{1+\lambda} v(x_T) \\ [v''(x_T)] = v_3''(x_T) - v_2''(x_T) & = & \dfrac{2(aA-1)}{c(1+\lambda)} v(x_T) \\ [v'''(x_T)] = v_3'''(x_T) - v_2'''(x_T) & = & \dfrac{2(1-a^3A)}{c(1+\lambda)} v(x_T) + \dfrac{2\alpha(aA-1)}{1+\lambda} v'(x_T^-) \end{cases}$$

where $v(x_T) = v_3(x_T)$ and $v'(x_T^-) = v_2'(x_T)$.

There are two unknown coefficients c_3 and c_4 in $v_2(x_T)$. c_5 and c_6 are the unknown coefficients in $v_3(x_T)$. If I simplify the above system and substitute numbers for a, A, α, x_T, u_T given by the stationary solution $u(x)$, I obtain a 4×4 homogeneous linear system with 4 unknown free parameters c_3, c_4, c_5, c_6. The coefficient matrix of this system must be singular for some λ in order to have a non-trivial solution (c_3, c_4, c_5, c_6), which means the determinant $D(\lambda)$ of the coefficient matrix must be equal to zero for some λ. The λ for which $D(\lambda) = 0$ is an eigenvalue and it determines the stability of the stationary solution. If there exists a λ such that $0 < \lambda < \lambda_b$ and $D(\lambda) = 0$, then the standing pulse is unstable. If there is no positive λ such that $0 < \lambda < \lambda_b$ and $D(\lambda) = 0$, the standing pulse is stable. This approach is similar to the Evans Function [20, 21, 22, 23].

3.8.1 Examples

Consider the stationary pulse solutions for $a = 2.4$, $A = 2.8$, $\alpha = 0.22$, $u_T = 0.40073$ and $\beta = 1$. There are two single-pulse solutions. One has higher amplitude and bigger width. I call it $u^{\mathbf{l}}(x)$. The other one is called $u^{\mathbf{s}}(x)$ which is slightly above threshold and much narrower than $u^{\mathbf{l}}(x)$. From chapter 2, I am able to explicitly calculate both single pulse solutions and they are given as

$$u^{\mathbf{l}}(x) = \begin{cases} 0.665\cos(0.31x)\cosh(1.49x) - 3.775\sin(0.31x)\sinh(1.49x) + 0.328, & -x_T \le x \le x_T \\ 6.237e^{-2.4|x|} - 1.61e^{-|x|}, & \text{otherwise} \end{cases}$$

where $x_T = 0.683035$.

$$u^{\mathbf{s}}(x) = \begin{cases} 0.216\cos(0.31x)\cosh(1.49x) - 8.031\sin(0.31x)\sinh(1.49x) + 0.328, & -x_T \le x \le x_T \\ 1.203e^{-2.4|x|} - 0.416e^{-|x|}, & \text{otherwise} \end{cases}$$

where $x_T = 0.202447$.

Using the stability criteria, the large pulse turns out to be stable and the small pulse is unstable. For the small pulse, there exists a positive value $\lambda \le \lambda_b$ such that $D(\lambda) = 0$. There is no positive value of $\lambda \le \lambda_b$ such that $D(\lambda) = 0$, therefore the large pulses stable.

3.8.2 Stability of the large pulse $u^{\mathbf{l}}(x)$

I first calculate the upper bound for λ. The upper bound λ_b for the large pulse and small pulse are different because λ_b depends on x_T. Let $\lambda_b^{\mathbf{l}}$ be the upper bound of λ for the large pulse and $\lambda_b^{\mathbf{s}}$ be the upper bound for the small pulse. For the following parameter set, I calculate $\lambda_b^{\mathbf{l}} = 1.25917$ and $\lambda_b^{\mathbf{s}} = 1.66628$. by theorem 3.3

$$\{a = 2.4, \quad A = 2.8, \quad \alpha = 0.22, \quad u_T = 0.40073\}$$

For the above set of parameters. $v_3(x)$ always has the following form.

$$v_3(x) = c_5 e^{-ax} + c_6 e^{-x}$$

However, the form of $v_2(x)$ depends on ω_1 and ω_2. For this specific set of parameters, $\lambda_l = -0.627692$ and $\lambda_r = 0.192861$. When $0 \le \lambda \le \lambda_r = 0.192861$, both ω_1 and ω_2 are complex. Therefore

$$v_2(x) = \begin{cases} 2c_3\cos qx\cosh px + 2c_4\dfrac{\sin qx}{q}\sinh px & v_2(x) \text{ is even} \\ 2c_3\cos qx\sinh px - 2c_4\dfrac{\sin qx}{q}\cosh px & v_2(x) \text{ is odd} \end{cases}$$

where p, q are real, and c_3, c_4 are unknown.

Plug $v_2^{\mathrm{e}}(x)$ and $v_3(x)$ into system $T1$. This system is a very complicated 4×4 linear system in c_3, c_4, c_5 and c_6. I do not show the actual system here. Mathematica [67] can calculate the

determinant of the coefficient matrix. The determinant $D(\lambda)$ is a function of λ. Plotting $D(\lambda)$ against λ on domain $[0, \lambda_r]$ to obtain figure 3.6. Repeat the same procedure to $v_2^o(x)$ to get figure

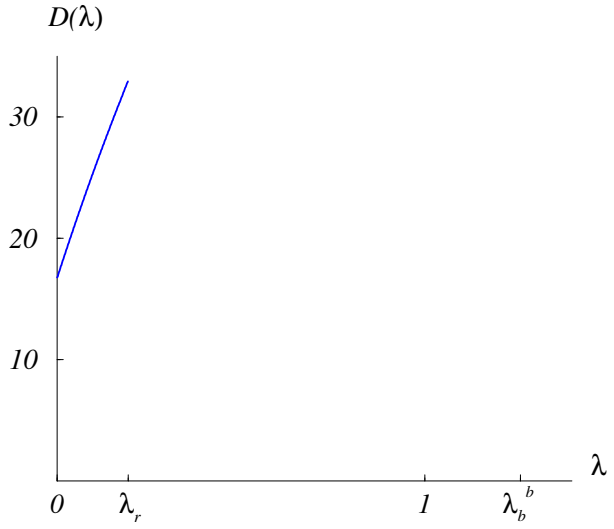

Figure 3.6. Plot of $D(\lambda)$ when both ω_1 and ω_2 are complex. $v_2(x)$ is even. $a = 2.4$, $A = 2.8$, $\alpha = 0.22$, $x_T = 0.683035$, $\lambda_r = 0.192861$, $\lambda_b^1 = 1.25917$.

3.7 of $D(\lambda)$. When $0.192861 = \lambda_r \leq \lambda \leq \lambda_b^1 = 1.25917$, $v_2(x)$ has the following exponential form

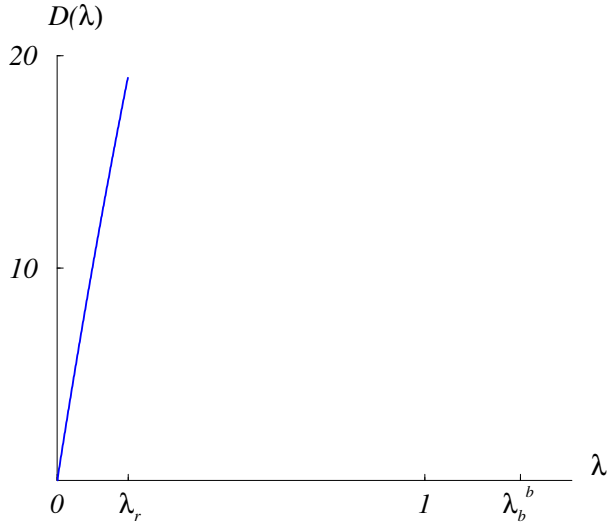

Figure 3.7. Plot of $D(\lambda)$ when both ω_1 and ω_2 are complex. $v_2(x)$ is odd. $D(\lambda)$ passes through the origin where $\lambda = 0$. $a = 2.4$, $A = 2.8$, $\alpha = 0.22$, $x_T = 0.683035$, $\lambda_r = 0.192861$, $\lambda_b^1 = 1.25917$.

---

because both ω_1 and ω_1 are real.

$$v_2(x) = \begin{cases} c_3(e^{\omega_1 x} + e^{-\omega_1 x}) + c_4 \dfrac{(e^{\omega_1 x} + e^{-\omega_1 x}) - (e^{\omega_2 x} + e^{-\omega_2 x})}{\omega_1 - \omega_2} & v_2(x) \text{ is even} \\ c_3(e^{\omega_1 x} - e^{-\omega_1 x}) - c_4 \dfrac{(e^{\omega_1 x} - e^{-\omega_1 x}) - (e^{\omega_2 x} + e^{-\omega_2 x})}{\omega_1 - \omega_2} & v_2(x) \text{ is odd} \end{cases}$$

Plotting $D(\lambda)$ for both even $v_2(x)$ and odd $v_2(x)$ gives figure 3.9 and figure 3.9. Combining

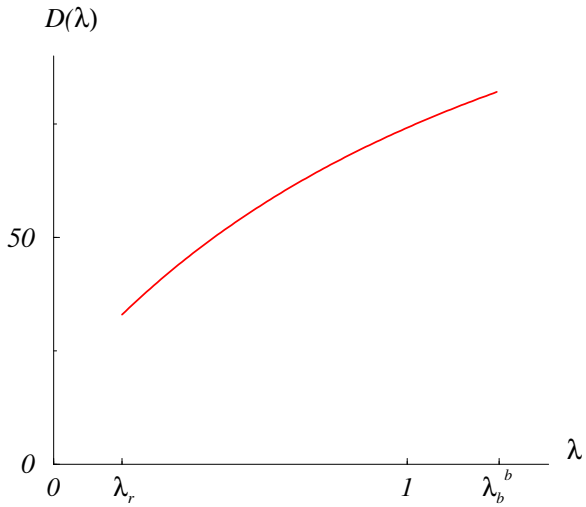

Figure 3.8. Plot of $D(\lambda)$ when both ω_1 and ω_2 are real. $v_2(x)$ is even $a = 2.4$, $A = 2.8$, $\alpha = 0.22$, $x_T = 0.683035$, $\lambda_r = 0.192861$, $\lambda_b^1 = 1.25917$.

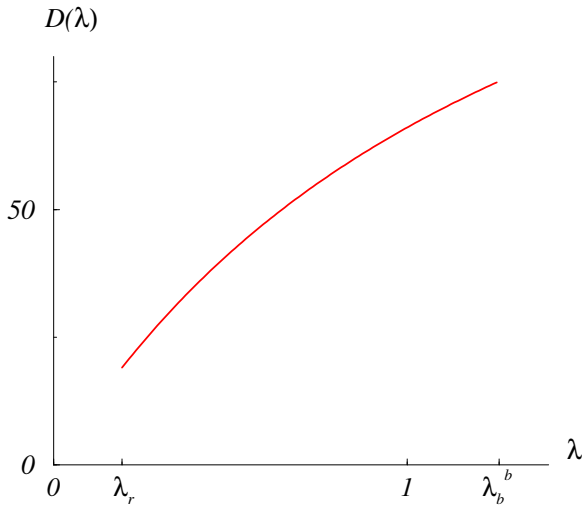

Figure 3.9. Plot of $D(\lambda)$ when both ω_1 and ω_2 are real. $v_2(x)$ is odd. $a = 2.4$, $A = 2.8$, $\alpha = 0.22$, $x_T = 0.683035$, $\lambda_r = 0.192861$, $\lambda_b^1 = 1.25917$.

$D(\lambda)$ with complex and real characteristic values gives figure 3.10 (even $v(x)$) and figures 3.11 (odd

$v(x)$.) From figure 3.10, $D(\lambda)$ has no zero. In figure 3.11, $D(\lambda) = 0$ only when $\lambda = 0$. There is no positive λ that satisfies $D(\lambda) = 0$. Hence, the large pulse solution is stable. Figure 3.11 shows that $\lambda = 0$ is an eigenvalue. This result is consistent with theorem 3.6.

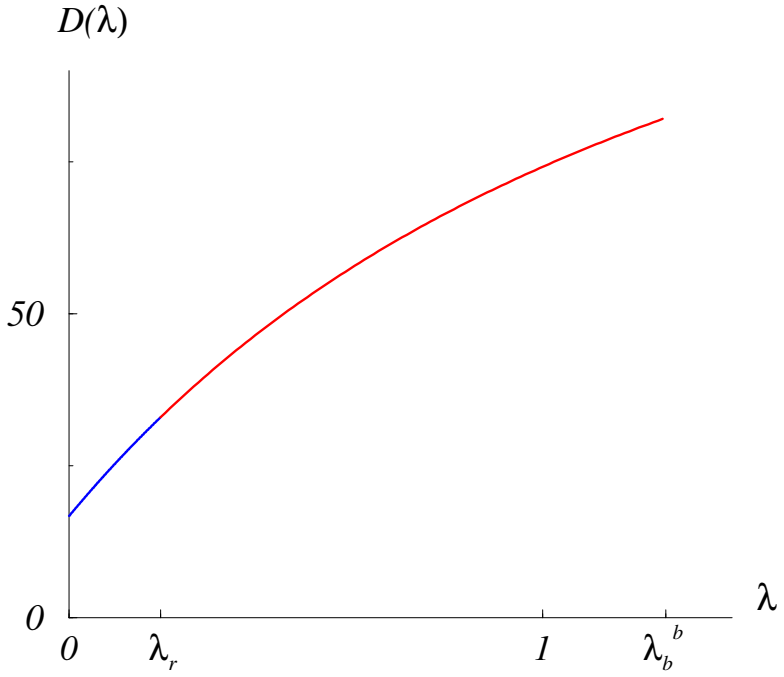

Figure 3.10. Plot of $D(\lambda)$ when $v_2(x)$ is even $a = 2.4$, $A = 2.8$, $\alpha = 0.22$, $x_T = 0.683035$, $\lambda_r = 0.192861$, $\lambda_b^{\mathbf{l}} = 1.25917$. There is no positive λ such that $D(\lambda) = 0$, $\lambda \leq \lambda_b^{\mathbf{l}}$.

3.8.3 Instability of the small pulse $u^{\mathbf{s}}(x)$

Let $\lambda_b^{\mathbf{s}}$ be the upper bound for the small pulse. For the following set of parameter, $\lambda_b^{\mathbf{s}} = 1.66628$ by theorem 3.3.

$$\{a = 2.4, \quad A = 2.8, \quad \alpha = 0.22, \quad u_T = 0.40073\}$$

Repeating the same procedure to plot $D(\lambda)$ for both $v_2^{\mathrm{e}}(x)$ and $v_2^{\mathrm{o}}(x)$ as in section 3.8.2. The positive eigenvalue $\lambda = \lambda^*$ such $D(\lambda^*) = 0$ in figure 3.12 implies the instability of the small single-pulse. The plot of $D(\lambda)$ corresponding to $v^{\mathrm{o}}(x)$ in figure 3.13 identifies the zero eigenvalue.

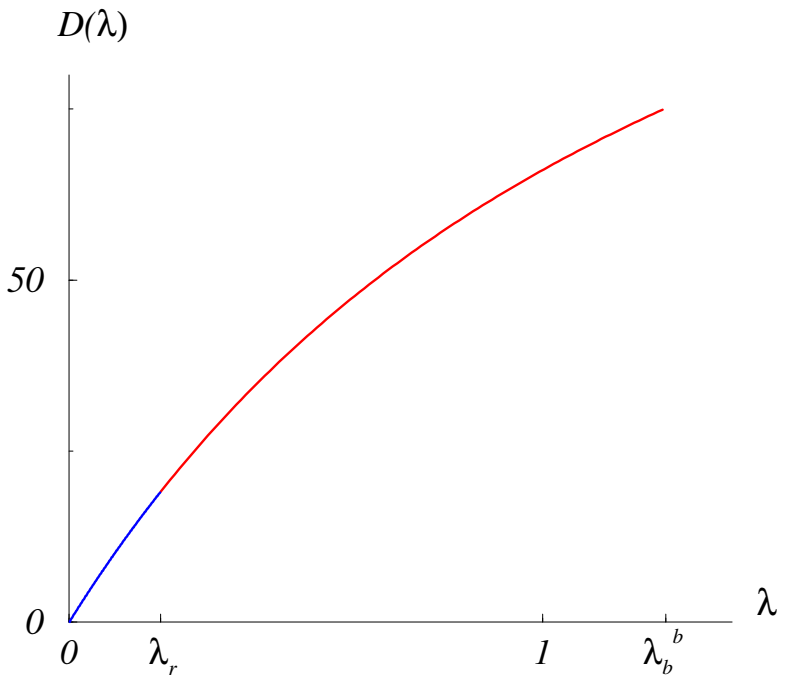

Figure 3.11. Plot of $D(\lambda)$ when $v_2(x)$ is odd. $a = 2.4$, $A = 2.8$, $\alpha = 0.22$, $x_T = 0.683035$, $\lambda_r = 0.192861$, $\lambda_b^{\mathbf{l}} = 1.25917$. There is no positive λ such that $D(\lambda) = 0$, $\lambda \leq \lambda_b^{\mathbf{l}}$. When $v_2(x)$ is odd, $D(\lambda)$ does identify the zero eigenvalue..

3.8.4 Stability of the dimple-pulse $u^{\mathbf{d}}(x)$ and the instability of the third pulse

When there are only two single-pulses, the large pulse could be a dimple-pulse instead of a single-pulse. This dimple pulse is stable by the stability criteria (figure 3.14 and 3.15.) There could be three pulses coexisting (examples in section 2.8.2 and 2.10.2.) Applying the same stability criteria to the third pulse, it shows that the third pulse is unstable. For example, the third pulse (the right dimple-pulse shown in figure 2.23) at P_2 (figure 2.22) in section 2.8.2 is unstable (figure 3.16.)

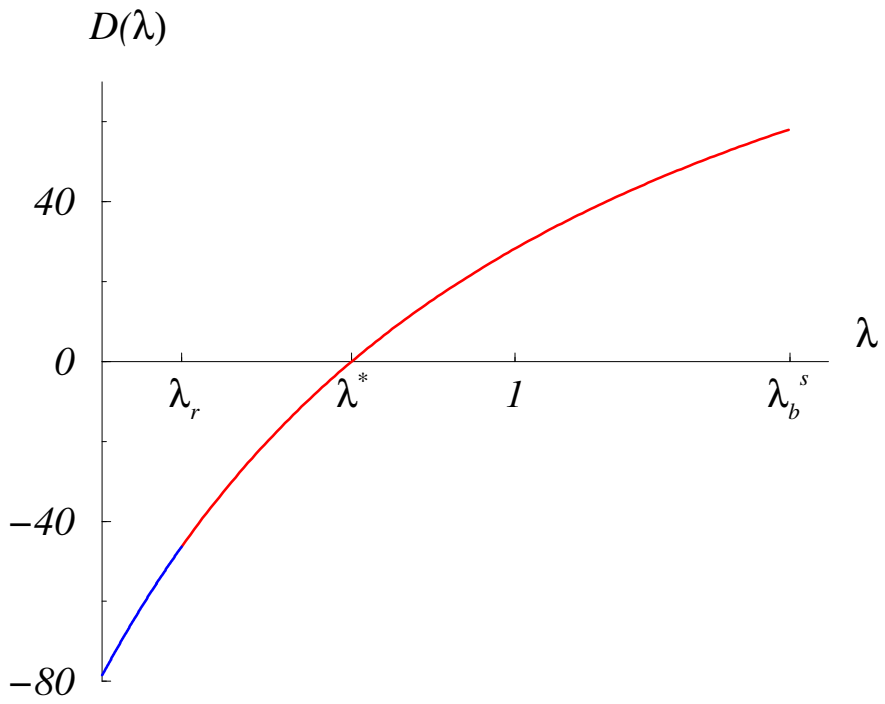

Figure 3.12. Plot of $D(\lambda)$ when $v_2(x)$ is even $a = 2.4$, $A = 2.8$, $\alpha = 0.22$, $x_T = 0.683035$, $\lambda_r = 0.192861$, $\lambda_b^{\mathbf{s}} = 1.66628$. $\lambda^* = 0.603705$ There is one positive $\lambda = \lambda^*$ such that $D(\lambda^*) = 0$, $\lambda^* \leq \lambda_b^{\mathbf{s}}$.

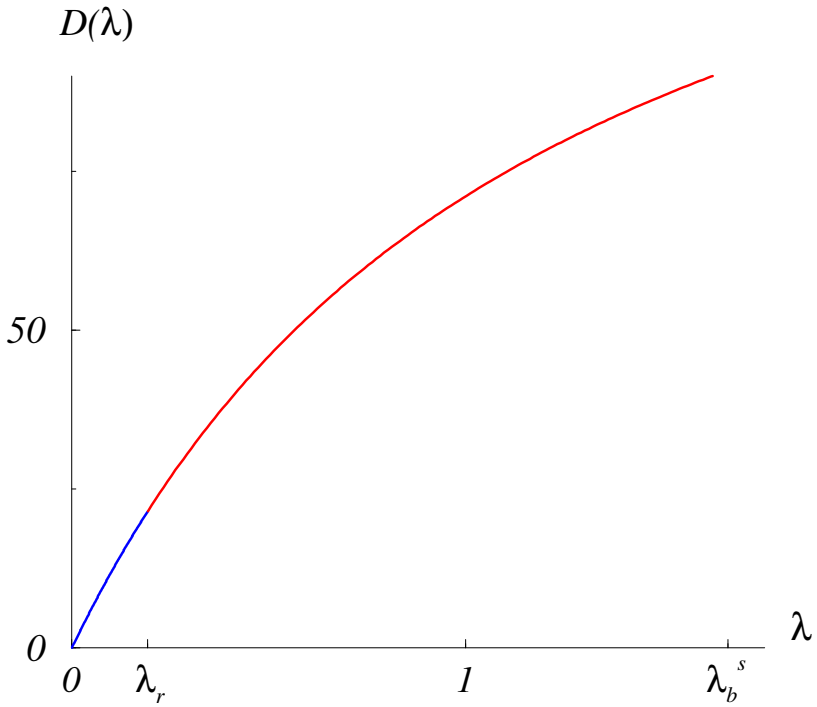

Figure 3.13. Plot of $D(\lambda)$ when $v_2(x)$ is odd. $a = 2.4$, $A = 2.8$, $\alpha = 0.22$, $x_T = 0.683035$, $\lambda_r = 0.192861$, $\lambda_b^{\mathbf{s}} = 1.66628$. There is no positive λ such that $D(\lambda) = 0$, $\lambda \leq \lambda_b^{\mathbf{s}}$. When $v_2(x)$ is odd, $D(\lambda) = 0$ at $\lambda = 0$ identifies the zero eigenvalue..

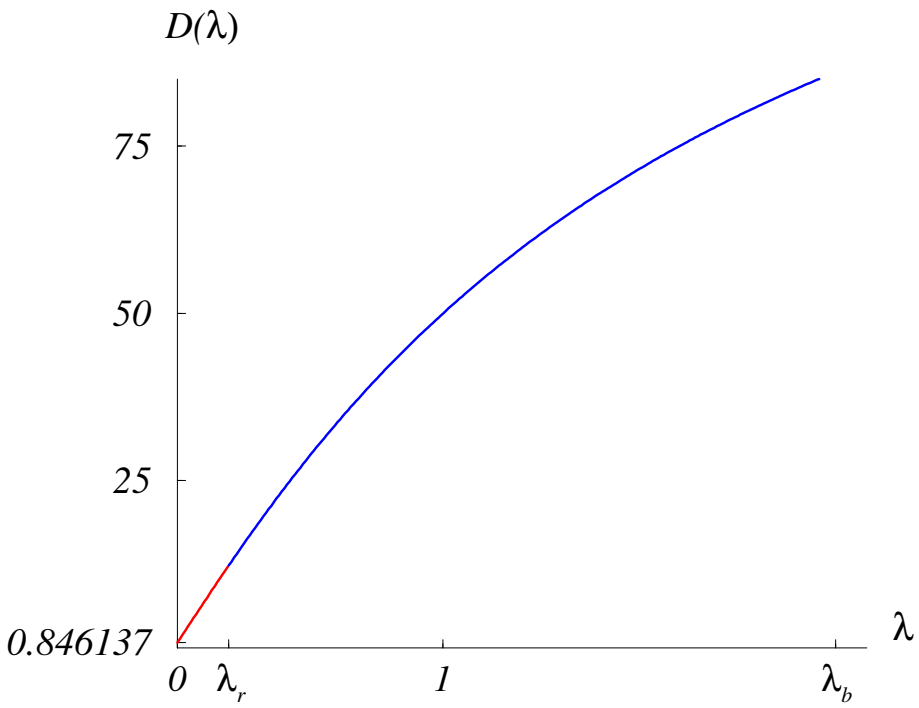

Figure 3.14. Plot of $D(\lambda)$ when $v_2(x)$ is even $a = 2.4$, $A = 2.8$, $\alpha = 0.22$, $x_T = 2.048246$, $\lambda_r = 0.192861$, $\lambda_b^{\mathbf{d}} = 2.48147$. There is no positive λ such that $D(\lambda) = 0$.

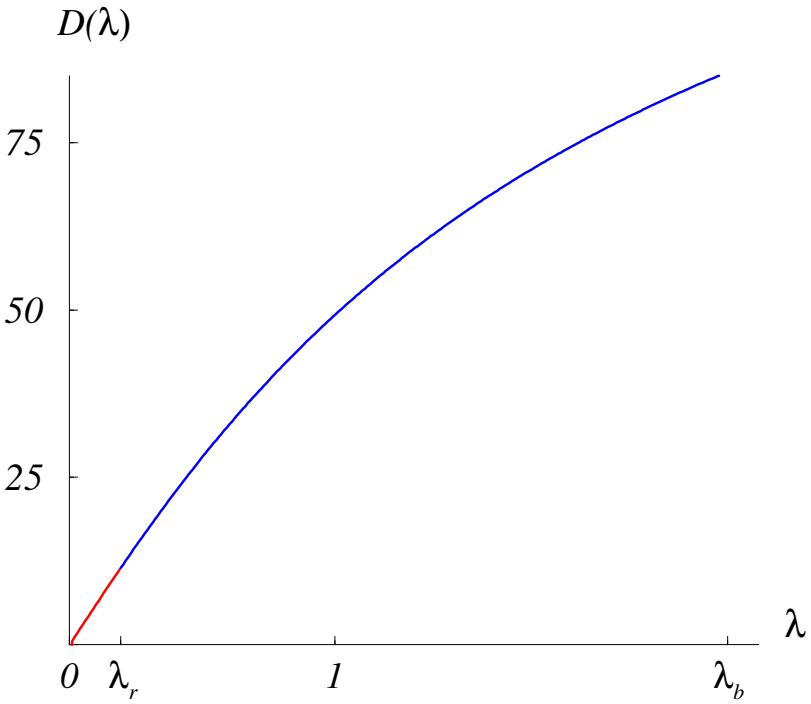

Figure 3.15. Plot of $D(\lambda)$ when $v_2(x)$ is odd. $a = 2.4$, $A = 2.8$, $\alpha = 0.22$, $x_T = 2.048246$, $\lambda_r = 0.192861$, $\lambda_b^{\mathbf{s}} = 2.48147$. There is no positive λ such that $D(\lambda) = 0$, $\lambda \leq \lambda_b^{\mathbf{d}}$. When $v_2(x)$ is odd, $D(\lambda)$ does identify the zero eigenvalue because $D(\lambda) = 0$ at $\lambda = 0$. This is consistent with theorem.

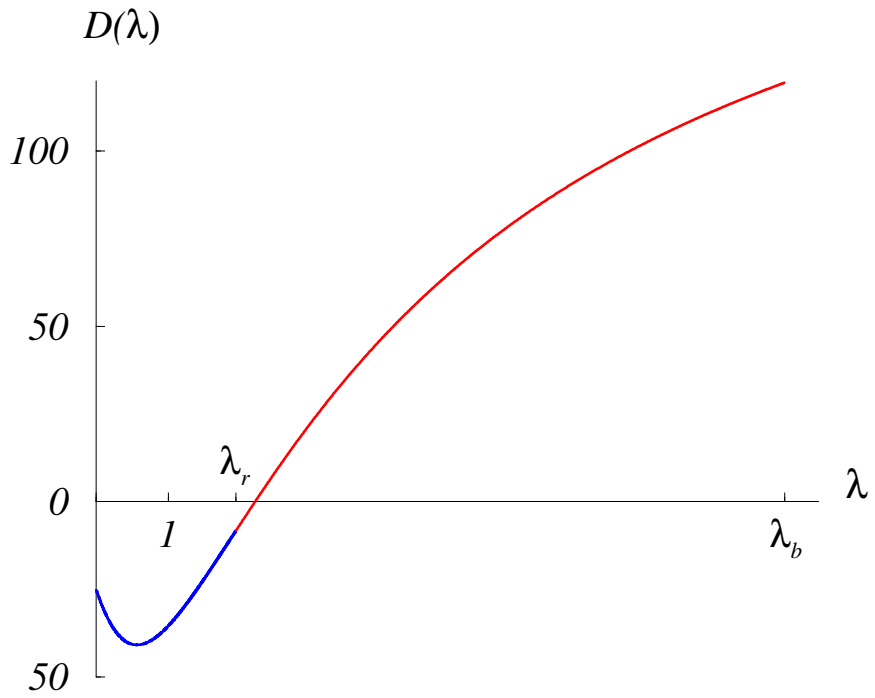

Figure 3.16. Plot of $D(\lambda)$ when $v_2(x)$ is even $a = 2.6$, $A = 2.8$, $\alpha = 0.6187$, $x_T = 1.98232$, $c = 0.588426$, $\lambda_r = 1.93376$, $\lambda_b^s = 9.52688$. There is a positive λ such that $D(\lambda) = 0$.

Chapter 4

Double-pulse solutions and future directions

In this chapter, I investigate double-pulse (2-pulse) solutions of equation

$$u(x) = \int_{-\infty}^{\infty} w(x-y) f[u(y)] dy \tag{4.1}$$

where $f[u(x)]$ is the gain function

$$f[u] = [\alpha(u - u_T) + \beta]\Theta(u - u_T) \qquad \alpha,\, u_T,\, \beta > 0 \tag{4.2}$$

$w(x)$ is coupling function

$$w(x) = Ae^{-a|x|} - e^{-|x|} \qquad A > 1,\, a > 1. \tag{4.3}$$

Both $f[u]$ and $w(x)$ are described in section 2.1.

A double-pulse (2-pulse) refers to a standing pulse (or localized excitation) with two disjoint, finite and open intervals (excitation regions).

Definition 4.1. Double-pulse solution: *A solution $u(x)$ of (4.1) is called a double-pulse or a 2-pulse if there are $x_1 > 0$ and $x_2 > 0$ such that*

$$u(x) \begin{cases} > u_T & \text{if } x \in (x_1, x_2) \cup (-x_2, -x_1),\ x_{1,2} > 0 \\ = u_T & \text{if } x = -x_2, -x_1, x_1, x_2 \\ < u_T & \text{otherwise} \end{cases}$$

with

$$(u, u', u'', u''') \to (0, 0, 0, 0)$$

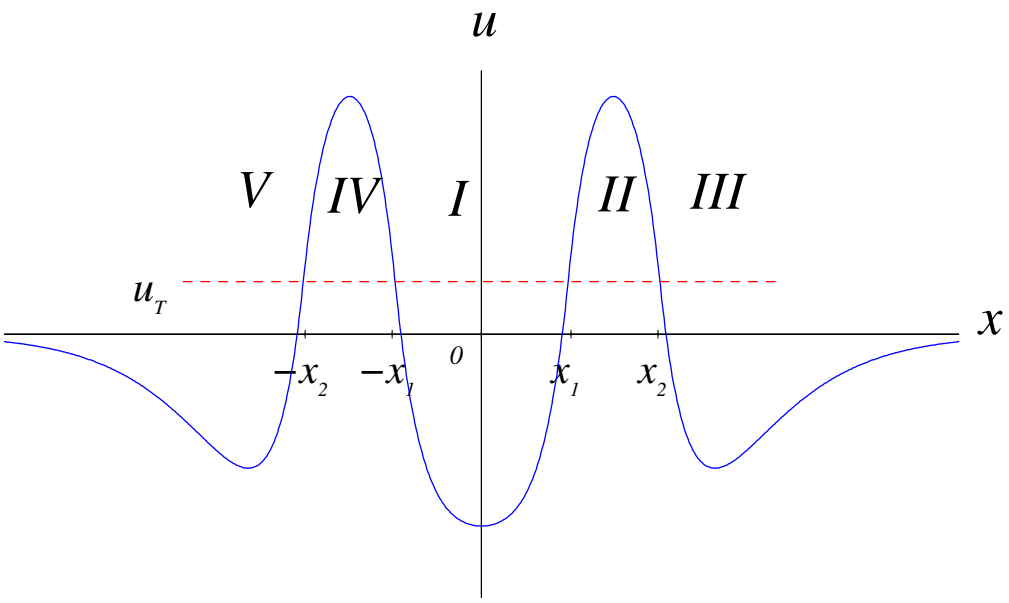

Figure 4.1. Double-pulse sketch.

exponentially fast as $x \to \pm\infty$. *Here* u, u' *are bounded and continuous on* $\Re$. u'', u''' *and* u'''' *are continuous everywhere for* $x \in \Re$ *except* $x = \pm x_{1,2}$ *and bounded everywhere on* $\Re$, *and.* $u(x)$ *is symmetric with* $u''(0) > 0$; $u(0)$ *is the minimum between* $-x_1$ *and* x_1 (seefigure 4.1).

4.1 Construction of double-pulse

The approach to find and construct a double-pulse is similar to that for a single-pulse as detailed in section 2.4. The coupling weight $w(x)$ is the same exponential function (2.3). Applying a Fourier Transform to (4.1), I obtain the same equation as (2.16)

$$F[u'''' - \left(a^2 + 1\right) u'' + a^2 u] = F[2\left(aA - a^2\right) f] + 2\left(aA - 1\right) F[s^2 f] \tag{4.4}$$

The $F[s^2 f]$ in equation (4.4) is different from the one in (2.16) because $F[s^2 f]$ is related to the threshold points. For a double-pulse, there are four threshold points $-x_{1,2}$ and $x_{1,2}$ instead of just the two $\pm x_T$for a single-pulse. Hence, I must recalculate $F[s^2 f]$ and re-derive the fourth order ODE

to look for a double-pulse solution. Consider

$$
\begin{aligned}
&F\left[s^2 f\right] \\
&= \int_{-\infty}^{\infty} s^2 e^{isx} f\left[u\left(x\right)\right] dx \\
&= -is\int_{x_1}^{x_2} \left(e^{isx}\right)' f\left[u\left(x\right)\right] dx - is\int_{-x_2}^{-x_1} \left(e^{isx}\right)' f\left[u\left(x\right)\right] dx \\
&= -ise^{isx} f\left[u\left(x\right)\right]\mid_{x_1}^{x_2} + \int_{x_1}^{x_2} ise^{isx}\frac{df\left[u\left(x\right)\right]}{dx}dx - ise^{isx} f\left[u\left(x\right)\right]\mid_{-x_2}^{-x_1} + \int_{-x_2}^{-x_1} ise^{isx}\frac{df\left[u\left(x\right)\right]}{dx}dx \\
&= -ise^{isx_2} f\left[u\left(x_2\right)\right] + ise^{isx_1} f\left[u\left(x_1\right)\right] + e^{isx_2} f'\left[u\left(x_2\right)\right] u'\left(x_2\right) - e^{isx_1} f'\left[u\left(x_1\right)\right] u'\left(x_1\right) \\
&\quad - \int_{x_1}^{x_2} e^{isx}\frac{d^2 f\left[u\left(x\right)\right]}{dx^2}dx - ise^{-isx_1} f\left[u\left(-x_1\right)\right] + is^{-isx_2} f\left[u\left(-x_2\right)\right] \\
&\quad + e^{-isx_1} f'\left[u\left(-x_1\right)\right] u'\left(-x_1\right) - e^{-isx_2} f'\left[u\left(-x_2\right)\right] u'\left(-x_2\right) - \int_{-x_2}^{-x_1} e^{isx}\frac{d^2 f\left[u\left(x\right)\right]}{dx^2}dx \\
&= -is\left(e^{isx_2} - e^{-isx_2}\right) f\left[u\left(x_2\right)\right] + is\left(e^{isx_1} - e^{-isx_1}\right) f\left[u\left(x_1\right)\right] \\
&\quad - f'\left[u\left(x_1\right)\right] u'\left(x_1\right)\left(e^{isx_1} + e^{-isx_1}\right) + f'\left[u\left(x-2\right)\right] u'\left(x_2\right)\left(e^{isx_2} + e^{-isx_2}\right) \\
&\quad - \left(\int_{x_1}^{x_2} e^{isx}\frac{d^2 f\left[u\left(x\right)\right]}{dx^2}dx + \int_{-x_2}^{-x_1} e^{isx}\frac{d^2 f\left[u\left(x\right)\right]}{dx^2}dx\right)
\end{aligned}
$$

Apply the inverse Fourier Transform to obtain the fourth order ODE on $x \in (-\infty, \infty)$

$$
\begin{aligned}
&u^{(\prime\prime\prime\prime)} - (a^2+1)u'' + a^2 u = \\
&\quad 2a(A-a) f\left[u(x)\right] + 2(aA-1)\left\{f[u(x_2)]\Delta_2'(x) - f[u(x_1)]\Delta_1'(x)\right\} - \\
&\quad 2(aA-1)\left\{f'[u(x_1)]u'(x_1)\Delta_1(x) + f'[u(x_1)]u'(x_1)\Delta_2(x)\right\} - \\
&\quad 2(aA-1)\frac{d^2 f\left[u(x)\right]}{dx^2}
\end{aligned}
\tag{4.5}
$$

where

$$
\begin{aligned}
\Delta_1(x) &= \delta(x-x_1) + \delta(x+x_1) \\
\Delta_2(x) &= \delta(x-x_2) + \delta(x+x_2) \\
\Delta_1'(x) &= \delta'(x-x_1) - \delta'(x+x_1) \\
\Delta_2'(x) &= \delta'(x-x_2) - \delta'(x+x_2)
\end{aligned}
$$

Integrating the fourth order ODE (4.5) over $(x_1-\epsilon, x_1+\epsilon)$ $(\epsilon \to 0)$ gives the jump of $u'''(x)$ at x_1.

$$u'''(x_1^+) - u'''(x_1^-) = -2(aA-1)f'[u(x_1)]u'(x_1)$$

Integrating the fourth order ODE with respect to x to get a third order ODE, then integrating the third order ODE over (x_1^-, x_1^+)

$$u''(x_1^+) - u''(x_1^-) = -2(aA-1)f[u(x_1)]$$

Similarly, the jumps at x_2 are

$$\begin{aligned} u'''(x_2^+) - u'''(x_2^-) &= 2(aA-1)f'[u(x_2)]u'(x_2) \\ u''(x_2^+) - u''(x_2^-) &= 2(aA-1)f[u(x_2)] \end{aligned}$$

Now I have ten equations for the matching conditions at both x_1 and x_2.

$$u_I(x_1) = u_T \tag{4.6}$$

$$u_{II}(x_1) = u_T \tag{4.7}$$

$$u_{II}(x_2) = u_T \tag{4.8}$$

$$u_{III}(x_2) = u_T \tag{4.9}$$

$$u_I'(x_1) = u_{II}'(x_1) \tag{4.10}$$

$$u_I''(x_1) = u_{II}''(x_1) + 2(aA-1)f(u(x_1)) \tag{4.11}$$

$$u_I'''(x_1) = u_{II}'''(x_1) + 2(aA-1)f'(u(x_1))u'(x_1) \tag{4.12}$$

$$u_{II}'(x_2) = u_{III}'(x_2) \tag{4.13}$$

$$u_{II}''(x_2) = u_{III}''(x_2) - 2(aA-1)f(u(x_2)) \tag{4.14}$$

$$u_{II}'''(x_2) = u_{III}'''(x_2) - 2(aA-1)f'(u(x_2))u'(x_2) \tag{4.15}$$

In Region I and III, ODE (4.5) can be reduced to

$$u'''' - (a^2+1)u'' + a^2 u = 0 \tag{4.16}$$

Solution of (4.16) on I is in the form of $u_{\rm I}(x) = C(e^{ax} + e^{-ax}) + D(e^{x} + e^{-x})$. In region III, $u_{\rm III}(x) = Ge^{-ax} + He^{-x}$.

In region II , ODE (4.5) can be reduced to

$$u'''' - (a^2+1)u'' + a^2b^2u = 2ab(bA-a)f\left[u(x)\right] - 2(aA-1)\frac{d^2f\left[u(x)\right]}{dx^2}$$

where $f\left[u(x)\right] = \alpha(u-u_T) + \beta$ and $\dfrac{d^2f\left[u(x)\right]}{dx^2} = \alpha u''(x)$.

It can be further simplified to

$$u'''' - \left[a^2 + 1 + 2\alpha(aA-1)\right]u'' + (a^2 - 2a\alpha(A-a))u = 2a(A-a)(\beta - \alpha u_T) \tag{4.17}$$

The ODE for double-pulse on region II is the same as ODE (2.27). Therefore, the four eigenvalues $\omega_{1,2}$ and $-\omega_{1,2}$ of ODE (4.17) have the same structures as those of ODE (2.27) for single-pulses in section 2.6. Hence the eigenvalues $\omega_{1,2}$ of ODE (4.17) satisfies

$$\omega_1^2 = R + S \tag{4.18}$$

$$\omega_2^2 = R - S \tag{4.19}$$

where

$$\Delta = (a^2 + 1 - 2\alpha(aA-1))^2 - 4(a^2 - 2a\alpha(A-a))$$

$$R = \frac{(a^2 + 1 - 2\alpha(aA-1))}{2} \qquad S = \frac{\sqrt{\Delta}}{2}$$

$\omega_{1,2}$ could be both real, both complex, or one real and complex for the other. There is no need to go over all similar details as for single-pulses. I only give the solution forms here.

If $\omega_{1,2}$ are real, the solution of ODE (4.17) in region II can be written as

$$u_{\rm II}(x) = Ee^{\omega_1(x-\frac{x_1+x_2}{2})} + Fe^{-\omega_1(x-\frac{x_1+x_2}{2})} + Se^{\omega_2(x-\frac{x_1+x_2}{2})} + Te^{-\omega_2(x-\frac{x_1+x_2}{2})} + \frac{2(A-a)(\beta-\alpha u_T)}{a-2\alpha(A-a)}$$

where E, F, S, $T \in \Re$. (Figure 4.2)

If $\omega_{1,2}$ are both complex, let $\omega_1 = p + iq$, then

$$u_{\mathrm{II}}(x) = 2Ee^{px}\cos qx - 2Fe^{px}\sin qx + 2Se^{-px}\cos qx + 2Te^{-px}\sin qx + \frac{2(A-a)(\beta-\alpha u_T)}{a-2\alpha(A-a)}$$

where $p = \Re\omega_1 \in \Re$, $q = \Im\omega_1 \in \Re$ and ω_1 is the complex conjugate of ω_2. E, F, S, $T \in \Re$. (Figure 4.3)

If ω_1 is real and ω_2 is complex, ω_1 satisfies (4.18) and $q = \sqrt{\dfrac{\sqrt{\Delta - R}}{2}}$, then

$$u_{\mathrm{II}}(x) = Ee^{w_1 x} + Fe^{-w_1 x} + 2S\cos qx + 2T\sin qxf + \frac{2(A-a)(\beta-\alpha u_T)}{a-2\alpha(A-a)}$$

where E, F, S, $T \in \Re$.

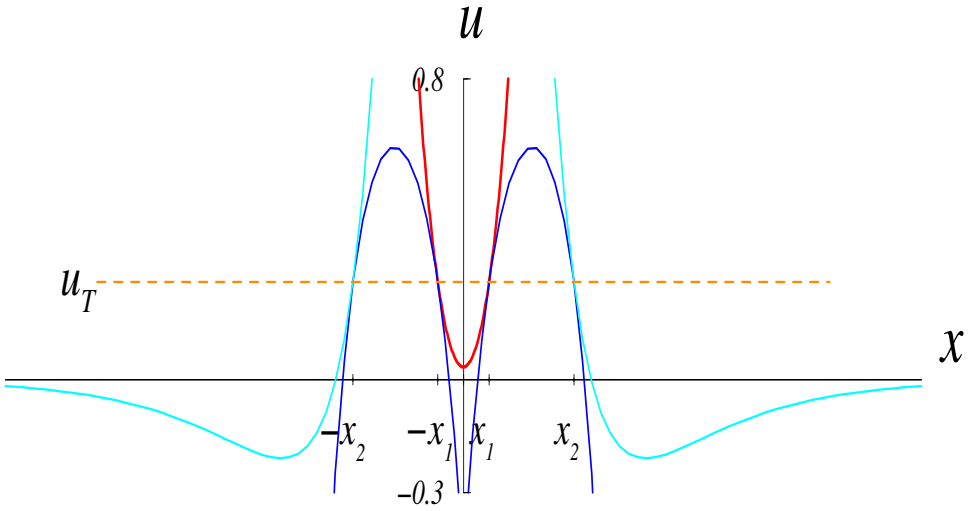

Figure 4.2. Double-pulse for Amari case in which $\alpha = 0$. $A = 2.8$, $a = 2.6$, $\alpha = 0$, $u_T = 0.26$, $x_1 = 0.279525$, $x_2 = 1.20521$.

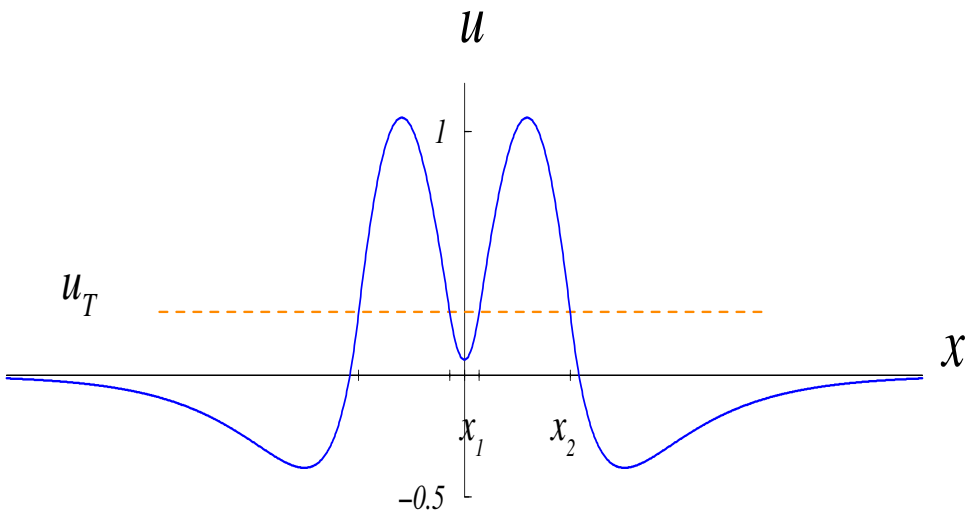

Figure 4.3. Double-pulse with complex $\omega_{1,2}$. $A = 2.8$, $a = 2.6$, $\alpha = 0.98$, $u_T = 0.26$, $x_1 = 0.19266$, $x_2 = 1.38376$.

4.2 Future directions

There are a number of directions to extend this work. One continuation of this work is to analyze the stability of double-pulses. Laing and Troy [42] develop criteria for the existence and stability of 2-pulse solutions for Amari's model with the Heaviside gain function. Their results imply that lateral inhibition type of coupling is not sufficient to produce stable 2-pulses. I would like to explore if the model with the non-saturating piece-wise linear gain function (4.2) can support stable double-pulse patterns. I will use a similar approach as the stability analysis of single-pulses (Chapter 3.) But the analysis of double-pulses will be much more complicated because there are more threshold points. This study will generalize part of Laing and Troy's to non-saturating gain.

In the one population rate model, I use a lateral-inhibition coupling such that each neuron in the network excites nearby neurons and inhibits distant ones. However, a neuron is either excitatory or inhibitory but cannot be both. Therefore, I will consider a two-population rate model:

$$u_t(x,t) = -u(x,t) + \int_{-\infty}^{\infty} w_{ee}(x-y) f_e[u(y,t)]dy - \int_{-\infty}^{\infty} w_{ie}(x-y) f_i[v(y,t)]dy \quad (4.20)$$

$$v_t(x,t) = -v(x,t) + \int_{-\infty}^{\infty} w_{ei}(x-y) f_e[u(y,t)]dy - \int_{-\infty}^{\infty} w_{ii}(x-y) f_i[v(y,t)]dy \quad (4.21)$$

Here, u and v represent the average neural activity in a population of excitatory (e) and inhibitory

(i) neurons, respectively, at spatial point x and time t; w_{jk} is the coupling weight function representing the strength of connectivity from population j to k $(j, k \in \{e, i\})$; f_j is the firing rate of population j. This two-population rate model is derived from a corresponding spiking neuron model using averaging methods.

Pinto and Ermentrout [52] study the two-population rate model with a linear f_i, the Heaviside f_e and lateral-inhibition type of connectivity. I can investigate this two-population rate model using a non-saturating piece-wise linear function (4.2) for f_e. My goal is to show the existence of standing pulses and examine their stability. Gutkin *et al.* [32] investigate a one-dimensional conductance-based network including both excitatory and inhibitory neurons. I can do a similar study of the corresponding spiking model. Then I can compare the neural activity of the two-population rate model with the simulations of the spiking model. I hope to find the correspondence between the rate model and the spiking model in the same manner as Laing and Chow [41].

Appendix

Appendix

Proposition A.1. *Both α_1 and α_3, the roots of equation $\Delta = 0$, are positive and they are never equal to each other, i.e. $\Delta(\alpha) = 0$ always has two different positive roots α_1 and α_2. And*

$$\alpha_1 = \frac{a^3A + a^2 - aA - 1 - 2\sqrt{aA}}{2(aA-1)^2} \tag{A.1}$$

$$\alpha_3 = \frac{a^3A + a^2 - aA - 1 + 2\sqrt{aA}}{2(aA-1)^2} \tag{A.2}$$

Proof of proposition A.1: Rearrange Δ and write it as a quadratic form of α.

$$\Delta = 4(aA-1)^2\alpha^2 + [4(aA-1)(a^2+1) + 8a(A-a)]\alpha + (a^2-1)^2 \tag{A.3}$$

The constant term $(a^2-1)^2$ is positive because $a > 1$. Thus, there is no zero solution for $\Delta = 0$ and the two solutions have the same sign, either both positive or both negative. Now we eliminate the possibility that both are negative by contradiction. Suppose the two roots, α_1 and α_3 are both negative. Then the following must be true.

$$\begin{aligned} \frac{4(aA-1)(a^2+1) + 8a(A-a)}{4(aA-1)^2} &< 0 \\ 4(aA-1)(a^2+1) + 8a(A-a) &< 0 \end{aligned} \tag{A.4}$$

Simplify (A.4),

$$A < \frac{3a^2+1}{a(a^2+3)} \tag{A.5}$$

Since $A > 1$, $\dfrac{3a^2+1}{a(a^2+3)} > 1$, which means $(a-1)^3 < 0$. Therefore, $a < 1$, which contradicts the

assumed condition on parameter a. So α_1 and α_3 must be both positive. Solve $\Delta = 0$ and simplify to obtain

$$\alpha_1 = \frac{a^3A + a^2 - aA - 1 - 2\sqrt{aA}}{2(aA-1)^2} \tag{A.6}$$

$$\alpha_3 = \frac{a^3A + a^2 - aA - 1 + 2\sqrt{aA}}{2(aA-1)^2} \tag{A.7}$$

Proposition A.2. *For the balanced case in which $A = a$, $\alpha_1 < 1/2$, $\alpha > 1/2$. When A gets bigger, α_1 moves closer to α_3, but never reaches it.*

Proof of proposition A.2: Replace A by a. Δ becomes

$$\Delta = (a^2 + 1 - 2\alpha(a^2-1))^2 - 4a^2 \tag{A.8}$$

Solve two equations

$$\Delta = a^2 + 1 - 2\alpha(a^2-1) = 2a \tag{A.9}$$

$$\Delta = a^2 + 1 - 2\alpha(a^2-1) = -2a \tag{A.10}$$

(A.10) gives $\alpha_1 = \frac{a-1}{2(a+1)}$, therefore $\alpha_1 < \frac{a+1}{2(a+1)} = \frac{1}{2}$. (A.9) gives $\alpha_3 = \frac{a+1}{2(a-1)}$, therefore $\alpha_3 > \frac{a-1}{2(a-1)} = \frac{1}{2}$.

Lemma A.1. *λ_B, the zero of B is always between -1 and λ_r. When $a^3 > A$, $\lambda_l < \lambda_B < \lambda_r$. When $a^3 < A$, $\lambda_B < \lambda_l < \lambda_r$.*

Proof of lemma A.1: Set

$$B = (1+\lambda)(a^2+1) + 2\alpha(1-aA) = 0$$

The zero of B is

$$\lambda_B = -\frac{a^2+1+2\alpha-2aA\alpha}{a^2+1} = -1 + \frac{2\alpha(aA-1)}{a^2+1}.$$

Since both a and A are bigger than unity and α is positive, $\lambda_B > -1$. Δ is a quadratic function in

λ and it has two zeros. The left zero is

$$\lambda_l = \frac{1 - a^2 + 2aA\alpha + 2\alpha - 4\alpha\sqrt{aA}}{a^2 - 1}$$

The right zero is

$$\lambda_r = \frac{1 - a^2 + 2aA\alpha + 2\alpha + 4\alpha\sqrt{aA}}{a^2 - 1}$$

The difference between λ_r and λ_B is

$$\lambda_r - \lambda_B = \frac{4a\alpha(a + A) + 4\alpha\sqrt{aA}(a^2 + 1)}{a^4 - 1} > 0$$

Therefore $-1 < \lambda_B < \lambda_r$.

The difference between λ_B and λ_l is

$$\lambda_B - \lambda_l = \frac{4\alpha(\sqrt{aA} - 1)(a^2 - \sqrt{aA})}{a^4 - 1}.$$

The sign of $\lambda_B - \lambda_l$ depends on $a^2 - \sqrt{aA}$.

If $a^2 - \sqrt{aA}$ is positive, *i.e.* $a^3 > A$, then $\lambda_l < \lambda_B < \lambda_r$.

If $a^2 - \sqrt{aA}$ is negative, *i.e.*, $a^3 < A$, then $\lambda_B < \lambda_l < \lambda_r$. $\Diamond$

Lemma A.2. *(i). When $a^3 > A$, $\lambda_l < \lambda_B < \lambda_r$, B does not intersect the left branch or the right branch of $\sqrt{\Delta}$. (ii). When $a^3 < A$, $\lambda_B < \lambda_l < \lambda_r$, B intersects only the left branch of $\sqrt{\Delta}$ once at λ_I.*

Proof of lemma A.2: It is not difficult to see that B does not intersect the right branch of $\sqrt{\Delta}$ for both (i) and (ii). $\sqrt{\Delta}$ is linear in λ with slope $a^2 - 1$ for large λ. The slope of B is $a^2 + 1$. Both $a^2 - 1$ and $a^2 + 1$ are positive and $a^2 + 1 > a^2 - 1$, therefore, B and the right branch of $\sqrt{\Delta}$ never meet. When $\lambda_l < \lambda_B < \lambda_r$, $B < 0$ for $\lambda < \lambda_B$ and $\sqrt{\Delta} > 0$ for $\lambda < \lambda_l < \lambda_B$. Therefore B and $\sqrt{\Delta}$ never intersect. In (ii), B intersects the left branch of $\sqrt{\Delta}$ at $\lambda_I = \frac{2A\alpha - 2a\alpha - a}{a}$. $\Diamond$

Bibliography

1. Charalambos Aliprantis. *Problems in real analysis: a workbook with solutions*. Academic Press, 1999.

2. Charalambos D. Aliprantis and Burkinshaw. *Principles of real analysis*. Academic Press, 1998.

3. S. Amari. Dynamics of pattern formation in lateral-inhibition type neural fields. *Biol. Cybernetics*, 27:77–87, 1977.

4. Michael A. Arbib, editor. *The Handbook of Brain Theory and Neural Networks*. MIT Press, 1995.

5. Kendall E. Atkinson. *Numerical solution of integral equations of the second kind*. Cambridge University Press, 1997.

6. Alan Baddeley. *Working Memory*. Oxford University Press, 1986.

7. Carl M. Bender and Steven A. Orszag. *Advanced mathematical methods for scientists and engineers I: Asyptotic methods and perturbation theory*. Springer, 1999.

8. William E. Boyce and Richard C. DiPrima. *Introduction to differential equations*. John Wiley and Sons, 1970.

9. M Camperi and X.J. Wang. A model of visuospatial working memory in prefrontal cortex: recurrent network and cellular bistability. *J. Comp. Neurosci*, 5:383–405, 1998.

10. A. R. Champneys and J. P. McKenna. On solitary waves of a piece-wise linear suspended beam model. *Nonlinearity*, 10:1763–1782, 1997.

11. C. L. Cobly, J.-R. Duhamel, and M. E. Goldberg. Oculocentric spatial representation in parietal cortex. *Cerebral Cortex*, 5:470–481, 1995.

12. S. Coombes, G. J. Lord, and M. R. Owen. Waves and bumps in neuronal networks with axo-dendritic synaptic interactions. *Physica D*, 178:219–241, 2002.

13. L. M. Delves and J. L. Mohamed. *Computational methods for integral equations*. Cambridge University Press, 1988.

14. Dean G. Duffy. *Green's functions with applications*. Chapman and Hall/CRC, 2001.

15. S. A. Ellias and S. Grossberg. Pattern formation, contrast control, and oscillations in the short-term memory of shunting on-center off-surround networks. *Biol. Cybern.*, 20:69–98, 1975.

16. G. Bard Ermentrout. Xppaut, simulation software tool.

17. G. Bard Ermentrout. Reduction of conductance-based models with slow synapses to neural nets. *Neural Comp*, 6:679–695, 1994.

18. G. Bard Ermentrout. Neural networks as spatio-temporal pattern-forming systems. *Rep. Prog. Phys.*, 61:353–430, 1998.

19. G. Bard Ermentrout. *Simulating, Analyzing, and Animating Dynamical Systems: A Guide to XPPAUT for Researchers and Students*. SIAM, 2002.

20. J. W. Evans. Nerve axon equations, i: Linear approximations. *Indiana Univ. Math. J.*, 21:877–955, 1972.

21. J. W. Evans. Nerve axon equations, ii: Stability at rest. *Indiana Univ. Math. J.*, 22:75–90, 1972.

22. J. W. Evans. Nerve axon equations, iii: Stability of the nerve impulse. *Indiana Univ. Math. J.*, 22:577–594, 1972.

23. J. W. Evans. Nerve axon equations, iv: The stable and unstable impulse. *Indiana Univ. Math. J.*, 24:1169–1190, 1975.

24. G. B. Folland. *Fourier analysis and its applications*. Wadsworth and Brooks/Cole Advanced Books and Software, 1992.

25. S. Funahashi, Bruce G. J., and R. Goldman-Rakic. Mnemonic coding of visual space in the monkey's dorsolateral prefrontal cortex. *J. Neurophys.*, 61:331–349, 1989.

26. J. Fuster and G. Alexander. Neuron activity related to short-term memory. *Science*, 173:652–654, 1971.

27. Joaquin M Fuster. *Prefrontal cortex: anatomy, physiology, and neuropsychology of the frontal lobe*. Lippincott-Raven Publishers, 1997.

28. Frank Garvan. *The Maple Book*. Chapman and Hall, 2001.

29. Christopher Denis Green. *Integral equation methods*. Nelson, 1969.

30. D. H. Griffel. *Applied functional analysis*. Ellis Horwood, 1985.

31. Yixin Guo and Carson Chow. Existence of standing pulses in neural networks. 2003 in preparation.

32. B.S. Gutkin, C.R. Laing, C. L. Colby, C.C. Chow, and G. B. Ermentrout. Turing on and off with excitation: the role of spike-timing asynchrony and synchrony in sustained neural activity. 11, 2001.

33. Tosio Kato. *Perturbation theory for linear operators*. Springer, 1995.

34. K Kishimoto and S. Amari. Existence and stability of local excitations in homogeneous neural fields. *J. Math. Biology*, 7:303–318, 1979.

35. Erwin Kreyszig. Introductory functional analysis with applications. pages 443–444, 1978.

36. Erwin Kreyszig. Introductory functional analysis with applications. pages 454–455, 1978.

37. Erwin Kreyszig. Introductory functional analysis with applications. pages 421–422, 1978.

38. Erwin Kreyszig. Introductory functional analysis with applications. pages 454–455, 1978.

39. Erwin Kreyszig. Introductory functional analysis with applications. page 449, 1978.

40. Yuri A. Kuznetsov. *Elements of applied bifurcation theory*. Springer, 1998.

41. Carlo R. Laing and Carson C. Chow. Stationary bumps in networks of spiking neurons. *Neural Comp.*, 13:1473–1493, 2001.

42. Carlo R. Laing and William C. Troy. Two-bump solutions of amari type models of working memory. *submitted to Physica D*, 2002.

43. Carlo R. Laing, William C. Troy, Boris Gutkin, and G. Bard Ermentrout. Multiple bumps in a neuronal model of working memory. *submitted to SIAM J. of Applied Math.*, 2001.

44. E. K. Miller, C. A. Erickson, and R. Desimone. Neural mechanisms of visual working memory in prefrontal cortex of the macaque. *J. Neurosci.*, 16:5154–5167, 1996.

45. Norman Morrison. *Introduction to Fourier analysis*. Wiley-Interscience, 1994.

46. James Dickson Murray. *Mathematical biology*. Springer, 2002.

47. John G. Nicholls. *From neuron to brain: a cellular molecular approach to the function of the nervous system*. Sinauer Associates, 1992.

48. Y. Nishiura and M. Mimura. Layer oscillations in reactoin-diffusion systems. *SIAM J. Appl. Math.*, 49:481–514, 1989.

49. Eva Pärt-Enander, Anders Sjöberg, Melin Bo, and Isaksson Pernilla. *The MATLAB handbook*. Addison-Wesley, 1998.

50. Lambertus A. Peletier and William C. Troy. *Spatial patterns: higher order models in physics and mechanics*. Birkhauser, 2001.

51. E. Pelinovsky, D and V. G. Yakhno. Generation of collective-activity structures in a homogeneous neuron-like medium. i. bifurcation analysis of static structures,. *Bifurcation Chaos Appl. Sci. Eng.*, 6:81–87, 89–100, 1996a,b.

52. J. D. Pinto and Ermentrout G. B. Spatially structured activity in synaptically coupled neuronal networks:1 traveling fronts and pulses. *SIAM J. Appl. Math.*, 62:206–225, 2001.

53. J. D. Pinto and Ermentrout G. B. Spatially structured activity in synaptically coupled neuronal networks:2 lateral inhibition and standing pulses. *SIAM J. Appl. Math.*, 62:226–243, 2001.

54. Andrei Dmitrievich Polianin and Alexander V. Manzhirov. *Handbook of integral equations*. CRC Press, 1998.

55. David L. Powers. *Boundary value problems*. Harcourt Academic Press, 1999.

56. Matiur Rahman. *Complex variables and transform calculus*. Computational Mechanics Publications, 1997.

57. Jonathan E Rubin, David Terman, and Carson C Chow. Localized bumps of activity sustained by inhibition in a two-layer thalamic network. *J Comp Neurosci*, 10:313–331, 2001.

58. Jonathan E Rubin and C. William Troy. Sustained spatial patterns of activity in neuronal populations with or without lateral inhibition. *Preprint*, 2002.

59. Walter Rudin. *Principles of mathematical analysis*. McGraw-Hill, 1976.

60. E. Salinas and L. F. Abbott. A model of multiplicative neural responses in parietal cortex. *Proc Natl Acad Sci USA*, 93:11956–11961, 1996.

61. S. H. Seung. How the brain keeps the eyes still. *Proc Natl Acad Sci USA*, 93:13339–44, 1996.

62. Steven H. Strogatz. *Nonlinear dynamics and chaos*. Perseus Books, 1994.

63. X-J Wang. Synaptic reverberation underlying mnemonic persistent activity. *Trends in Neurosci*, 24:455–463, 2001.

64. Stephen Wiggins. *Introduction to applied nonlinear dynamical systems and chaos*. Springer, 1990.

65. H. R. Wilson and J. D. Cowan. Excitatory and inhibitory interactions in localized populations of model neurons. *Biophys. J.*, 12:1–24, 1973.

66. H. R. Wilson and J. D. Cowan. A mathematical theory of the functional dynamics of cortical and thalamic nervous tissue. *Kybernetic*, 13:55–80, 1973.

67. Stephen Wolfram. *The Mathematica Book*. Cambridge University Press, 4th Edition, 1999.

68. Eberhard Zeidler. *Nonlinear functional analysis and its applications I: fixed-point theorems*. Springer, 1986.